

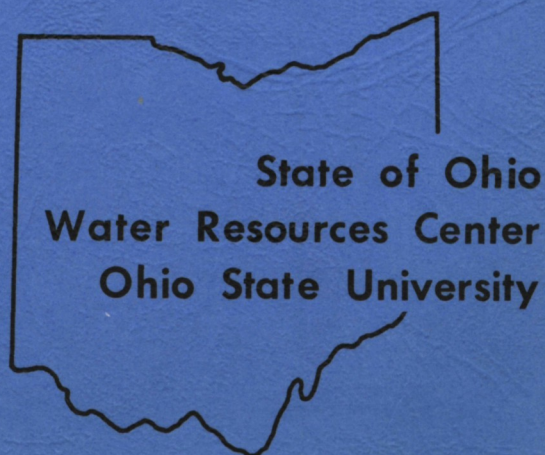
1974

Bacterial Methane Oxidation
and its Influence in the
Aquatic Environment

Patrick R. Dugan
and
Terry L. Weaver
Department of Microbiology
The Ohio State University

Office of
Water Research and Technology
United States Department
of the Interior

PROJECT
A-027-OHIO.



BACTERIAL METHANE OXIDATION AND ITS INFLUENCE
IN THE AQUATIC ENVIRONMENT

by

Patrick R. Dugan and Terry L. Weaver
Department of Microbiology
The Ohio State University

August 1974

This study was supported in part by the Office of Water Resources Research, U.S. Department of the Interior under Project A-027-OHIO. Parts of this report were not sponsored by OWRR but are included to give subject continuity to the report. Much of the research reported constituted the Ph.D. dissertation of Terry L. Weaver.

TABLE OF CONTENTS

	page
Table of Contents	i
List of Tables	iii
List of Figures	iii
1. Introduction	1
2. Review of the Literature	2
3. Mixed Culture Growth Studies	10
Materials and Methods	10
Results and Discussion	11
4. Pure Culture Growth Studies	27
Materials and Methods	27
Results and Discussion	30
5. Morphology of Methane Oxidizing Bacteria	42
Materials and Methods	42
Results and Discussion	44
6. Isolation of Intracytoplasmic Membranes	65
Materials and Methods	65
Results and Discussion	66
7. Lipids of Cells and Membranes	73
Materials and Methods	73
Results and Discussion	78
8. Proteins of Cells and Membranes	97
Materials and Methods	97
Results and Discussion	101
9. Summary	122
10. Conclusions and Recommendations	124

LIST OF TABLES

<u>Table Number</u>		<u>page</u>
1	Values showing size distribution (%) and cation exchange capacity for four different clay types	11
2	Components of mineral salts medium CM listed in grams per liter of distilled water	28
3	Organic compounds tested for the ability to support growth of <u>Methylosinus trichosporium</u>	33
4	Gaseous substrate and product balances during methane oxidation by <u>Methylosinus trichosporium</u> grown in CM medium at 21 C.	40
5	Relative weight of protein, hexose, and PHB in various differential centrifugation fractions of broken <u>M. trichosporium</u> cells	71
6	Gravimetric analysis of lipid components of whole cells and membranes	80
7	R _f values of cell and membrane simple lipids and standards of silica gel TLC in hexane-diethyl etheracetic acid	82
8	Quantitative analysis of simple lipids from whole cells and membranes	83
9	Summary of silica gel TLC data concerning membrane phospholipids	85
10	R _v values of phospholipid standards	86
11	R _f values for membrane phospholipids on argenation TLC plates.	87
12	R _f values for the hydrolysis products of phosphatidyl ethanolamine compared to standards.	88
13	Formaldehyde quantitation after periodate oxidation of phospholipids.	89
14	Relative peak areas from radiochromatogram scanner tracing of P ³² labeled phospholipids separated by TLC . . .	93

LIST OF TABLES (cont)

<u>Table Number</u>		<u>page</u>
15	Scintillation spectrophotometric quantitation of p ³² labeled phospholipids scraped from TLC plate	94
16	Fatty acid compositions of the phospholipids of <u>M.</u> <u>trichosporium.</u>	95
17	R _f values for amino acids on silica gel TLC plates developed with ethanol and ammonium hydroxide	103
18	Polarity of amino acids in various protein samples from <u>M. Trichosporium</u>	104
19	Migration distances and molecular weights of membrane proteins and bovine serum albumin standard as related to polyacrylamide gel electrophoresis	107
20	Enzyme nomenclature listing CEIUB number, systematic name, trivial name, and reaction	112
21	Initial velocities and activities of enzymes in membrane and cytoplasmic preparation	120

LIST OF FIGURES

<u>Figure Number</u>		<u>page</u>
1	Curves showing methane oxidized and carbon dioxide produced by a mixed bacterial population versus time of incubation. Curves represent different kaolinite suspension concentrations.	17
2	Curves showing methane oxidized and carbon dioxide produced by a mixed bacterial population versus time of incubation. Curves represent a 4.0% concentration of different clay types.	18
3	Curves showing methane oxidized and carbon dioxide produced by a mixed bacterial population versus time of incubation. Curves represent a 4.0% concentration of different size vermiculite particles.	19
4	Curves showing methane oxidized and carbon dioxide produced by a mixed bacterial population versus time of incubation. Curves show the effects of the addition of kaolinite (4.0%) to actively growing cells.	20
5	Curves showing methane oxidized and carbon dioxide produced by a mixed bacterial population versus time of incubation. Curves represent a 4.0% concentration of various types of insoluble inorganic particulates. . .	21
6	Curves showing methane oxidized and carbon dioxide produced by a mixed bacterial population versus time of incubation. Curves represent a 4.0% concentration of various types of insoluble organic particulates. . . .	22
7	Curves showing methane oxidized and carbon dioxide produced by a mixed bacterial population versus time of incubation. Curves represent a 0.4% concentration of extracellular polysaccharide polymers.	23
8	Curves showing methane oxidized and carbon dioxide produced by a mixed bacterial population versus time of incubation. Curves represent 3.0 ml of various algae under constant illumination.	24
9	Curves showing methane oxidized and carbon dioxide produced by a mixed bacterial population versus time of incubation. Curves represent 3.0 ml of various algae incubated in the dark.	25
10	Curves showing methane oxidized and carbon dioxide produced by a mixed bacterial population versus time of incubation. Curves represent 3.0 ml of various cell free algal culture media.	26

LIST OF FIGURES (cont)

<u>Figure Number</u>		<u>page</u>
11	Growth curve for <u>Methylosinus trichosporium</u> cultivated in liquid CM medium at 21 C. and pH 7.	31
12	Curves showing micromoles of methane oxidized by <u>Methylosinus trichosporium</u> . Curves represent $10^{-2}M$ concentrations of various organic acids.	35
13	Curves showing micromoles of methane oxidized by <u>Methylosinus trichosporium</u> . Curves represent $10^{-2}M$ concentrations of various amono acids.	36
14	Curves showing micromoles of methane oxidized by <u>Methylosinus trichosporium</u> . Curves represent $10^{-2}M$ concentrations of various pentoses.	37
15	Curves showing micromoles of methane oxidizing by <u>Methylosinus trichosporium</u> . Curves represent $10^{-2}M$ concentrations of various hexoses.	38
16	Electron microbraph of a freeze etch preparation of <u>M. trichosporium</u>	45
17	Electron micrograph of a carbon replica of <u>M. methanica</u> .	47
18	Electron micrograph of a freeze etch preparation of <u>M. trichosporium</u>	48
19	Electron micrograph of a freeze etch preparation of <u>M. trichosporium</u>	49
20	Electron micrograph of a freeze etch preparation of <u>M. trichosporium</u>	50
21	Electron micrograph of a freeze etch preparation of <u>M trichosporium</u>	51
22	Electron micrograph of a freeze etch preparation of <u>M. trichosporium</u> showing extend of internal membranes.. .	52
23	Electron micrograph of a freeze etch preparation of build building <u>M. trichosporium</u> cell showing the division of membranes.	53
24	Electron microbraph of a freeze etch preparation of a <u>M. trichosporium</u> spore.. . . .	54
25	Electron microbraph of a freeze etch preparation of <u>M. trichosporium</u>	56

LIST OF FIGURES (cont)

<u>Figure Number</u>		<u>page</u>
26	Electron micrograph of a freeze etch preparation of <u>M. trichosporium</u>	57
27	Electron micrograph of negatively stained sample of liquid <u>M. trichosporium</u> culture showing an intercellular bridge.	58
28	Electron micrograph of a freeze etch preparation of <u>M. trichosporium</u>	59
29	Illustration representing the proposed morphology of <u>M. trichosporium</u>	60
30	Electron micrograph of a freeze etch preparation of <u>M. methanica</u> showing Type I membranes	61
31	Electron micrograph of a thin section preparation of <u>M. methanica</u>	62
32	Electron micrographs of thin sections of membranes in <u>M. methanica</u> showing	63
33	Electron micrograph of a thin section preparation of <u>M. methanica</u>	64
34	Negative stain of the 5P differential centrifugation fraction of disrupted <u>M. trichosporium</u> cells.	67
35	Negative stain of the 20P differential centrifugation fraction of disrupted <u>M. trichosporium</u> cells.	68
36	Negative stain of the 80P differential centrifugation fraction of disrupted <u>M. trichosporium</u> cells.	69
37	Thin section of an intracytoplasmic membrane preparation 20P, 40P, 80P, fractions from <u>M. trichosporium</u>	70
38	Infrared spectra of methanol precipitate from total lipids of <u>M. trichosporium</u> and purified PHB	79
39	Autoradiogram of P ³² labeled phospholipids separated by TLC.	91
40	Radiochromatogram scanner tracing of P ³² labeled phospholipids separated by TLC.	92
41	Histogram showing polarity of 2 membrane associated enzymes and distribution of polarity among 100 nonmembrane proteins.	102

LIST OF FIGURES (cont)

<u>Figure Number</u>		<u>page</u>
42	Photograph of electrophoretic polyacrylamide gels containing brovine serum albumin and membrane proteins, and brovine serum albumin	106
43	Absorption spectra of a 80P membrane preparation from <i>M. trichosporium</i> when oxidized and reduced	108
44	Difference spectrum of oxidized 80P membranes versus reduced 80P membranes	109
45	Absorption spectra of 20S centrifugation fractions. Spectra represent oxidized spectrum, sample plus methane, and sample plus methanol, formaldehyde, formate, or NADH.	111
46	Graphs showing activity of serine transhydroxymethylase .	113
47	Graphs showing methanol dehydrogenase activity.	114
48	Graphs showing formaldehyde dehydrogenase activity. . . .	115
49	Graphs showing formate dehydrogenase activity	116
50	Graphs showing cytochrome C reductase activity.	117
51	Graphs showing hydroxypyruvate reductase activity	118
52	Graphs showing beta-hydroxuburyate dehydrogenase activity.	119

1. INTRODUCTION

Organic material is inevitably present in natural waters. As man's activities in the watershed areas increase, so do hominoid discharges into a body of water increase. These discharges add organic materials directly, and they also indirectly increase the organic content of water by stimulation of the growth of organic organisms through the fixation of inorganic carbon, nitrogen and other minerals into an organic form. Thus, organic material will be present in a body of water to a greater or lesser extent depending upon many factors.

Organic material in a body of water ultimately finds its way to the bottom where it is degraded by a myriad of microorganisms. Anaerobic bacteria produce and liberate great quantities of methane gas from the organic material in the anaerobic ferment in the bottom sediments. Since methane is only slightly soluble in water, it often exceeds its solubility, bubbles up through the water column, and is released into the atmosphere. Methane gas lost to the atmosphere represents a way for a body of water to "rid itself" of extraneous organic material and prevent carbon buildup. However, several species of bacteria oxidize methane as an energy source and convert it either into cellular material or much more soluble carbon dioxide. This results in some of the methane carbon being recycled back into the aquatic ecosystem. Therefore, the accumulation and recycling of methane carbon plays a key role in aquatic carbon buildup because the carbon remains "locked into" the system while other processes such as photosynthesis continually add or fix new carbon. The amount of methane carbon that is recycled and the amount that escapes from the ecosystem are determined by the conditions in the water at that particular time. Hence, the purpose of these studies was to investigate environmental factors that affect aquatic methane oxidation, to determine the effects these processes have on aquatic ecosystems, to develop methods to examine these processes, and ultimately, to reveal ways to control microbial methane oxidation and carbon buildup.

Major portions of this report were not sponsored by OWRR but the entire effort is included as a single report in order to maintain continuity of presentation of research data.

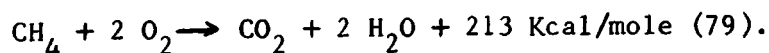
2. REVIEW OF THE LITERATURE

Methane Production and Fixation

Methane as an end product of microbial metabolism has been recognized since 1903 when Maze' reported its production by bacteria (77). Barker (2, 3) described several different kinds of bacteria that produce methane from the anaerobic decomposition of organic materials. The natural existence of methane in the environment is readily observed as natural gas, "fire damp" in coal mines, or "marsh gas" bubbling to the surface of swamps and lakes (79). Methane production in Lake Erie bottom sediments has recently been reported as $1.71 \text{ cm}^3 \text{ CH}_4 \text{ produced/meter}^2 \text{ of bottom sediment/minute}$ (53). Due to its low solubility in water, some methane escapes into the atmosphere where it has been reported to exist in concentrations of 1.2 to 1.5 parts per million (123). While methane production tends to remove extraneous carbon from natural waters, refixation of methane carbon by microbial oxidation and assimilation can also occur.

Bacterial methane oxidation was first reported by Kaserer in 1905 (60). One year later, Söhngen (117) reported isolation of a methane oxidizing bacterium, a Gram negative bacillus since named Pseudomonas methanica. These discoveries spurred interest in methane oxidizing microorganisms and their occurrence was soon reported to be widespread in soil and both fresh and salt water (34, 47, 54). Since Söhngen's first isolation, many different kinds of methane oxidizing bacteria have been isolated including Gram negative rods of various sizes, Gram negative cocci, vibrios, and even nitrogen fixing methane oxidizers (18, 32, 68, 132). Whittenbury (132) isolated over 70 pure cultures of methane oxidizing bacteria that could be separated into at least 15 morphologically distinctive groups.

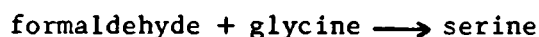
Some isolates are obligate methane oxidizers while others can grow in gaseous alkanes, methanol, formaldehyde, or a variety of other organic compounds in addition to methane (25, 68, 121). The complete oxidation of methane can be represented as follows:



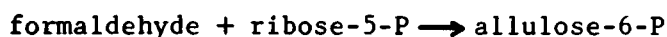
It has been shown that in microorganisms the reaction proceeds stepwise through

a series of intermediates, i.e. methane to methanol to formaldehyde to formic acid to carbon dioxide (9). However, all the methane is not oxidized to carbon dioxide; much of it is fixed into cellular material short of the complete oxidation to carbon dioxide. The ratio of methane consumed to oxygen used varies from 1:1.1 to 1:1.9 and the percentage of methane carbon fixed into cellular material varies from 40 to 80% depending upon the condition of the cells used in the determination (9, 32, 54, 109, 125, 132). Also, more methane carbon is fixed into cellular material when oxygen rather than methane is limiting (109). While the methane oxidizers exhibit many different morphological types, they seem to fall into two different physiological groups based upon the method of methane carbon fixation (66). One type of fixation is the hydro-oxymethylation of glycine by formaldehyde which was produced from methane to yield the amino acid serine and the other involves coupling of a one carbon unit (e.g. formaldehyde) with a pentose phosphate to form a six carbon unit, hexose phosphate (61, 62).

1. Serine Pathway:



2. Pentose Phosphate Pathway:



Thus, the methane oxidizers include several different types of bacteria existing in both fresh and marine waters that may fix as much as 80% of the carbon from oxidized methane into cellular material. The exact amount of methane carbon fixed in a natural aquatic ecosystem will depend upon environmental conditions at that time and the types of organisms present in that environment. The quantity and type of suspended particulate material in the water is one of the more important environmental factors involved in these interactions.

Particulate Effects on Microorganisms

In 1936, Zobell and Anderson (137) reported that they obtained greater increases in numbers of bacteria in sea water stored in small volumes as compared to larger volumes. This was attributed to the contact of the sea water with the proportionate larger solid surface area in small containers. In a more extensive study based upon this observation, Heukelekian and Heller (51) found that glass beads would increase bacterial growth in dilute nutrient

solutions. They indicated that this growth increase was due to a concentration of nutrients on the glass beads thus making the nutrients more readily available to the bacteria in the dilute solution. These two early reports were the basis of extensive investigation later concerning the relation between surfaces (particles) and microbial growth.

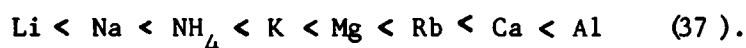
The existence of particulates in natural waters has been reported by Pfister et al (94, 95). Relatively large quantities of various particulates were found in water from Lake Erie. The size range of the particles was from $0.007\mu\text{m}$ to $30\mu\text{m}$ with the majority of the particles being less than $0.5\mu\text{m}$. Meadows (78) found that microorganisms including bacteria, blue green algae, diatoms, and yeasts congregate and grow on marine and freshwater sand particles.

Clays are very common soil constituents and are readily transported into lakes and streams by wind and water erosion and are probably the most common and most extensively studied groups of suspended inorganic particulates. They characteristically exist as small particles (less than $2\mu\text{m}$) and so can remain in suspension in water for long periods of time.

Clays are crystalline hydrous aluminosilicates comprised of aggrates of layered "unit cells" (16). The clays used in this investigation (kaolinite, illite, vermiculite, and bentonite) were chosen to be representative of commonly occurring clay types. Two types of structural units make up the layers of the unit cells of clays. One layer is comprised of octahedral arrangements of oxygens and hydroxyls in which aluminum atoms are embedded, and the other type consists of tetrahedral arrangements of oxygens and hydroxyls containing silicon atoms (91). Kaolinite has a two layer unit cell (1:1 type) and the structure Si-Al. Thus, when these unit cells are aggregated as in a particle, a silicon layer is always strongly attached to an aluminum layer. The other three clays have a three layer unit cell of the 2:1 type where the structure is Si-Al-Si (37). Aggregates of these unit cells always have a silicon layer facing a silicon layer and are not bound together as tightly as the unit cells of the 1:1 clays. Therefore, water can hydrate the interlayers between the unit cells causing the lattice to expand. The degree of hydration and expansion is governed by the composition, bonding, and organization within and between the unit cells.

Another important characteristic of clays that varies with the composition, bonding, and organization within and between the unit cells, i.e. varies with

clay type, is the ability to exchange cations. This cation exchange ability results from broken bonds around the edges of the unit cells, charge imbalances in the lattice structure, and/or the hydrogen of exposed hydroxyl groups (37). The exchangeability of a cation varies mostly with the valence and the radius of the hydrated ion (135). Some ions replace others very readily but are difficult to remove once the exchange has taken place while other ions may attach only with great difficulty but are very easy to remove. A typical replacement series is as follows:



Because of a high ratio of surface area to volume and their ion exchange capabilities, clays can have profound effects on microbial metabolism.

Stimulation of bacterial growth by clays was first reported by Conn and Conn in 1940 (8). They attributed this stimulation to increased surface area, adsorption of harmful products of growth, and/or increased aeration in the presence of the flocculated colloid. Stotzky and Rem (119) found that kaolinite and montmorillonite served equally as a source of magnesium, sulfur, and/or nitrogen for the growth of Agrobacterium radiobacter. They also reported a stimulation of bacterial respiration and shortening of the lag phase of growth by montmorillonite with several species of Pseudomonas, Bacillus, Flavobacterium, Aerobacter, Proteus, and Escherichia coli. The stimulation was attributed to a buffering effect of the clays to changes in pH in the medium. Stimulation was observed by clay concentrations as low as 0.1% and increased with increasing clay concentrations up to 8%. In a later report (120), they showed that the respiration of mycelial homogenates of 27 fungal species representing 4 classes was generally not affected by pH nor by montmorillonite or kaolinite at concentrations below 4%. At montmorillonite concentrations above 4% and at kaolinite concentrations above 40% respiration was inhibited. The inhibition was related to viscosity of the systems which, in turn, influenced the rate of oxygen diffusion.

Investigations involving insoluble inorganic particulates other than clays have been very limited. Bigger and Nelson (4) reported stimulation of E. coli by several insoluble phosphates, sulfates, and silicates. They suggested that the stimulation was due to the concentration of nutrients by the insoluble particles.

Organic particulates, usually polysaccharide polymers relatively resistant

to degradation, can serve as both nutrient sources and in providing surface area around which microorganisms and nutrients may aggregate (16). Cellulose, pectin, chitin, and the extracellular polysaccharides of algae and bacteria are all relatively stable organic compounds that exist as suspended micro-particulates in natural aquatic ecosystems. Cellulose is β 1-4 linked poly D-glucose, pectin is a α 1-4 linked poly D-galacturonic acid, chitin is a β 1-4 linked poly N-acetyl-D-glucosamine, and the extracellular polysaccharides of algae and bacteria are highly variable polymers usually containing glucose, galactose, and/or mannose (47, 89). In photographs of Lake Erie water samples, Dugan et al (24) have shown associations of microorganisms and inorganic particles with the extracellular polymers of algae and bacteria. However, bacterial decomposition of chitin, cellulose, and lignin has been reported by several investigators (29, 126). Thus, while these compounds must surely play an important role in water ecology, their resistance to degradation or persistence as particles is relative and dynamic.

Other common organic particulates present in natural waters are living cells such as algae. Algae have been reported to cover several hundred square miles of water with a layer of suspended cells several feet thick (13). It is also well known that algae can have profound effects on other microorganisms in their environment. For example, pathogenic and coliform bacteria die out rather quickly in sewage oxidation ponds in which there is abundant algal growth (74). Antibiotic substances from algal cells and from algal cultures have also been reported (58, 105, 108).

Hence, there exists an abundance of naturally occurring particulates known to affect microbial metabolism in a variety of ways that could also affect bacterial oxidation and fixation of methane in the aquatic environment.

Biological Membranes

One of the most obvious and distinctive morphological characteristics of the methane oxidizing bacteria is the presence of complex systems in intracytoplasmic membranes. Before proceeding with a description of these membranes, however, a very cursory examination of biological membrane literature in general should be beneficial.

The idea of a distinct boundary membrane at cell surfaces originated in 1855 when Nageli and Cramer studied pigment penetration into intact and

damaged cells and concluded they were bounded by a plasma membrane. They further suggested that the osmotic properties of cells were due to this membrane. On the basis of permeability studies, Overton (86) reported that the plasma membrane contains lipids. Then Gorter and Grendel (35) extracted the lipids from red blood cell membranes, spread the extracted lipid as monomolecular film and found the lipid occupied twice the area of the membranes. They postulated that the lipid must exist as a bilayer with the hydrophobic parts of the lipid molecules facing inward. Danielli and Dawson (17) reported that membranes also contain protein. They postulated that this protein coats both sides of the lipid bilayer of Gorter and Grendel. With the development of electron microscopy, osmium fixed membranes were seen to exist as a 10 nanometer trilamellar unit with two dense lines separated by a region of low density; this was readily related to the lipoprotein sandwich of Danielli and Dawson. Because of the seeming universality of this structure, Robertson (102) proposed that all biological membranes have the same basic structure, the so called unit membrane theory. The Lipid-Globular Protein mosaic model of membrane structure was proposed by Lenard and Singer (72). This model suggests that hydrophobic portions of lipids (phospholipids) and a large fraction of the nonpolar amino acid residues of the protein are sequestered away from contact with water in hydrophobic interior of the membrane while the ionic groups of both the lipids and the proteins are in direct contact with water. The phospholipids in this mosaic model are primarily arranged in a bilayer form, but the ionic groups of the lipids are exposed directly to the aqueous phase, and the bilayer is not continuous. Recently, Singer and Nicolson (112) revised this concept to the fluid mosaic model of membrane structure. This theory describes membranes to exist basically as lipid structures wherein amphipathic proteins are found floating in fluid liquid matrix. This model has strong appeal in that it is thermodynamically sound and can explain certain phenomena that no other model explains. For example, membrane antigens can be observed to migrate to a uniform distribution over the new cell surface within a short time after two antigenically different cells fuse together. More recently, Singer (111) cited numerous reports published since he proposed the fluid mosaic model in 1972 establishing the mobility of molecular components in cell membranes. Thus, while our knowledge has increased concerning cell membranes, the newest ideas are not drastically different from the earlier proposals of Gorter and Grendel and Danielli and

Dawson. Membranes play many varied roles in biological systems. As was obvious very early but nevertheless remains very significant is the idea that membranes contain and wall in cell components isolating these components from the surrounding environment. Also recognized very early were the osmotic and permeability properties of cells which are regulated by membranes (Nageli and Cramer (80) and Overton (86). Membranes possess enzymes as an integral part of their structure that catalyze a variety of reactions including oxidations, reductions, electron transport, phosphorylation, active transport and synthetic reactions for cell components (14).

Intracytoplasmic Membranes of the Methane Oxidizing Bacteria

The first report that methane oxidizing bacteria contained intracytoplasmic membranes was in Whittenbury's (132) publication. He published two electron micrographs of thin sections of two of his isolates each showing a distinctive arrangement of intracytoplasmic membranes. The first thin section described was of his Methylosinus trichosporium isolate. He wrote one sentence describing these intracytoplasmic membranes as a tubular membrane system. Since this first description involving one photograph of one thin section, this organism has not been further described in the literature with respect to its intracytoplasmic membranes. The other organism described as possessing a lamellated membrane system in this report was a Methylabacter isolate. A report by Proctor et al. (96) soon followed in which they observed in Methylococcus capsulatus what Whittenbury had called a lamellar arrangement of intracytoplasmic membranes in his Methylabacter isolate. Additionally they described a peripheral intracytoplasmic membrane system in an unidentified methane utilizing isolate that was similar to the tubular system Whittenbury described for Methylosinus trichosporium. These investigators went on to point out the similarity between these intracytoplasmic membranes and those reported previously in photosynthetic bacteria and nitrifying bacteria; they speculated that the membranes probably play a role in the respiratory activity of the cells. Davies and Whittenbury (19) were the first to point out that methane oxidizing bacteria possessed one of two arrays of intracytoplasmic membranes. They either had the tubular membrane system consisting of pairs of membranes extending through the cytoplasm or near the cell periphery or they had the lamellar system comprised of vesicular discs organized into distinct bundles

Methylococcus minimus, Methylobacter vinelandii, Methylomonas vibrum, and Methylomonas albus contained the latter type membrane which they termed Type I membrane system. Connections between the plasma membrane and the intracytoplasmic membranes of Methylomonas were reported and is the only report of connections between these two membranes to date. Methylocystis parvis and Methylosinus sporium have the "tubular" type membrane arrangement which they called a Type II membrane system. Smith and Ribbons (115) described the intracytoplasmic membranes of Methanomonas methanoxidans. They reported these membranes were arranged in concentric layers near the cell periphery and existed as flattened sacs. Chemical analysis of these membranes revealed phosphatidyl chlorine as the major phospholipid with an 18:1 fatty acid accounting for over 90% of the total esterified fatty acids. Smith et al. (115) described the intracytoplasmic membranes of Methylococcus capsulatus as saccules limited by a 7.5 nanometer unit membrane arranged in stacked arrays.

Classification of Methane Oxidizing Bacteria

It has become obvious that the two main differences known to date to exist between methane oxidizing bacteria are the method of methane fixation and the type of membrane system they possess. Apparently the methane oxidizers with a Type II membrane system all incorporate methane via the serine pathway, while those that have a Type I membrane system fix methane by the allulose phosphate pathway. With the existing data, most known isolates of obligate methane oxidizing bacteria can be placed into one of these two broad groups. It should be emphasized that some of the data are sketchy and incomplete (e.g. Lawrence and Quayle (66) assayed for hydroxypuruvate reductase rather than serine hydroxymethyl transferase), however, the following is a reasonable categorization:

Group	Genus	Type Membranes	Hydroxy- Dyruvate Reductase	Hexose Phosphate Synthetase
A.	<u>Methylomonas</u>	I	-	+
	<u>Methylobacter</u>	I	-	+
	<u>Methylococcus</u>	I	-	+
B.	<u>Methylosinus</u>	II	+	-
	<u>Methylocystis</u>	II	+	-
	<u>Methanomonas</u>	II	+	+/-

3. MIXED CULTURE GROWTH STUDIES *

Aquatic ecosystems represent complex cultures of mixed populations of organisms. Therefore, mixed cultures were used to evaluate the effects of various parameters on microbial methane oxidation.

MATERIALS AND METHODS

The methane oxidizing bacteria used as inocula in this study were obtained by enrichment. One ml of lake water was added to 25 ml of N-1 mineral salts medium in a 74 ml serum bottle. The composition of n-1 medium in grams/1000 mls distilled water was as follows:
 KH_2PO_4 , 1.0; $\text{FeSO}_4 \cdot 7\text{H}_2\text{O}$, 0.01; NH_4NO_3 , 0.5; $\text{MgSO}_4 \cdot 7\text{H}_2\text{O}$, 0.2; $\text{MnCl}_2 \cdot 4\text{H}_2\text{O}$, 0.002; $\text{NaMnO}_4 \cdot 2\text{H}_2\text{O}$, 0.002; $\text{CaCl}_2 \cdot 2\text{H}_2\text{O}$, 0.01; $\text{CuSO}_4 \cdot 5\text{H}_2\text{O}$, 10^{-6} ; H_3BO_3 , 10^{-6} ; $\text{ZnSO}_4 \cdot 7\text{H}_2\text{O}$, 10^{-6} ; $\text{CoCl}_2 \cdot 6\text{H}_2\text{O}$, 10^{-6} ; pH 7.0. The bottle was sealed with a rubber serum stopper and 10 ml of 99.1% C.P. grade methane were injected with a syringe. The enrichment was incubated on a rotary shaker (21°C, 160 RPM) and transferred weekly. After several transfers this yielded a mixed population of Gram negative bacteria that oxidized methane quite rapidly and exhibited reproducible and predictable growth patterns. One ml of a 1 week culture was used to inoculate experimental vessels.

Chlorella vulgaris, Anacystis nidulans (Meyers), and Anabaena variabilis were obtained from the Department of Microbiology, The Ohio State University. Schizothrix calcicola (Drouet) was isolated from western Lake Erie. The algae were grown in medium N-1 to which sodium citrate (0.01 gm/liter) and sodium carbonate (0.02 gm/liter) were added. Three ml of a 2 week culture were used as inocula when required.

Kaolinite was obtained from the Georgia Kaolin Co. while the illite, bentonite, and vermiculite were obtained from the Agronomy Department, The Ohio State University. Characteristics of the clays are shown in Table 1. All were washed in 0.5 N NaOH to remove organic material. The diatomaceous earth was a commercial preparation from Johns-Manville called Celite, the cellulose was a preparation used in chromatography called Avicell, and the chitin was obtained from National Biochemicals Corporation. The polysaccharide exopolymers of Anacystis nidulans and Zoogloea ramigera were prepared in this

* Previously published as Ref. No. 128

TABLE 1

Values showing size distribution (%) and cation exchange capacity (milliequivalents/100 grams) for four different clay types.

Clay	C.E.C. * meg/100 gms	Size Distribution (%)		
		2 m	2-50 m	50 m
Kaolinite	9.7	45.6	54.3	0.1
Illite	24.6	36.7	63.0	0
Vermiculite	70.6	30	51.25	18.75
Ventonite	74.5	36.95	60.65	2.4

* Cation Exchange Capacity

laboratory by ethanol precipitation (90).

Experiments were performed in 74 ml serum bottles fitted with rubber serum stoppers. Additions were made to the bottles, and N-1 medium was used to bring the volume to 25 ml. After removing 2 ml of air through the rubber stopper with a needle and syringe, 2 ml of 99.1% methane were injected to start the experiments. The vessels were incubated on a rotary shaker (21°C, 160 RPM). Periodically, 100 μ l gas samples were withdrawn with a gas tight syringe and were analyzed for methane and carbon dioxide by gas chromatography. 100 μ l of N-1 medium were then injected into the bottles to replace the gas removed. Methane was added to the bottles at a rate equivalent to its uptake in order to maintain a concentration in the bottles of about 1.7 μ M/ml.

Chromatography was carried out with a Carle Model 8004 gas chromatograph equipped with 100 K ohm thermistor detectors. The column was 1/8 inch O.D. by 8 ft stainless steel packed with 50/60 mech silica gel. C.P. Grade helium at 20 ml/min was used as the carrier gas. Operating temperature was 60°C.

RESULTS AND DISCUSSION

Previous reports on interactions between clays and microorganisms have shown that clays can profoundly affect microbial growth (15, 119). The effects of various concentrations of kaolinite on the oxidation of methane by bacteria are shown in Figure 1. The kaolinite enhanced methane uptake by (a) decreasing the lag phase of growth, (b) by increasing the total methane consumed, and (c) by increasing the rate of methane oxidation. While all quantities of kaolinite enhanced methane uptake, the 4.0% suspension resulted in greatest stimulation; therefore the 4.0% concentration was used in subsequent experiments. No adsorption of methane by the clays could be detected in the controls although this does not preclude the possibility that some adsorption took place.

Figure 2 compares the effects of various types of clays on methane oxidation. It can be seen that there is no significant difference in the resulting effects although all stimulated methane uptake. This suggests that cation exchange capacity is not the primary cause of the observed methane oxidation enhancement. However, the data in Figure 3 suggest a surface phenomenon of some kind is involved because the smaller size vermiculite particles having a greater surface area per unit volume elicited a greater

stimulation than the larger size kaolinite particles. The observed methane oxidation enhancement by the clays can be explained in a variety of ways. The decreased lag phase of growth is probably due to the increased rate of methane oxidation. The rate increase may be due to the removal of a metabolic inhibitor or repressor either by adsorption to the clays or by other bacteria, or the clays may render the methane or oxygen more readily available to bacterial metabolism. The increase in total methane oxidized may also be due to either the removal of an inhibitor or repressor, or possibly conversion of methane to end products that are less oxidized than CO_2 , i.e. alcohol, aldehyde, or acid.

The significance of methane oxidation stimulation can best be shown in Figure 4. This experiment more nearly represents the situation that exists in the natural environment. That is, methane oxidizing bacteria would be continually growing and would be exposed to varying concentrations of clay particulates due to surface runoff and/or dispersion of bottom sediments through wind and wave action. Therefore, kaolinite was injected into an actively growing culture of methane oxidizing bacteria. The results show the utilization rate of methane doubled at the time of clay addition and the total methane uptake increased. It can be concluded that suspended clay minerals will increase the methane oxidized and thereby the methane carbon retained in an aquatic ecosystem.

Since clay minerals so greatly enhanced methane oxidation, it was thought that perhaps other naturally occurring relatively insoluble inorganic compounds might function similarly. The compounds tested were silica, ferrous phosphate, calcium phosphate and calcium carbonate. The results shown in Figure 5 reveal a variety of responses. Silicious remains a diatoms (celite) produced a slight stimulation of methane uptake. Ferrous phosphate had no significant effect, and the calcium carbonate and calcium phosphate nearly completely inhibited methane oxidation. In an attempt to explain the inhibition observed with the calcium compounds, the effects of various concentrations of calcium chloride were examined. However, the results revealed no inhibition of methane oxidation had occurred until the calcium chloride concentration reached 1.0% which suggests that the observed inhibition caused by insoluble calcium compounds was not due to solubilized calcium ions.

The diverse results observed with these insoluble inorganic particulates remains unexplained but is probably related to the surface chemistry of the individual chemical species of these particles. Nevertheless, it can be postulated that the type of non-clay insoluble inorganic particulates existing

in a body of water can have an important effect on retention of methane carbon in water.

Having observed widely varying magnitudes and types of effects on methane oxidation with the inorganic particles, similar studies were conducted with naturally occurring organic materials. The organic particulates tested included cellulose, chitin, and the extracellular polysaccharide polymers produced by Anacystis nidulans and Zoogloea ramigera. The results shown in Figures 6 and 7 reveal that none of the compounds tested stimulated methane uptake. By comparing the CO₂ evolution to methane uptake it is evident that the organic particles are degraded with varying rapidity by microorganisms in the enrichment culture. This degradation resulted in rapid production of carbon dioxide in the experimental vessels which was the probable reason for the observed inhibition of methane oxidation. In this instance carbon dioxide rather than methane is produced from the organic compounds because the experimental vessels, like most naturally occurring waters near the surface, are aerobic. Any effects in a natural ecosystem such as those observed in these experiments would be of relatively brief duration since the organic particles would disappear through microbial degradation to either soluble forms or to bottom sediments. This is not to say that these compounds have no effect on methane recycling, but rather than serving as particulates to effect methane oxidation, the most pronounced effect would be to serve as carbon sources, either directly or indirectly for the production of methane in the anaerobic bottom sediments.

In view of the results described in the preceding section with the organic materials, it was thought that living cells would act as organic particulates that would act as organic particulates that would not be susceptible to rapid microbial degradation. Algae, which are known to exist during blooms in Lake Erie in layers several feet thick and covering hundreds of square miles, were chosen as the experimental living particulates. Four species of algae selected were chosen to be representative of types known to exist in large numbers during algal blooms.

Figure 8 shows the effects of constantly illuminated algae upon methane oxidation. Varying degrees of inhibition were observed with 3 of the algae, whereas Schizothrix had no effect on methane uptake. It was also evident from control experiments that algal cells alone do not take up detectable quantities of methane. With time a gradual disappearance of methane oxidation inhibition was observed. This was paralleled by a drastic decrease in numbers of algae

and reflects unfavorable conditions for algal growth in the experimental bottles. The several days of inhibition observed before algal numbers declined would be representative of the situation that exists in a natural aquatic ecosystem with an actively growing population of algae.

Opaque bottles were used to determine whether similar effects could be observed when the algae were not exposed to light (i.e. non-photosynthesizing). The results shown in Figure 9 reveal that only Anacystis retained its inhibitory effects in the absence of light. The Chlorella slightly stimulated methane uptake in the dark, although it is impossible to say whether this was due to a particulate effect or a chemical effect from some algal cell derivative. Thus, except for Anacystis the algae must be exposed to light to be inhibitory.

Cell free culture medium from which the algae had been removed by centrifugation after four weeks growth was substituted for the algae to test for an extracellular inhibitory substance. Once again methane oxidation inhibition was observed with the Anacystis indicating that the inhibitory effects were due either to a secreted substance or an algal cell derivative. These results are presented in Figure 10. The Anacystis cell free culture medium was lightly yellow green and tested strongly positive for anthrone sugar and ninhydrin nitrogen. When extracted with cold 5% trichloroacetic acid (TCA), the inhibitory substance was in the cold TCA soluble fraction. The color and solubility in cold TCS suggest the possibility of a pigment compound as the inhibitory substance although it could also be a sugar, amino acid, or simple metabolic intermediate.

The extracellular inhibitory compound also explains the inhibition observed with Anacystis when incubated in the dark. There was enough of the inhibitory substance already present in the inoculum to produce the observed effects. However, the inhibition observed only with illuminated cultures of Anabaena and Chlorella is more difficult to explain. There have been previous reports of extracellular antibiotic substances from algae that require light activation through a photooxidation of the inhibitory compounds (58). If this were the situation, however, the cell free culture medium would be expected to be inhibitory since it was incubated in the light. Thus, it seems that the inhibition observed in the light with Chlorella and Anabaena may have been due to an extracellular substance that was degraded once outside the cell. Therefore only when the algae were actively photosynthesizing and the substance was being continually produced could the inhibition be observed.

Regardless of the explanation, certain algae have marked inhibitory effects upon the oxidation, fixation, and recycling of methane.

It is evident from the preceding results that the particulate material present in a body of water determines to a large extent how much methane will be oxidized and retained in that aquatic ecosystem. This in turn greatly influences carbon accumulation in the ecosystem which will at least partially govern the rate of eutrophication. This means that if man could select what type of particulates were present in a body of water, he could partially control the rate of eutrophication in that ecosystem. While this investigation was by no means exhaustive, some suggestions for practical application can be drawn from it.

One of the more important controls that can be effected is to encourage land management practices that result in decreased runoff of clay minerals. This will help prevent carbon retention due to clay enhancement of methane fixation.

Considering another aspect, if other factors were equal, it would be advantageous to build a reservoir in an area that drains a soil with large quantities of apatite (a calcium phosphate) rather than to drain an area of high clay content. More extensive studies of mineral particulate involvement would undoubtedly lead to similar conclusions for inorganic particles and would provide a much more complete picture of their involvement in methane recycling.

Another interesting speculation would be the seeding of lakes with algae known to inhibit methane oxidation. Algae would inevitably develop in the water, so this would be an attempt to select beneficial types. Theoretically, this would result in lower methane carbon retention in the ecosystem and a lower rate of eutrophication.

Thus, by "particulate management" we might be able to at least partially control the eutrophication rate of a body of water.

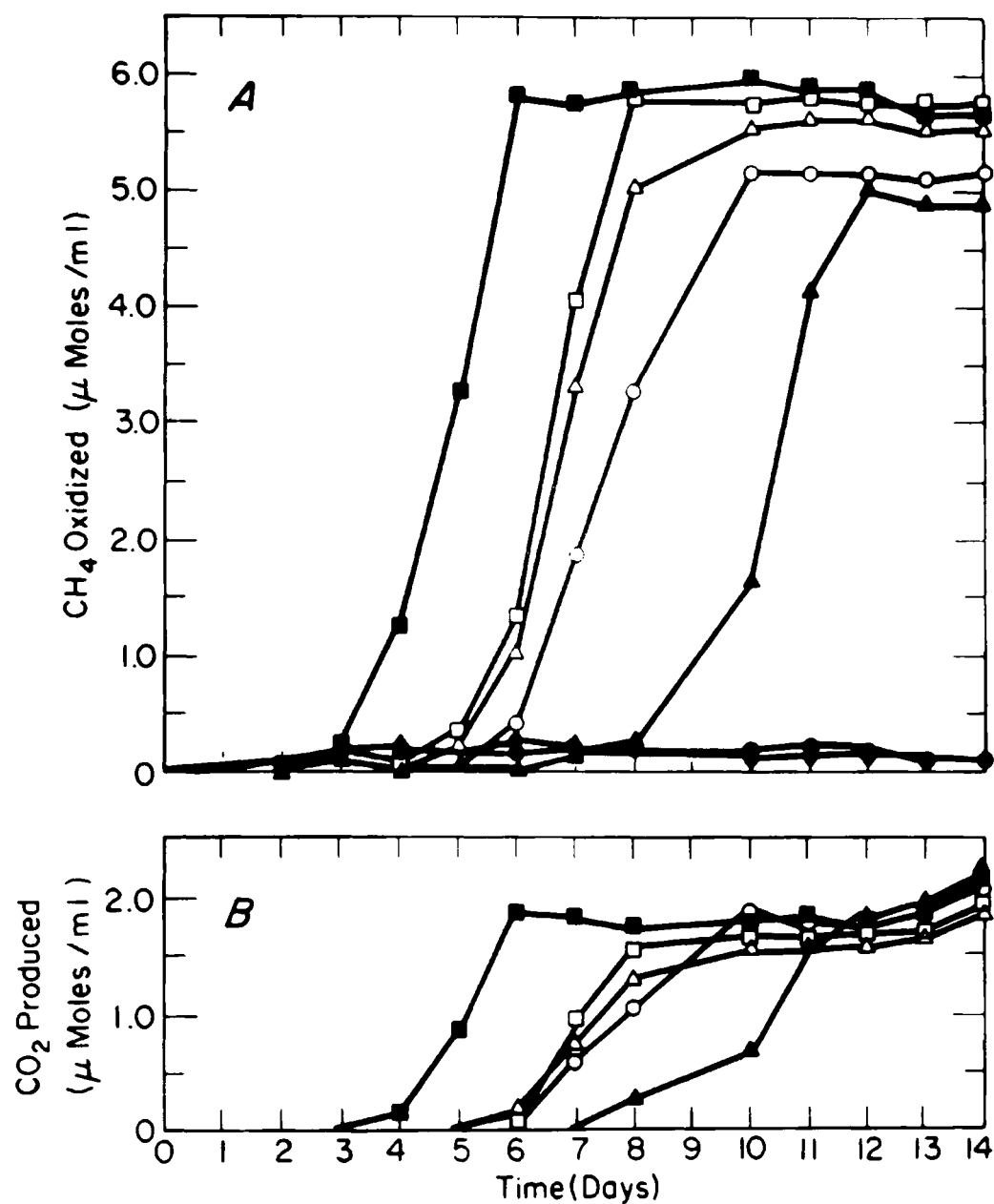


Figure 1. Curves showing (A) methane oxidized and (B) carbon dioxide produced by a mixed bacterial population versus time of incubation. Curves represent different kaolinite suspension concentrations.

- Control-sterile medium (n-1)
- ◆ Medium plus 4.0% kaolinite
- ▲ Medium plus cells
- Medium plus cells 4.0% kaolinite
- Medium plus cells plus 0.4% kaolinite
- △ Medium plus cells plus 0.04% kaolinite
- Medium plus cells plus 0.004% kaolinite

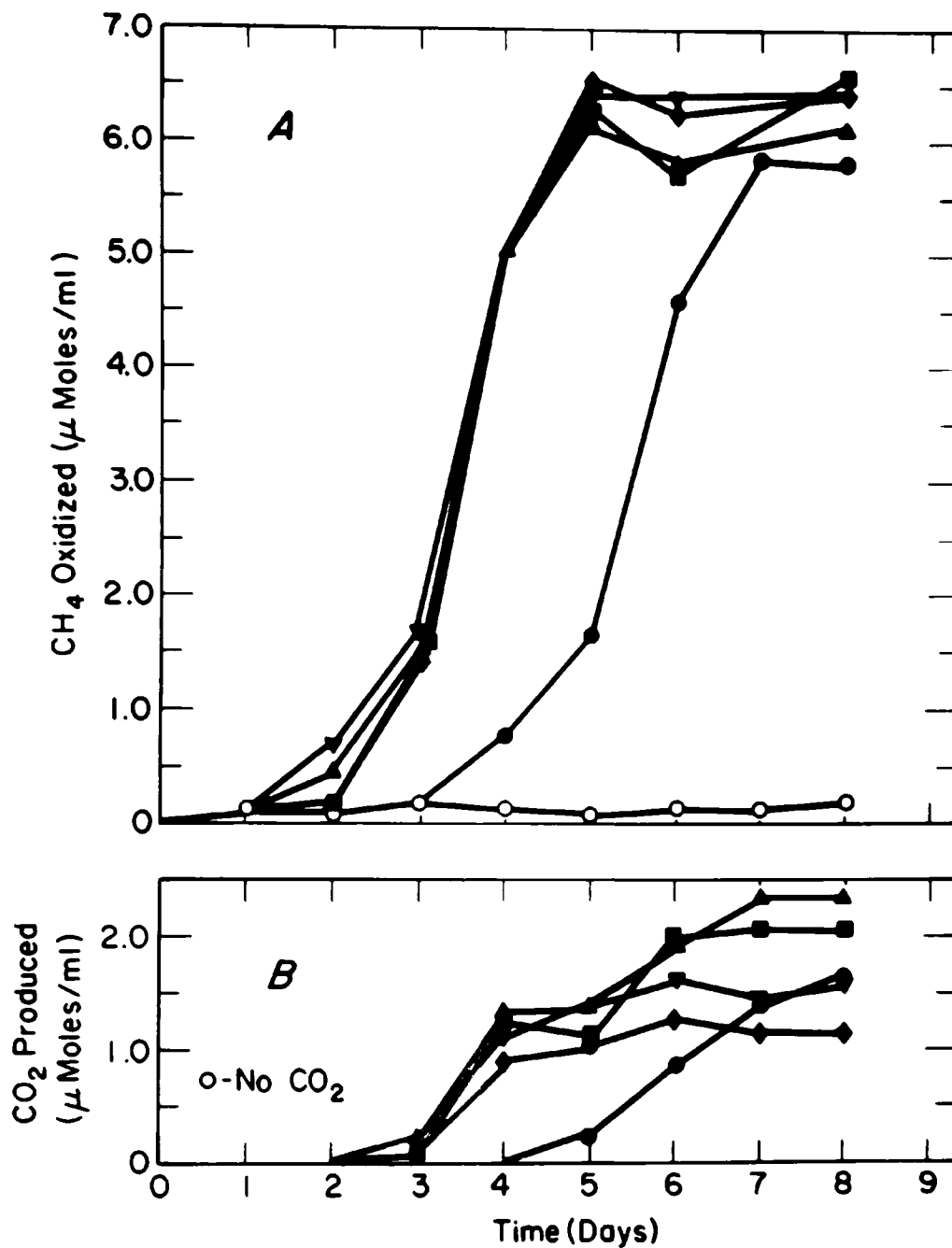


Figure 2. Curves showing (A) methane oxidized and (B) carbon dioxide produced by a mixed bacterial population versus time of incubation. Curves represent a 4.0% concentration of different clay types.

- Control-sterile medium (N-1)
- Medium plus cells
- ▲ Medium plus cells plus kaolinite
- Medium plus cells plus illite
- ◆ Medium plus cells plus vermiculite
- ▼ Medium plus cells plus bentonite

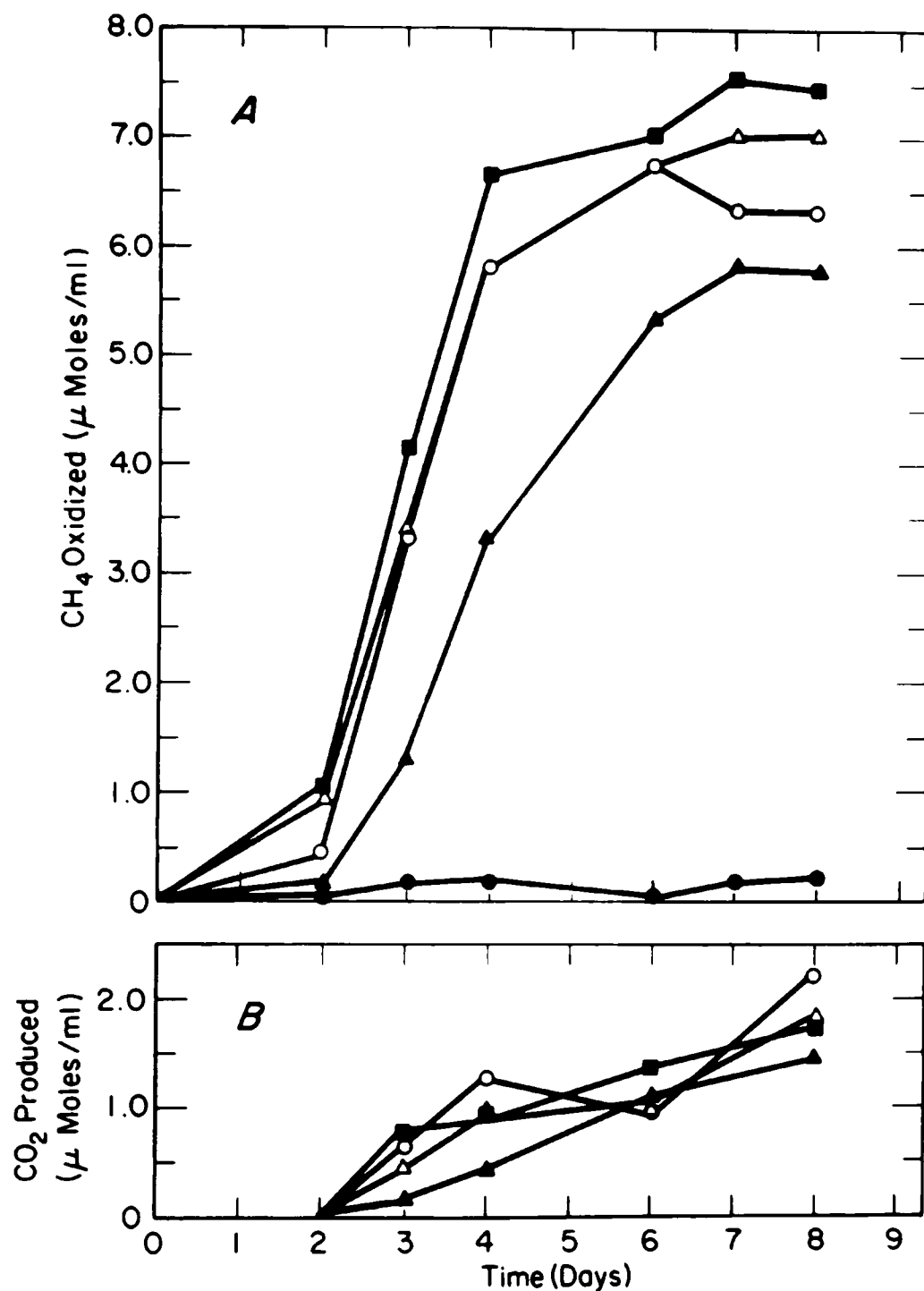


Figure 3. Curves showing (A) methane oxidized and (B) carbon dioxide produced by a mixed bacterial population versus time of incubation. Curves represent a 4.0% concentration of different size vermiculite particles.

- Control-sterile medium (N-1)
- ▲ Medium plus cells
- Medium plus cells plus less than 1 μm size particles
- Medium plus cells plus 2-50 μm size particles
- △ Medium plus cells plus greater than 50 μm size particles

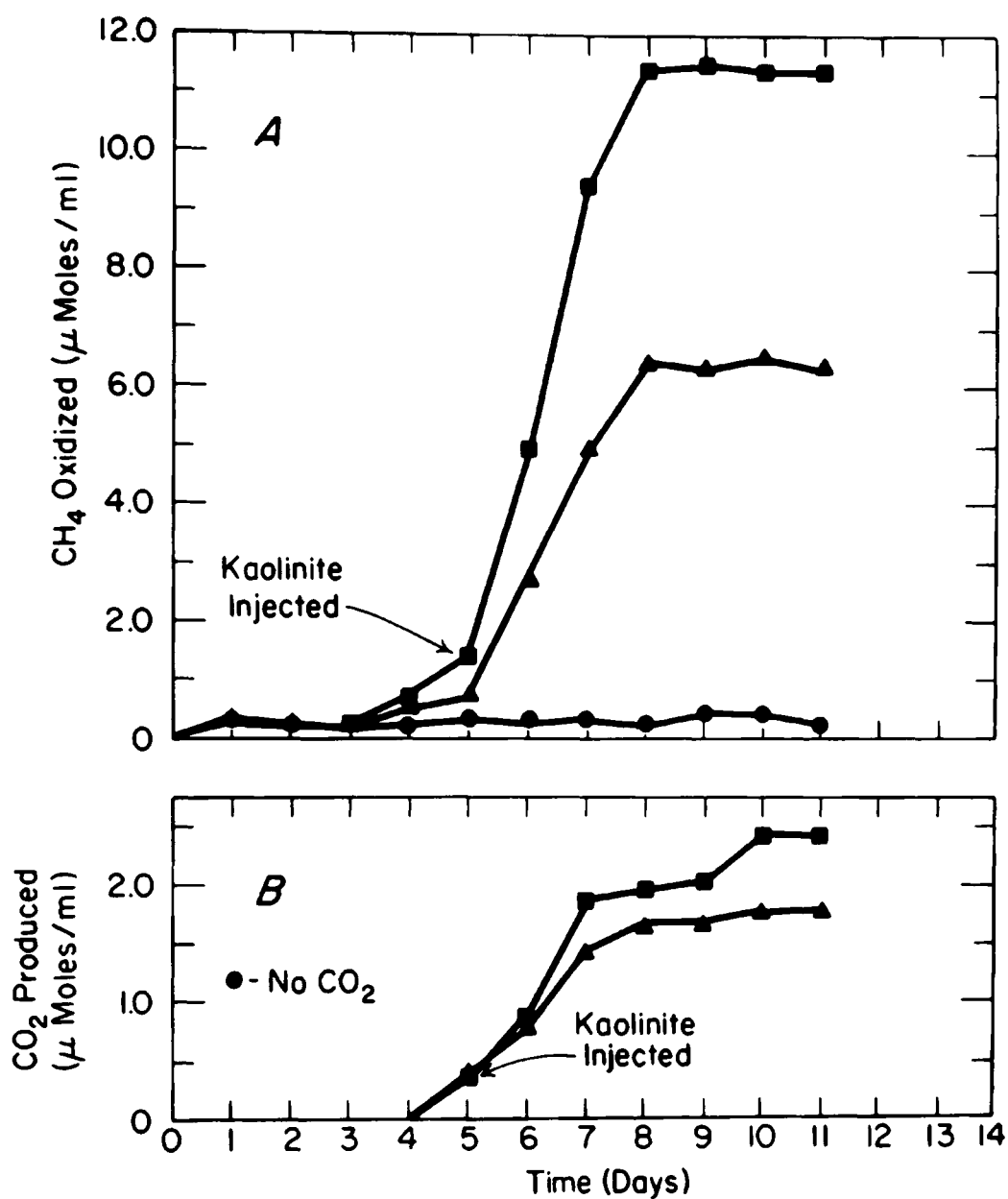


Figure 4. Curves showing (A) methane oxidized and (B) carbon dioxide produced by a mixed bacterial population versus time of incubation. Curves show the effects of the addition of kaolinite (4.0%) to actively growing cells.

- Control-sterile medium (N-1)
- ▲ Medium plus cells
- Medium plus cells to which kaolinite was added on the fifth day

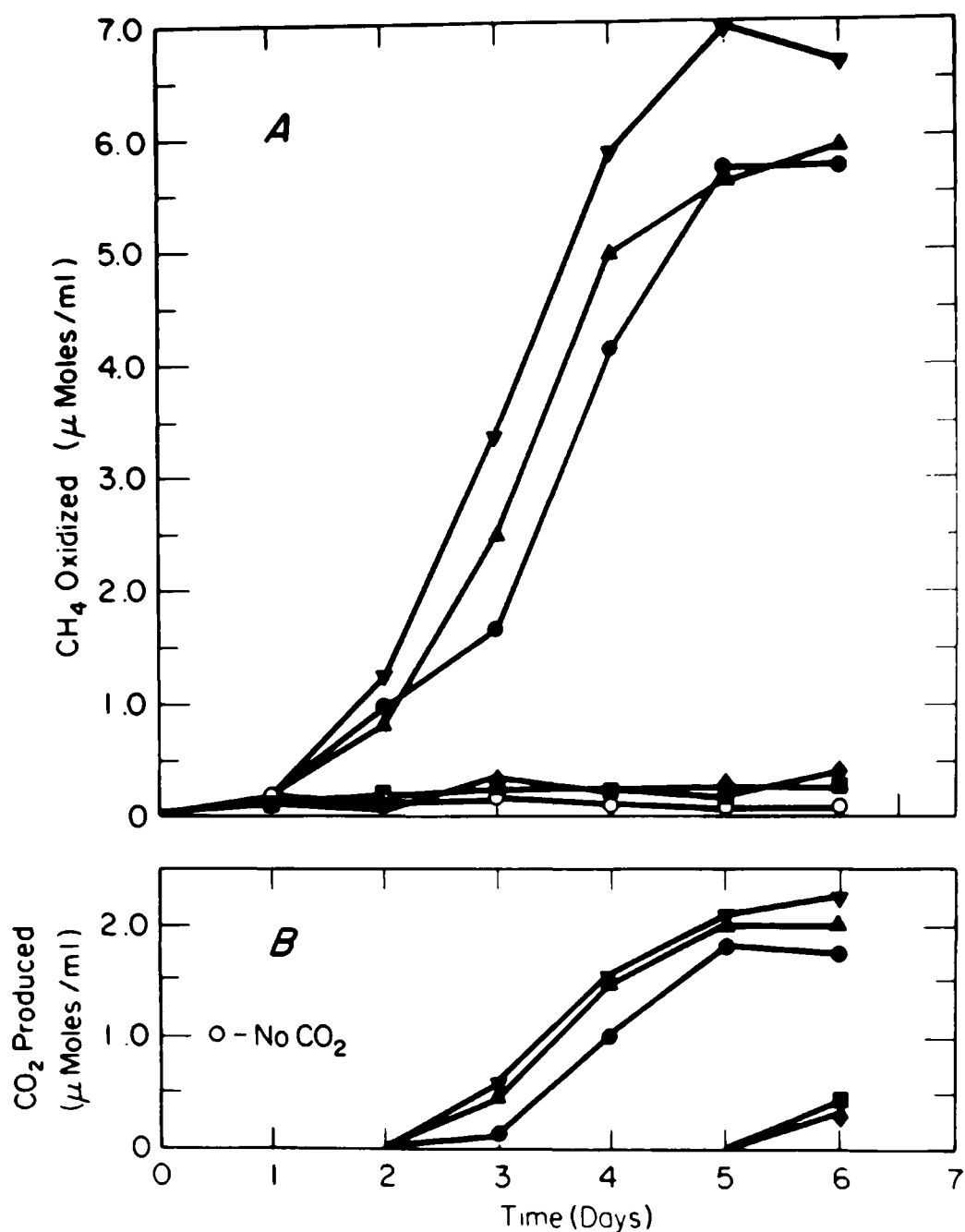


Figure 5. Curves showing (A) methane oxidized and (B) carbon dioxide produced by a mixed bacterial population versus time of incubation. Curves represent a 4.0% concentration of various types of insoluble inorganic particulates.

- Control-sterile medium (N-1) and Medium plus Fe₃(PO₄)₂, Ca₃(PO₄)₂, CaCO₃, or celite
- Medium plus cells
- ▲ Medium plus cells plus Fe₃(PO₄)₂
- Medium plus cells plus Ca₃(PO₄)₂
- ◆ Medium plus cells plus CaCO₃
- ▼ Medium plus cells plus celite

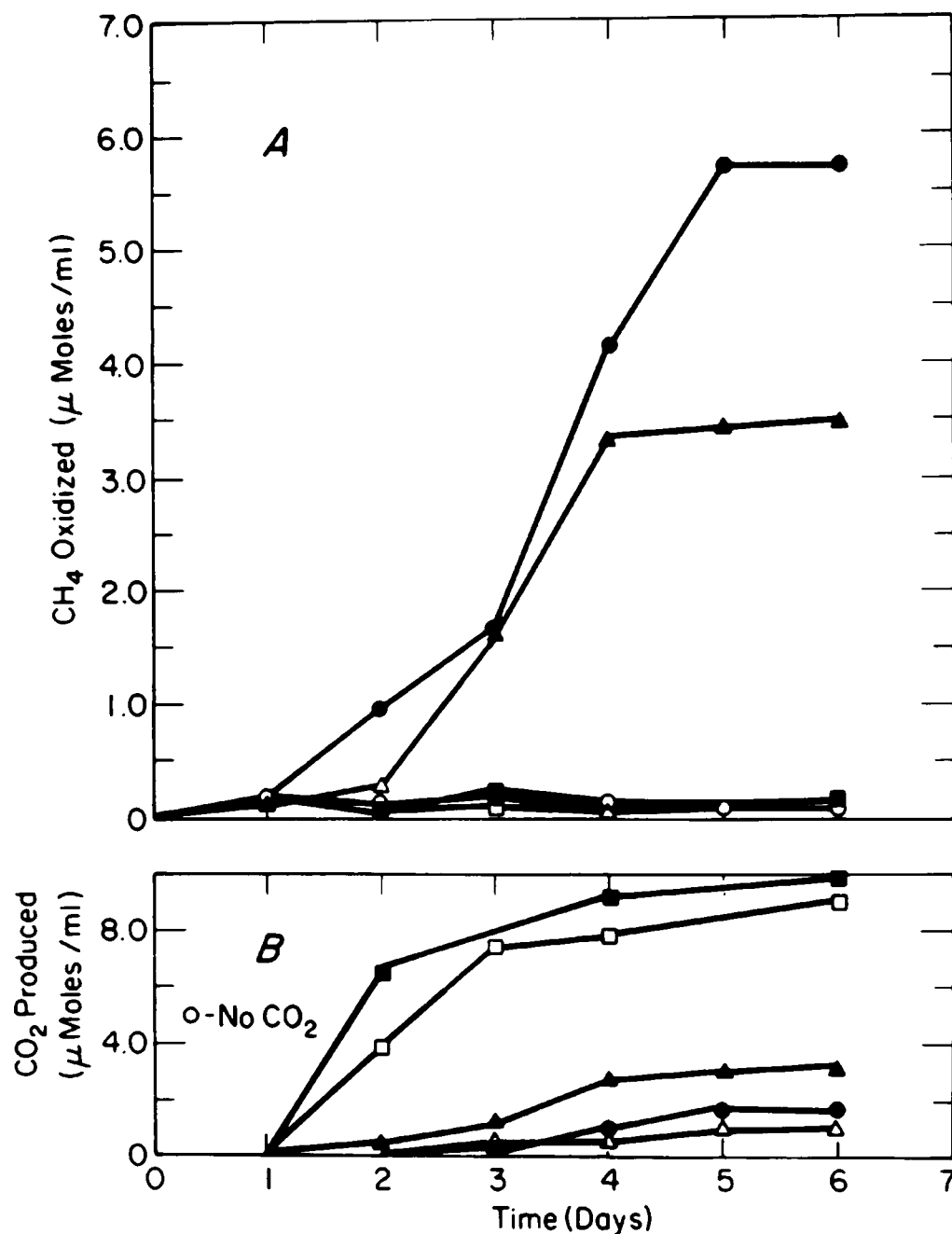


Figure 6. Curves showing (A) methane oxidized and (B) carbon dioxide produced by a mixed bacterial population versus time of incubation. Curves represent a 4.0% concentration of various types of insoluble organic particulates.

- Control-sterile medium (N-1)
- Medium plus cells
- △ Medium plus cellulose
- ▲ Medium plus cells plus cellulose
- Medium plus chitin
- Medium plus chitin plus cells

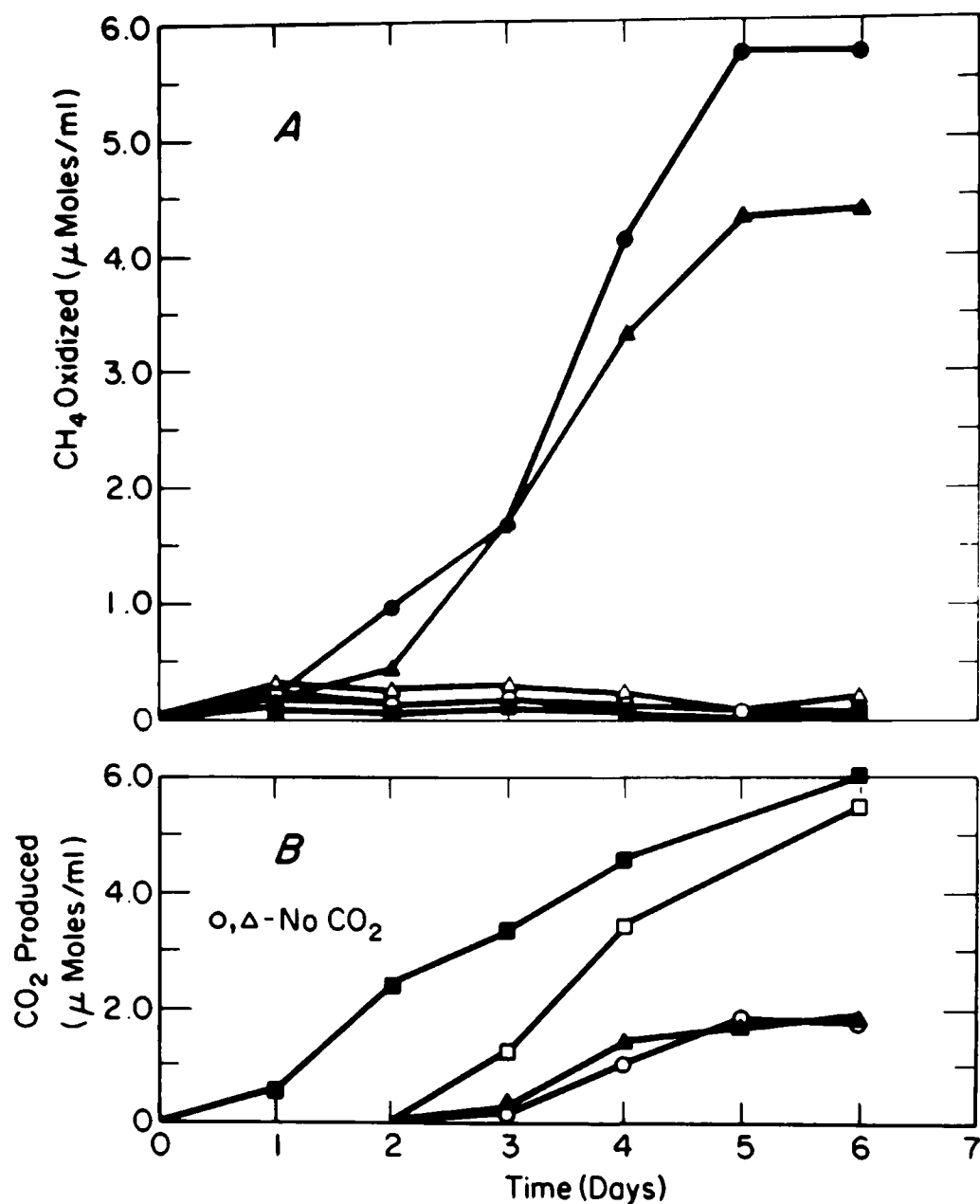


Figure 7. Curves showing (A) methane oxidized and (B) carbon dioxide produced by a mixed bacterial population versus time of incubation. Curves represent a 0.4% concentration of extracellular polysaccharide polymers.

- Control-sterile medium (N-1)
- Medium plus cells
- △ Medium plus *Anacystis* exopolymer
- ▲ Medium plus *Anachstis* exopolymer plus cells
- Medium plus *Zoogloea* exopolymer
- Medium plus *Zoogloea* exopolymer plus cells

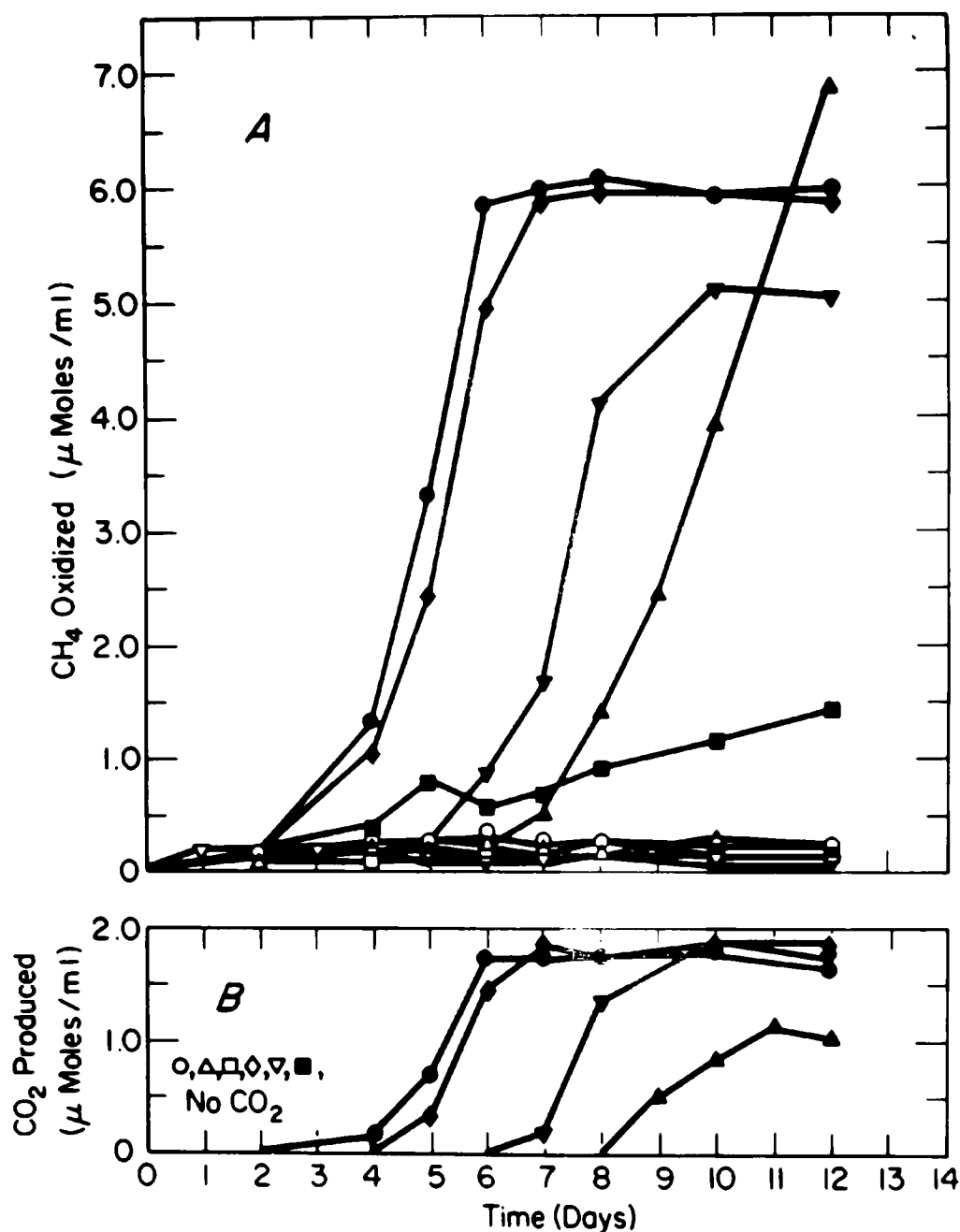


Figure 8. Curves showing (A) methane oxidized and (B) carbon dioxide produced by a mixed bacterial population versus time of incubation. Curves represent 3.0 ml of various algae under constant illumination.

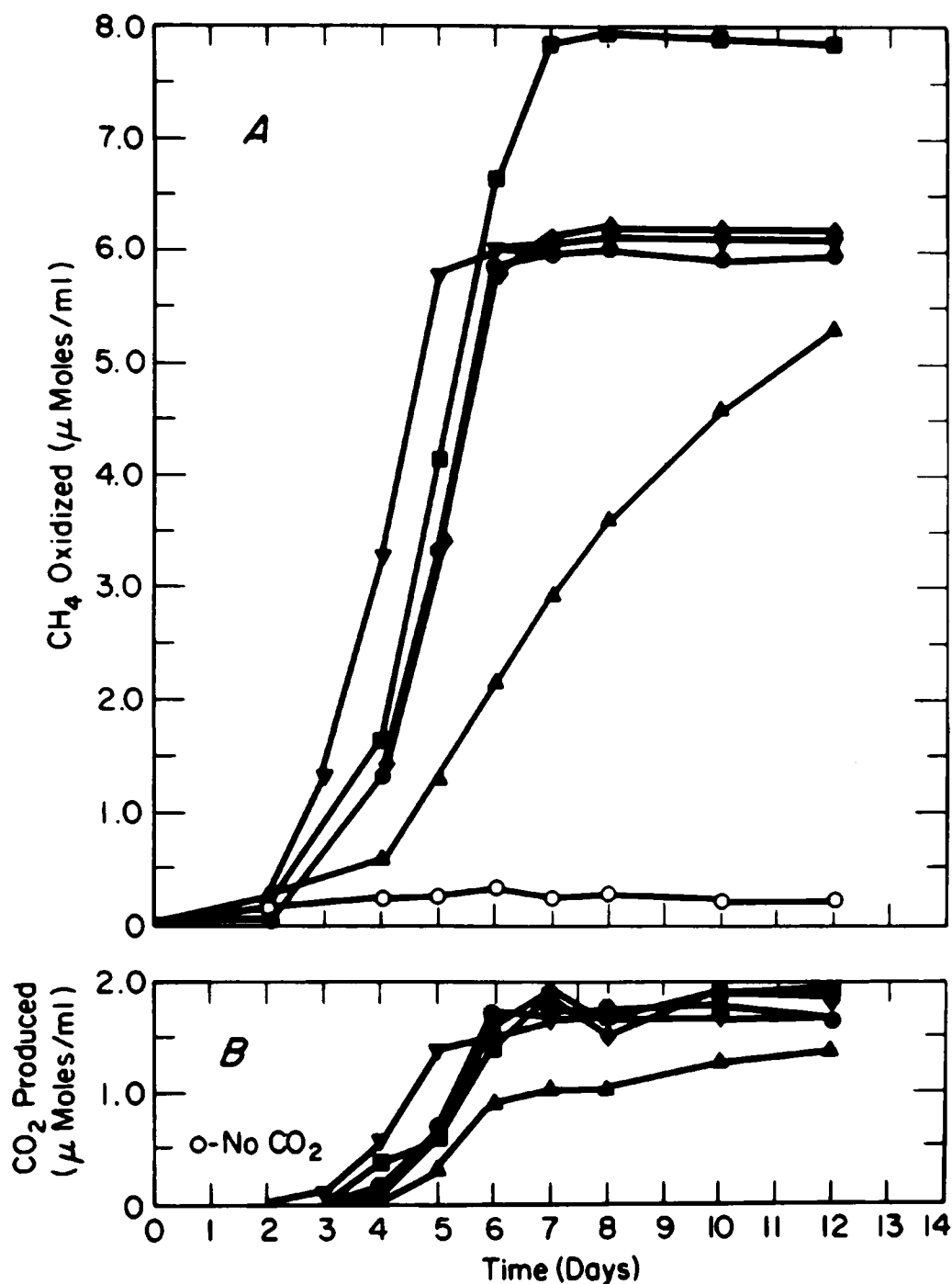


Figure 9. Curves showing (A) methane oxidized and (B) carbon dioxide produced by a mixed bacterial population versus time of incubation. Curves represent 3.0 ml of various algae incubated in the dark.

- Control-sterile medium (N-1)
- Medium plus cells
- ▲ Medium plus cells plus *Anacystis nidulans*
- Medium plus cells plus *Chlorella vulgaris*
- ◆ Medium plus cells plus *Schizothrix calcicola*
- ▼ Medium plus cells plus *Anabaena variabilis*

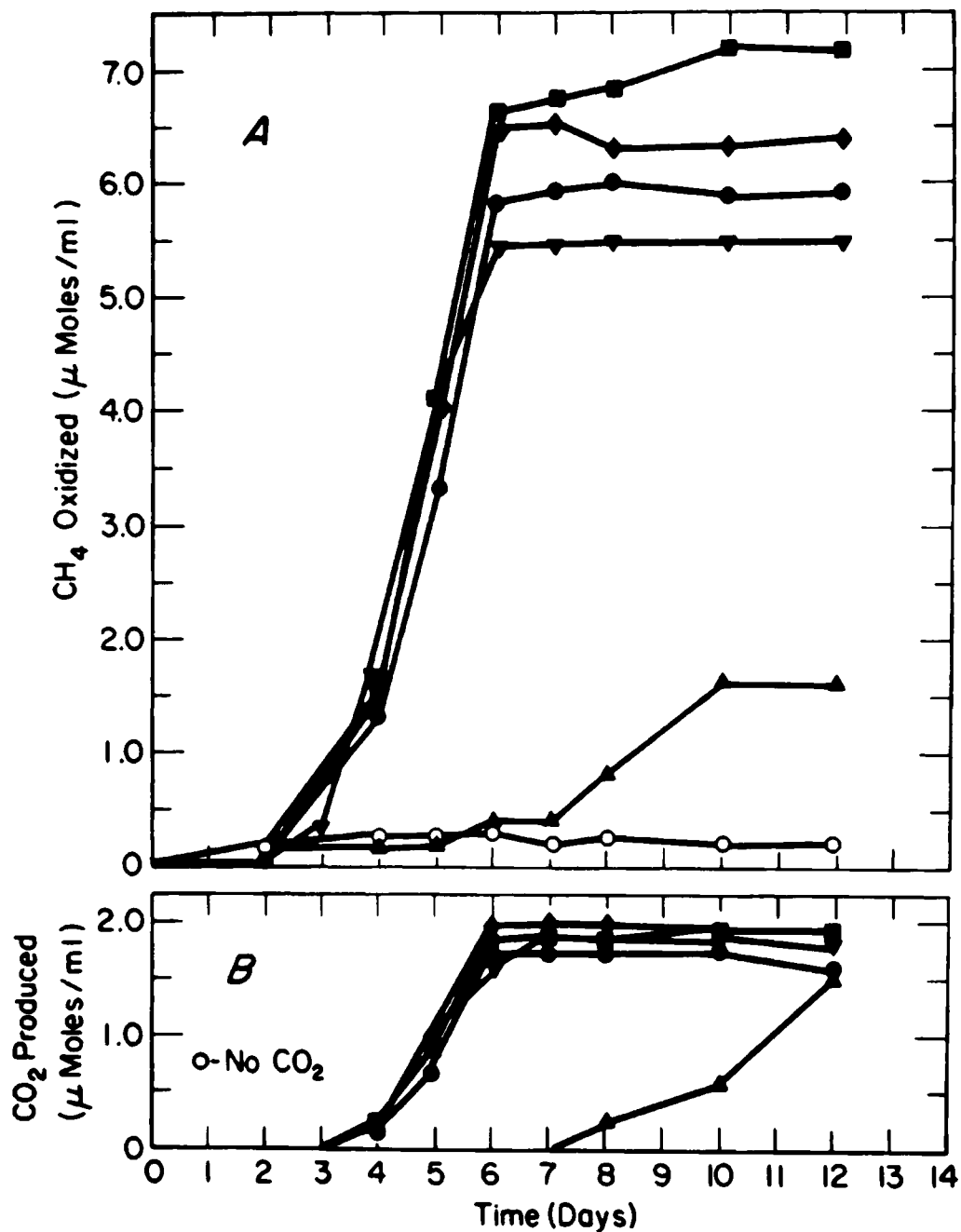


Figure 10. Curves showing (A) methane oxidized and (B) carbon dioxide produced by a mixed bacterial population versus time of incubation. Curves represent 3.0 ml of various cell free algal culture media..

- Control-sterile medium (N-1)
- Medium plus cells
- ▲ Medium plus cells plus *Anacystis nidulans* cell free culture medium
- Medium plus cell plus *Chlorella vulgaris* cell free culture medium
- ◆ Medium plus cells *Schizothrix caliciocla* cell free culture medium
- ▼ Medium plus cells plus *Anabaena variabilis* cell free culture medium

4. PURE CULTURE GROWTH STUDIES

Pure Culture studies were done to more accurately elucidate certain growth characteristics of a methane oxidizing bacterium. This information was compared to mixed culture growth and was related to ecological effects.

MATERIALS AND METHODS

A defined mineral salts culture medium was developed by combining various components of similar published media in an attempt to minimize undesirable precipitates and labor while providing a satisfactory medium for culturing methane oxidizing bacteria. The composition of this combined medium (medium CM) is listed in Table 2. The pH of the medium was adjusted to 7.0 following which the medium was dispensed as required and autoclaved for 20 minutes at 121 C. and 15 lbs/in² pressure. If a solid medium was desired, 2% Difco purified agar was added prior to sterilization.

The OB3b of Methylosinus trichosporium a lake water isolate was kindly provided by Dr. Roger Whittenbury, University of Warwick, Coventry. This isolate was used for pure culture studies because very little research had been done with type II methane oxidizers, particularly with this genus.

Cultures were maintained in both liquid medium and on solid medium and could be readily transferred from one to the other. Liquid cultures were kept in rubber stoppered 74 ml serum bottles containing 25 ml CM medium. Inoculations were made by injecting culture fluid through the rubber stopper with a sterile syringe. After inoculation, 10 ml of 99.1% methane (Matheson Gas Co.) were injected into the bottles using a sterile syringe equipped with a Swinney filter. The filter contained a 0.22 micrometer pore membrane filter (Millipore) to sterilize the injected methane. The bottles were agitated on a rotary shaker at 2 cycles/sec. Cultures were also maintained on CM plates by standard techniques. The plates were incubated in desiccators filled with methane and air (1:1). Incubation of all cultures was at 21 C.

Methylomonas methanica was isolated for comparative purposes in morphological studies. An enrichment culture was obtained by inoculating water from Lake Erie into a serum bottle followed by injecting methane into the bottle and incubating several weeks as described previously. This culture enriched in methane oxidizing bacteria was used to inoculate culture tubes containing 10 ml of CM medium. The culture tubes were stoppered with cotton and incubated in

Table 2. Components of mineral salts medium CM
listed in grams per liter of distilled water.

KNO_3	1
$\text{MgSO}_4 \cdot 7\text{H}_2\text{O}$	2×10^{-1}
CaCl_2	2×10^{-2}
$\text{FeSO}_4 \cdot 7\text{H}_2\text{O}$	1×10^{-2}
Na_2HPO_4	2.3×10^{-1}
NaH_2PO_4	7×10^{-2}
$\text{CuSO}_4 \cdot 5\text{H}_2\text{O}$	5×10^{-6}
H_3BO_4	1×10^{-5}
$\text{MnSO}_4 \cdot \text{H}_2\text{O}$	7×10^{-6}
$\text{ZnSO}_4 \cdot 7\text{H}_2\text{O}$	7×10^{-5}
MoO_3	1×10^{-5}

desicators as described previously. After several weeks, a reddish pink pellicle was obvious on the surface of the medium. A loopful of the pellicle was streaked onto CM agar plates from which isolated pink colonies could be picked. These colonies consisted of motile rod shaped bacteria that would not grow on nutrient agar. Based upon the method of isolation, the requirement for methane, and the morphology and pigmentation of the bacteria, this isolate was identified as Methylomonas methanica.

Large quantities of bacteria were grown in a Fermentation Design Model SA30-FLS 30 liter fermenter containing 15 liters of CM medium. The fermenter was modified so that the head space could be evacuated and filled with a glass wool filtered methane:air (1:1) gas mixture. The broth was stirred at one revolution per second and incubated at 21 C. After a week, cells were harvested using a Sharples continuous flow centrifuge.

Methylosinus trichosporium was tested for the ability to grow heterotrophically on 19 different carbohydrates; Bacto Differentiation Disks (Difco) were used for this purpose. For determining fermentative capacity, the disks were transferred septically to cotton stoppered culture tubes containing 10 ml of sterile CM medium, gas indicator tubes, and 0.04% bromocresol purple. The tubes were then inoculated with 0.2 ml of a 5 day culture and incubated at 21 C. The tubes were checked for acid and gas after 4 hours, 24 hours, and 1 week. In order to determine capacity for aerobic growth on the carbohydrates, the differential disks were aseptically transferred to plates of CM agar that had been heavily swabbed with culture. Incubation was aerobic at 21C and observation was at the above times.

Methylosinus trichosporium was tested for ability to grow on 20 different amino acids. For this purpose, sterile CM agar plates containing 0.5% amino acids were streaked with bacteria, and the plates were incubated aerobically or anaerobically (i.e. in CO₂ incubator at 21 C.). After 2 weeks the plates were examined for growth. Sodium salts of formate, acetate, propionate, and butyrate were tested.

In view of the fact that Methylosinus trichosporium was incapable of growth on 43 organic compounds tested, several of these compounds were tested for their ability to affect methane oxidation in any manner. Serum bottles containing 10⁻² Molar concentrations of various previously tested organic compounds in CM medium were prepared; pH was re-adjusted to 7 prior to sterilization by addition of 0.1 N HCl or 0.1 N NaOH. One ml of bacterial inoculum (Final

concentration 1.8×10^7 cells/ml) was injected into each bottle. This was followed by 2 ml of 99.1% sterile methane injected to start the experiment. Incubation was at 21 C. on a rotary shaker (2 cycles/second).

Since these bacteria could not be enumerated by plate count, a standard curve was prepared for rapid spectrophotometric estimates of cell numbers. Various dilutions through 10^{-4} were made of a cell suspension. The optical density of each dilution was read at 420 nm with a Gilford Model 2400 Recording Spectrophotometer and a cell count was done using a Petroff-Hauser counting chamber. Cell number was plotted against optical density to obtain a standard curve from which subsequent estimations of cell numbers could be made.

Fifteen identical serum bottles were prepared each of which contained 25 ml CM medium and bacterial inoculum (Final concentration 1.8×10^7 bacterial/ml). Two ml of 99.1% methane were added to each bottle to start the experiment. Incubation was at 21 C. on a rotary shaker (2 cycles/second). Samples were removed at various times; at each sampling the pH was measured using a Corning pH meter and cell numbers were determined spectrophotometrically as described previously.

The ratio of methane, oxygen, and nitrogen consumed to carbon dioxide produced by a cell suspension was determined. After adding 0.1 mg (wet weight) of cells to 25 ml CM medium, 2 ml 99.1% methane were added to start the experiment. Gas samples were withdrawn periodically and were analyzed by gas chromatography. After withdrawing a sample, an equal volume of sterile medium was injected into the bottle.

Gas samples were analyzed using a Carle Model 8004 gas chromatograph equipped with a 100K ohm thermistor detector. For analysis of methane and/or carbon dioxide, an 8 ft x 1/8 in, 50-60 mesh silica gel column was used. For analysis of oxygen, nitrogen, and methane a 12 ft x 1/8 in, 100-120 mesh molecular sieve column was used. In both cases column temperature was 80 C and helium was the carrier gas. Carrier gas was maintained at 18 ml/min with the silica gel column and at 12 ml/min with the molecular sieve column.

RESULTS AND DISCUSSION

Methylomonas methanica formed round pink colonies on CM agar and a red-pink pellicle in liquid CM medium. The bacteria were 0.7×1.5 micrometer

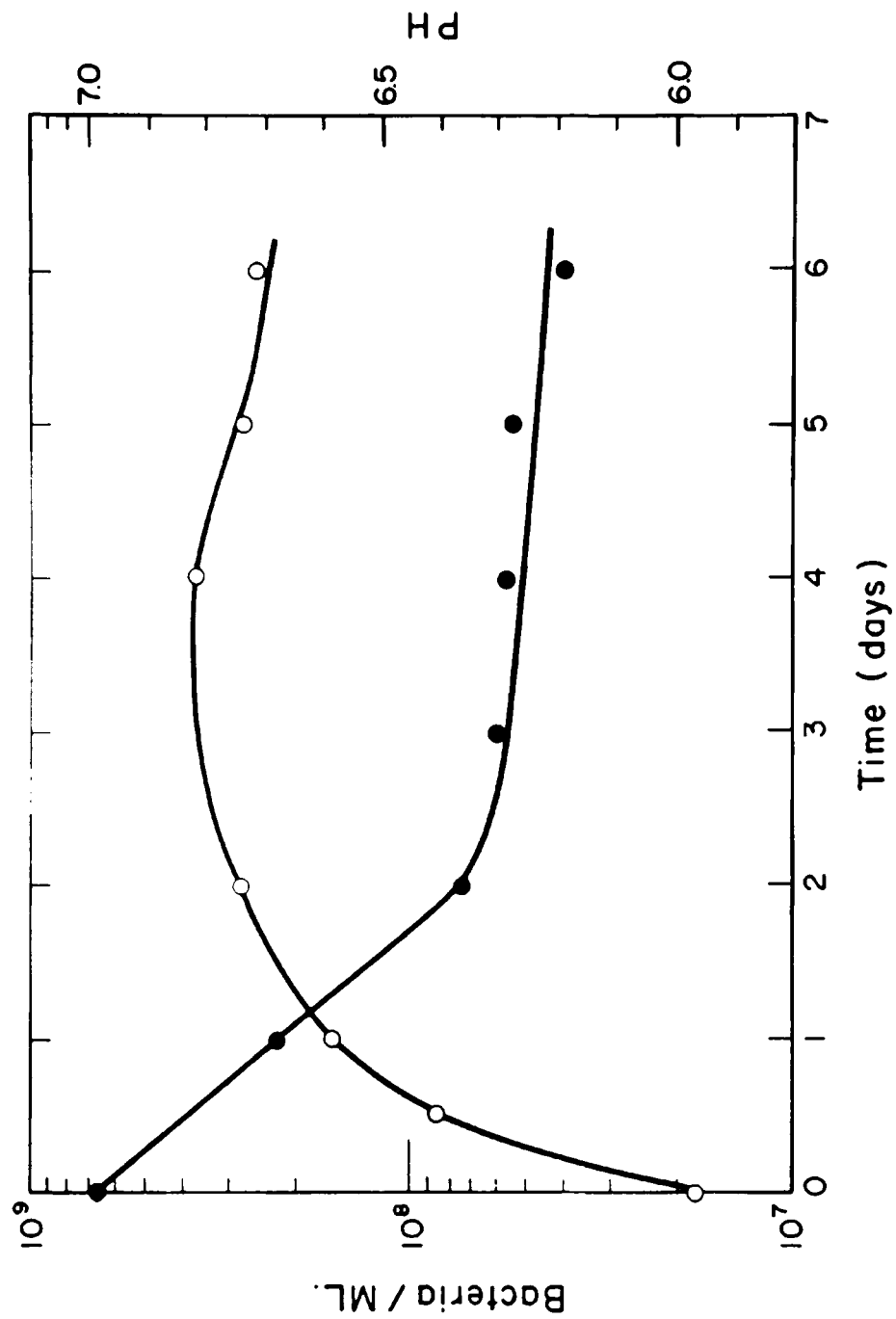


Figure 11. Growth curve for Methylosinus trichosporium cultivated in liquid CM medium at 21 C. and pH 7.

○ growth curve
● pH

rods. This bacterium formed a very thick (i.e. 1/2 inch) pellicle in enrichment cultures, but formed only a thin film on the surface of the medium in pure culture. By microscopic examination, the pellicle formed by the enrichment cultures appeared to consist almost entirely of Methylobacterium methanica; however, other bacteria in the pellicle were obvious when the culture was plated on nutrient agar. Thus, the thick pellicle did not seem to result from proliferation of other bacteria in the enrichment, rather, relatively few of these bacteria seemed to stimulate M. methanica to produce the thick pellicle.

Relatively light growth of Methylobacterium trichosporium was also observed on both liquid and solid media. For example, it took about 3 weeks for colonies to reach 1 millimeter in diameter on CM agar plates; in liquid culture, yields of 0.2 gm/liter (wet weight) were observed. If the growth of M. trichosporium in mixed culture is analogous to Methylobacterium methanica, the rates and quantities of methane oxidation may even be greater in the natural environment where mixed populations of bacteria are in maximum. This raises some question as to the relevance of pure culture studies and conclusions drawn from such studies as they relate to growth in the natural habitat. However, this cannot prevent continuance of pure culture studies since they are essential for controlled experiments; nevertheless, one should keep these shortcomings in mind.

The growth response of M. trichosporium in CM medium is illustrated in Figure 11. The curve resembles a typical bacterial growth curve. The gradual decline in pH in the medium is probably due to carbon dioxide production since formic acid did not accumulate. However, since a complete analysis of the post-growth medium was not done, the possibility of some other acidic product can not be ruled out. As is evident in the growth curve, bacterial numbers declined after the fifth day. For this reason, culture transfers were made weekly. If culture transfer was delayed longer than 2 weeks, there was an excessive lag period prior to the appearance of visible growth. This was apparently due to cell die off after the first week as suggested by the growth curve. Estimations of growth parameters can be obtained from these data. The logarithmic growth phase is restricted to the time period prior to 24 hours growth and probably even to less than 12 hours. Since there may be a lag phase in this growth response, rates calculated from these data may be slightly lower than actually exists.

Logarithmic phase bacteria growth can be represented by the following function:

TABLE 3

Organic compounds tested for the ability to
support growth of Methylosinus trichosporium.

<u>Carbohydrates</u>	<u>Amino Acids</u>	<u>Organic Acids</u>
adonitol	alanine	acetic acid
arabinose	asparagine	butyric acid
dulcitol	aspartic acid	formic acid
glactose	cysteine	propionic acid
glucose	glutamic acid	
inositol	glycine	<u>Alcohols</u>
insulin	histidine	butanol
levulose	hydroxproline	ethanol
maltose	isoleucine	methanol
mannitol	lisine	propanol
mannose	methionine	
melibiose	ornithine	
raffinose	phenylalanine	
rhamnose	proline	
salicin	serine	
sorbitol	threonine	
sorbose	tryptophane	
trehalose	tyrosine	
xylose	valine	

$$N = N_0 e^{ct}$$

N represents the number of bacteria at time t, N_0 is the number of bacteria at time zero, and C is a growth constant. By using the numbers of bacteria at time 0 and 12 hours in the growth curve as an approximation of logarithmic growth, the growth constant was calculated to be 0.1312 hours⁻¹. By knowing the growth constant, bacterial numbers at any time during logarithmic growth can be predicted, and bacterial generation time can be calculated. By definition, $N = 2N_0$ for N in the general equation and taking the natural log of both sides, the following equation was obtained:

$$\ln 2 = (0.1312 \text{ hours}^{-1})(GT)$$

Solving this equation for GT, the generation time was found to be 5.3 hours. This is somewhat longer than the 3 hour generation time reported by Vary and Johnson (125) for a mixed culture of methane oxidizing bacteria and may simply reflect the pure versus mixed culture growth. Alternatively, M. trichosporium may have an intrinsically longer generation time than the bacteria of Vary and Johnson. The value corresponds closely with the report of Whittenbury (132) of generation times around 5 hours for Methylosinus isolates.

Whittenbury (133) examined M. trichosporium for its ability to utilize 7 amino acids, 11 carbohydrates, and 7 organic acids as sole carbon and energy sources. He found that the organism was unable to grow on any substrates tested except methane or methanol. The results of a more extensive nutritional screening study involving 19 carbohydrates, 19 amino acids, 4 alcohols, and 4 organic acids were all negative; no growth was observed under aerobic or anaerobic conditions with any of the compounds listed in Table 2 nor was growth observed on methanol. This latter observation probably reflects a strain difference between the M. trichosporium used in this study and that tested by Whittenbury. Therefore, this organism appears to be an obligate methylotroph incapable of growth on any substrate other than methane. This does not imply inability of this organism to metabolize other organic compounds.

Figure 12 illustrates the effects of various organic acids on methane oxidation by M. trichosporium; Figure 13 shows effects of various amino acids; Figure 14 represents the effects of two pentoses; Figure 15 shows effects of several hexoses. These data show a general enhancement of methane oxidation

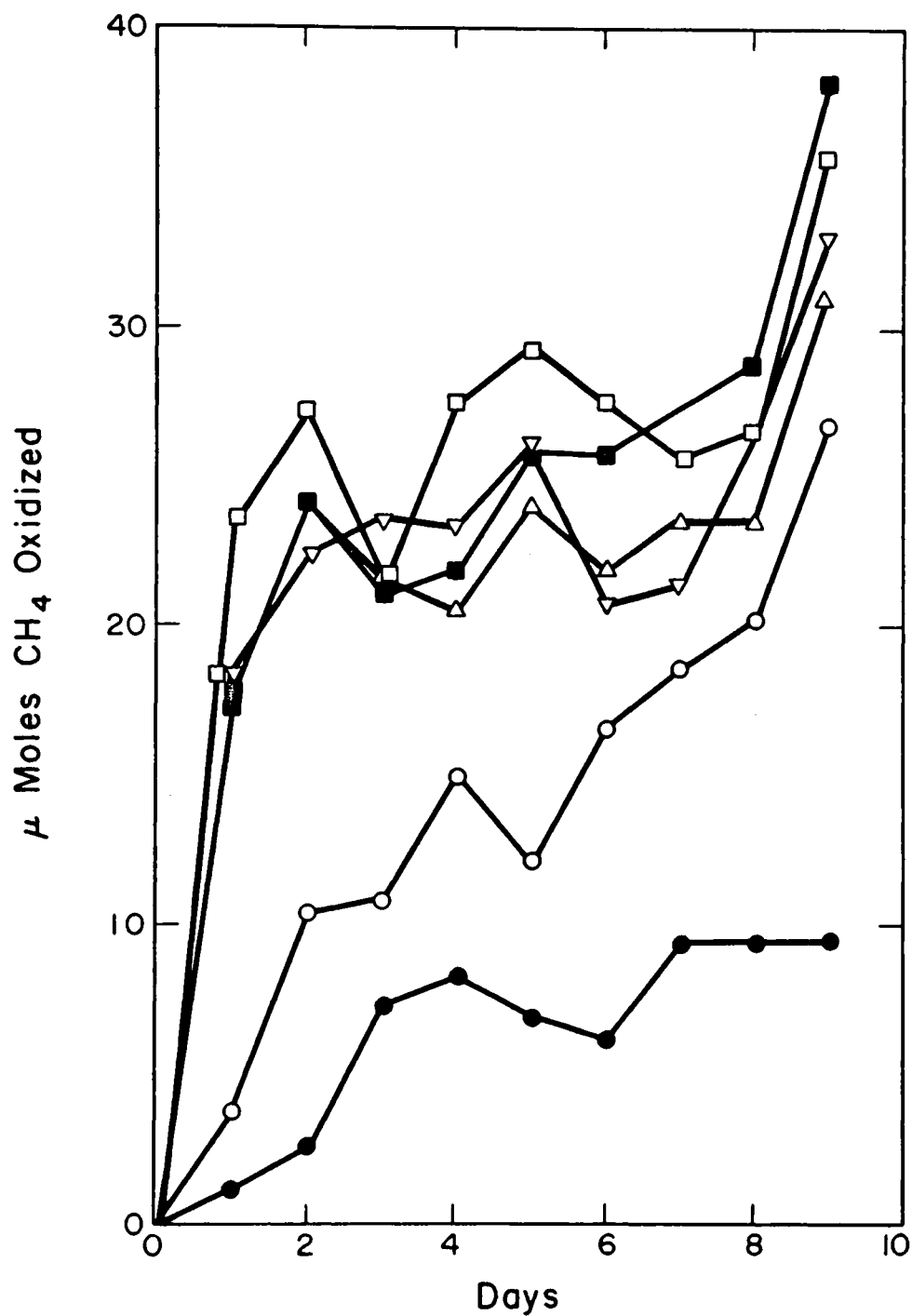


Figure 12. Curves showing micromoles of methane oxidized by Methylosinus trichosporium. Curves represent $10^{-2}M$ concentrations of various organic acids.

- Control-sterile CM medium
- Medium + cells
- Medium + cells + sodium formate
- ▲ Medium + cells + sodium acetate
- Medium + cells + sodium propionate
- ▽ Medium + cells + sodium butyrate

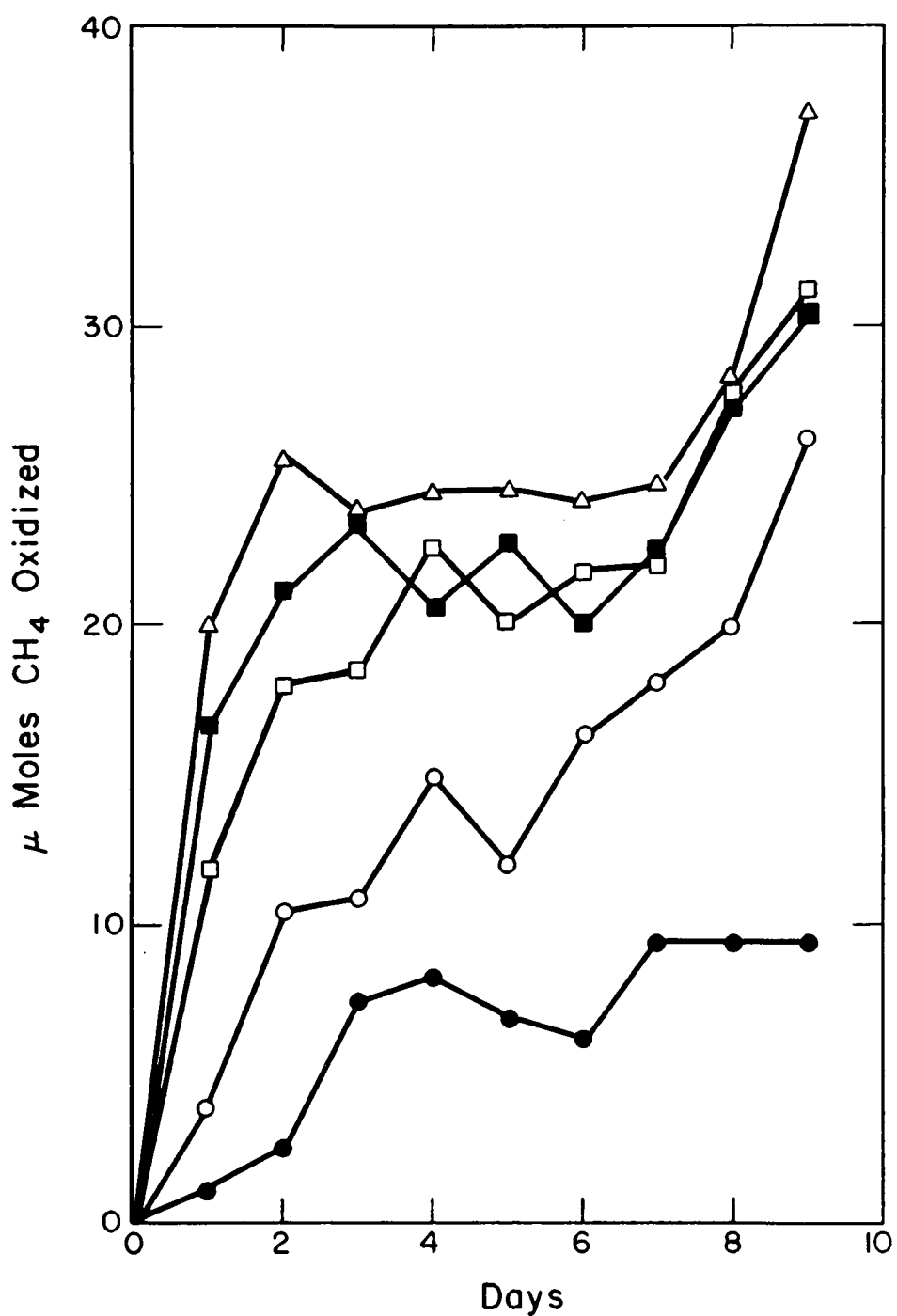


Figure 13. Curves showing micromoles of methane oxidized by Methylosinus trichosporium. Curves represent 10^{-2} M concentrations of various amino acids.

- Control-sterile CM medium
- Medium + cells
- △ Medium + cells + serine
- Medium + cells + alanine
- Medium + cells + glutamic acid

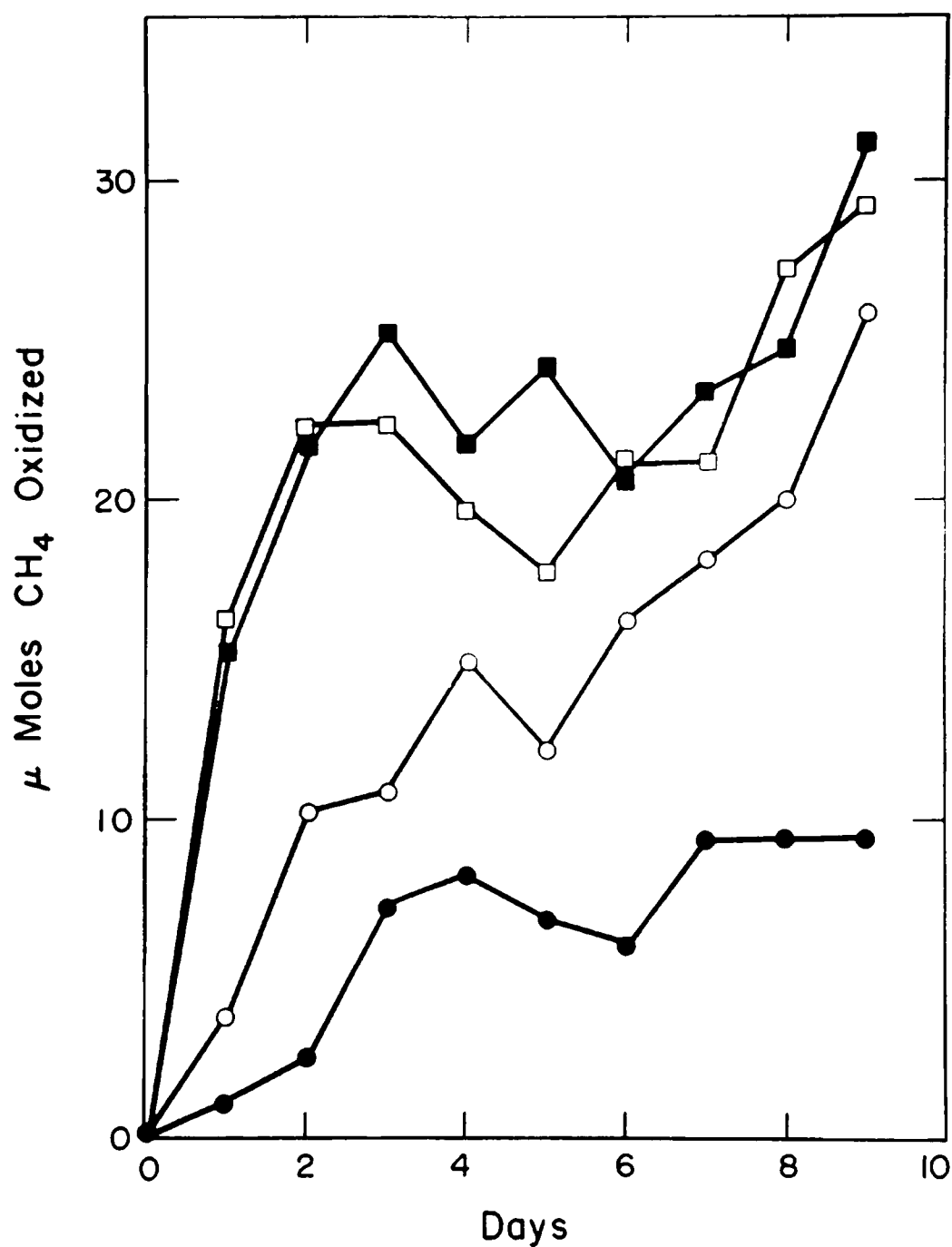


Figure 14. Curves showing micromoles of methane oxidized by Methylosinus trichosporium. Curves represent 10^{-2} M concentrations of various pentoses.

- Control-sterile CM medium
- Medium + cells
- Medium + cells + arabinose
- Medium + cells + xylose

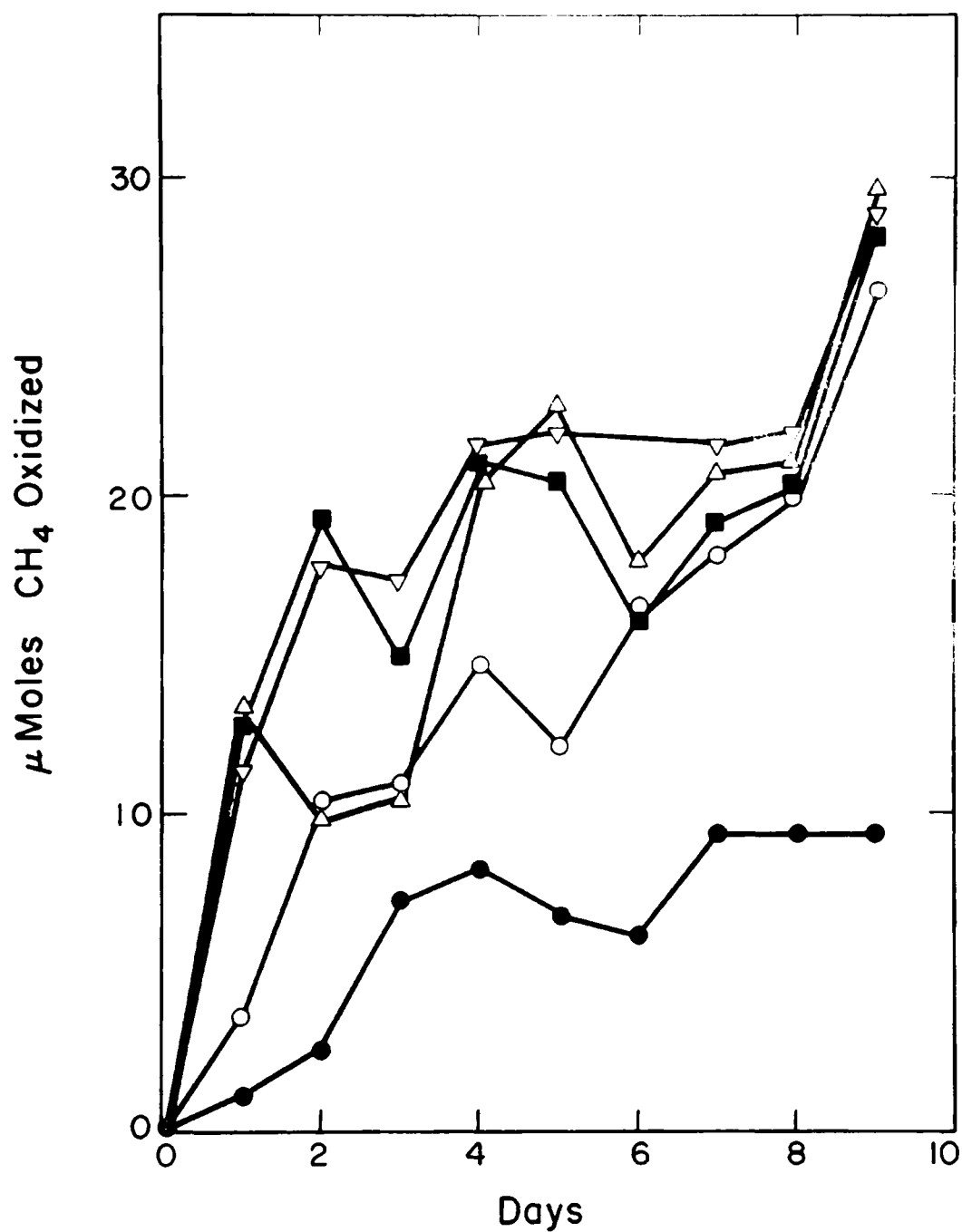


Figure 15. Curves showing micromoles of methane oxidizing by Methylosinus trichosporium. Curves represent 10^{-2} M concentrations of various hexoses.

- Control-sterile CM medium
- Medium + cells
- Medium + cells + glucose
- △ Medium + cells + galactose
- ▽ Medium + cells + mannose

by the organic compounds. This enhancement appeared as an increased initial rate of methane oxidation and a greater total amount of methane oxidized. All the graphs have general similarities. The bottles containing only cells oxidized methane at a relatively steady rate while the bottles to which organic compounds were added showed more rapid initial methane oxidation leveling off to some lesser rate. The organic acids elicited the greatest stimulation which was about a 4 fold increase in methane oxidation on the first day. The amino acids and pentoses resulted in a 3 fold increase in methane oxidation on the first day, while the hexoses enhanced methane oxidation only slightly. The relatively slight stimulation by the hexoses may be due to permeability effect.

The explanation for these observations is presently unknown. Perhaps the organic compounds stimulated cell division thereby increasing the number of methane oxidizing bacteria and the quantity of methane oxidized. Alternatively, the organic compounds could have affected the rate of methane oxidation without increasing cell numbers. This could have been done by directly affecting the methane oxidation process or by increasing the solubility and/or availability of methane to the bacteria. Regardless of the explanation, this phenomenon would have a tremendous effect on these bacteria in the natural environment. By secretion, leaking, or lysis, organisms of all kinds release variable quantities and types of organic materials into the environment that would affect methane oxidation by these bacteria. Less widespread but significant in restricted situations would be similar stimulating effects due to external organic pollutants entering aquatic ecosystems.

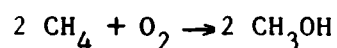
Results of the determination of gaseous substrate and product balances during methane oxidation by *M. trichosporium* are shown in Table 4. By comparing the amount of methane oxidized with the amount of carbon dioxide produced, it appears that about 50% of the methane that was oxidized was incorporated into cellular material. Therefore, only half as much carbon dioxide was produced as was methane oxidized. Since complete oxidation of methane to carbon dioxide via methanol, formaldehyde, and formate involves 4 oxidations, and because methane is incorporated at the formaldehyde level, the incorporation of 50% of the methane oxidized into cellular material decreases the number of oxidations from 8 per 2 methane molecules to 6 per 2 methane molecules. Therefore, the potential energy yielding oxidations were decreased by 25% while 50% of the methane was fixed into cell material.

TABLE 4

Gaseous substrate and product balances during methane
oxidation by Methylosinus trichosporium grown in CM medium at 21 C.

Time (days)	UTILIZATION (/ml)			PRODUCTION (micromoles/ml)		RATIOS	
	CH ₄	O ₂	N ₂	CO ₂		O ₂ /CH ₄	CH ₄ /CO ₂
1	1.67	2.85	0	0.74		1.7	2.2
2	4.69	7.06	0	2.27		1.5	2.1
3	4.75	7.64	0	2.39		1.6	2.0

Another interesting feature is the relationship between methane oxidized to oxygen consumed which was about 6 atoms of oxygen per 2 molecules of methane oxidized. Based upon incorporation of 50% of the methane at the formaldehyde level, there was 1 oxygen atom utilized per oxidative step. This stoichiometry is constant with either a mixed function oxidase or a hydration-dehydrogenation for the initial oxidation of methane. In view of the studies of Ledbetter and Foster (70) and Higgins and Quayle (52) showing O^{18} incorporation into methane oxidizing bacteria, M. trichosporium probably also utilizes a mixed function oxidase (monooxygenase) at the first oxidation. The relationship between methane and oxygen consumed shown in Table 3 suggests a 1:1 ratio for the initial oxidation or the following reaction:



This is as opposed to a mechanism involving 2 oxygen atoms per methane in the initial oxidation with some reduced hydrogen donor transporting hydrogen to the extra oxygen. The oxidation of methane to methanol has a $G_O' = -26.12$ Kcal mole⁻¹ (99). Although it is energetically feasible to recover ATP from this reaction, coupling of phosphorylation to monooxygenase has yet to be demonstrated. The remaining oxidative steps in the oxidation of methane are probably dehydrogenations coupled with electron transport and oxidative phosphorylation. These data show that aquatic methane oxidation not only increases carbon retention but also depletes reserves of dissolved oxygen in the water.

5. MORPHOLOGY OF METHANE OXIDIZING BACTERIA

Because of the rather limited culturing capabilities encountered with the methane oxidizing bacteria, standard techniques such as plate counts were useless in these studies. Therefore, other techniques for detecting and quantitating methane oxidizing bacteria were sought. The morphology of methane oxidizing bacteria was examined as a possible means of identifying these microorganisms.

MATERIALS AND METHODS

Methane oxidizing bacteria were grown as described in Section 4. These bacteria were examined electron microscopically after thin sectioning, freeze etching, and negative staining.

Freeze etching of bacteria was done as follows:

1. Concentrate cells by centrifugation.
2. Place a drop of the pellet on a gold specimen holder.
3. Freeze in liquid freon for 5 seconds.
4. Transfer quickly to liquid nitrogen.
5. Place on specimen platform cooled to -100 C.
6. Evacuate to 10^{-6} torr.
7. Fracture with knife cooled to -196 C.
8. Position the knife above specimen and etch for 4.5 minutes.
9. Shadow for 8 seconds, 110 volts, with 6 cm of 0.1 millimeters platinum wire at an angle of 32° .
10. Carbon coat for 11 seconds at 122 volts.
11. Vent to atmospheric pressure.
12. Float off the carbon replica in distilled water.
13. Transfer the carbon replica to 25% (v/v) H_2SO_4 for 15 minutes.
14. Transfer to 50% (v/v) H_2SO_4 for 15 minutes.
15. Transfer to 75% (v/v) H_2SO_4 for 15 minutes.
16. Transfer to concentrated H_2SO_4 for 15 minutes.
17. Reverse the H_2SO_4 sequence to distilled water.
18. Transfer to 5% (w/v) sodium hypochlorite (Clorox) for 2 hours.
19. Wash in distilled water.
20. Pick up the carbon replica on a 300 mesh uncoated copper grid.

For thin sectioning, the following reagents were prepared:

1. Veronal-Acetate Buffer Stock

Sodium acetate	19.428 g
Sodium barbital (Fisher)	29.428 g
Sodium chloride	34 g
Distilled water	1000 ml

2. Working concentration of Veronal-Acetate Buffer

Stock Mixture	5.0 ml
0.1N HCl	7.0 ml
1M CaCl_2	0.25 ml
Distilled H_2O	13.0 ml

3. 1% (w/v) OsO_4 (Mallinckrodt) in Veronal-Acetate Buffer.

4. 5% (w/v) (J. T. Baker) Uranyl-acetate in Veronal-Acetate Buffer.

5. Mixture A:

Dodecenyl succinic anhydride (Shell)	100 ml
Epon 812 (Shell)	62 ml

6. Mixture B:

Methylnadic anhydride (Shell)	89 ml
Epon 812	100 ml

7. Embedding resin: mix thoroughly 55A to 45B.

Fixation and embedding of samples were done as follows:

1. Add glutaraldehyde (Fisher) to the sample to a final concentration of 1%.
2. Incubate 16 hours at 5C.
3. Wash in veronal acetate buffer.
4. Fix 2 hours at room temperature in 1% (w/v) osmium tetroxide.
5. Wash in veronal acetate buffer.
6. Resuspend sample in 2% (w/v) agar and cool.
7. After agar solidifies, cut into small blocks.
8. Wash blocks in uranyl acetate for 2 hours.
9. Transfer to 30% (v/v) ethanol for 15 minutes.
10. Transfer to 50% (v/v) ethanol for 15 minutes.
11. Transfer to 70% (v/v) ethanol for 15 minutes.
12. Transfer to 80% (v/v) ethanol for 15 minutes.
13. Transfer to 95% (v/v) ethanol for 15 minutes.
14. Transfer to 95% (v/v) ethanol for 15 minutes.
15. Transfer to 100% ethanol for 15 minutes.

16. Transfer to 100% ethanol for 15 minutes.
17. Transfer to propylene oxide (Eastman Organic Chemicals) for 15 minutes.
18. Transfer to propylene oxide for 30 minutes.
19. Transfer to propylene oxide in resin (3:1) for 1 hour.
20. Transfer to propylene oxide in resin (1:1) for 1 hour.
21. Transfer to propylene oxide in resin (1:3) for 4 hours.
22. Transfer to pure embedding resin for 4-12 hours.
23. Transfer to Beem capsules filled with embedding resin.
24. Incubate capsules 12 hours at 37 C.
25. Incubate capsules 12 hours at 45 C.
26. Incubate capsules 12 hours at 60 C.
27. Blocks ready for sectioning when cool.

Thin sections were cut using a Porter Bloom MT 1 manual ultramicrotome or a LKB Model III ultramicrotome; in both cases, freshly prepared glass knives were used. In some cases sections were post stained with lead citrate for 5 minutes as described by Reynolds (98).

For negative stains, samples were mixed 1:1 with 1% (w/v) phosphotungstic acid (Fisher), pH 7.0, and sprayed onto formvar coated copper electron microscope grids.

Either a Zeiss EM-9 or a Phillips EM-300 electron microscope was used to examine the preparations. Photographs were taken on Kodak Electron Image glass negative plates. The plates were developed for 4 minutes (68-70 F.) in D-19 developer (Kodak) and fixed for 5-10 minutes.

RESULTS AND DISCUSSION

In Figure 16, M. trichosporium is observed to be a smoothly textured rod shaped bacterium. Measurements from a variety of electron micrographs revealed that the bacterium is 2-3 micrometers long and may be somewhat pear-shaped ranging from 0.5-1 micrometer in width. Figure 16 also shows the cell wall to be 15.4 nanometers thick with a distinct outer region 6 nanometers thick and an inner region 9.4 nanometers thick. This is similar to the cell wall of Escherichia coli which has an outer layer about 5 nanometers thick and an inner layer about 8.5 nanometers thick (21). These dimensions are smaller than Gram positive cell walls which are usually between 200 and

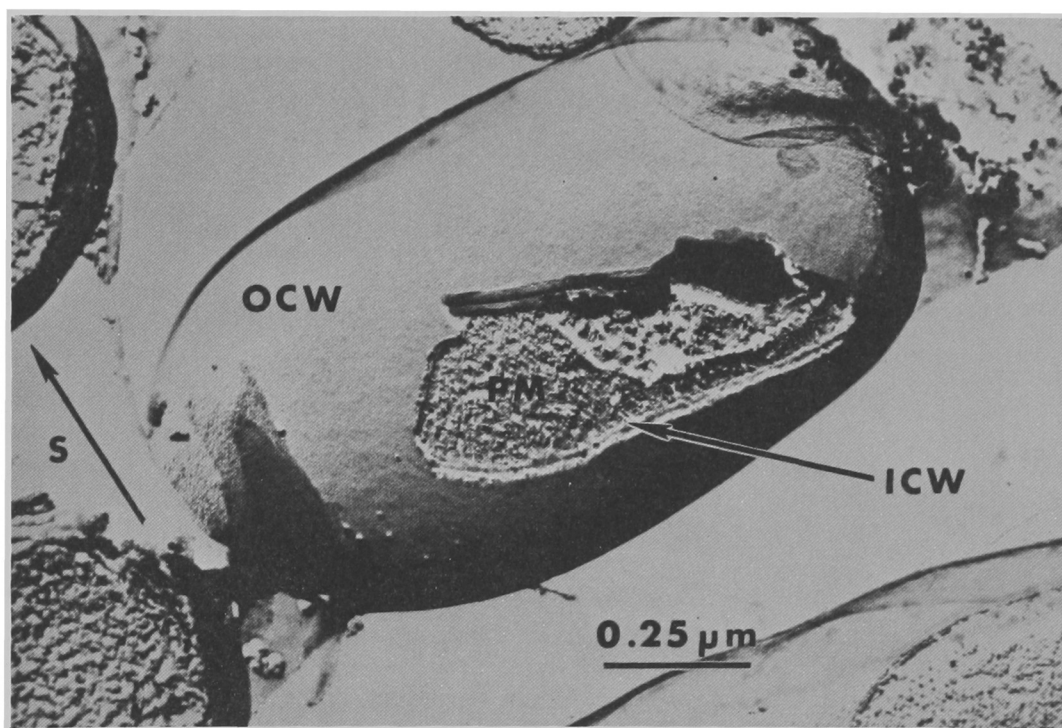


Figure 16. Electron micrograph of a freeze etch preparation of M. trichosporium showing:

OCW = outer cell wall
ICW = inner cell wall
S = direction of shadow

800 nanometers thick. The outer wall of the organism was seen to be rather smooth. This is similar in appearance to the somewhat smaller M. methanica shown for comparison in Figure 17.

Figure 8 shows slightly more extensive fracturing of M. trichosporium than was observed in the first freeze etching. Again the 2 layered cell wall is evident. Also, small fibers 10-70 nanometers long can be seen connecting the cell wall and plasma membrane. The fibers attach the plasma membrane to the cell wall which made it extremely difficult to obtain purified plasma membranes from these cells. These fibers have plagued membrane investigators working with Gram negative bacteria. Of further significance in Figure 18 are balloonlike intracytoplasmic membrane vesticles (V) where the cleavage plane broke over the surface of the vesticles rather than through them. This cleavage plane fracturing which resulted in the relief evident in this electron micrograph is one of the main advantages of freeze etching as compared to thin sections. Furthermore, this is in contradiction to Whittenbury's (132) description of the intracytoplasmic membranes as tubules.

Figure 19 shows a longitudinal fracture of M. trichosporium midway through the cell that is very similar to what one obtains with thin sections. The internal membranes are arranged in groups of vesticles 16-300 nanometers thick sometimes running the entire width and length of the cell near the periphery. Figure 20 is a transverse fracture showing essentially the same vesticular structure as in Figure 19. This reveals that the internal membranes may occupy almost all the peripheral cell area in these bacteria. In Figure 21, and enlargement of Figure 10 shows that these vesticle membranes are rather typical looking 9 nanometer thick membranes. The three dimensional effect in Figure 22 further emphasizes the extent of the internal membrane system.

The origin of these intracytoplasmic membranes is uncertain. In none of the electron micrographs could the plasma membrane be seen to be continuous with or in the process of forming vesticles, however, this does not eliminate the possibility that the internal membranes originate in the plasma membrane. In at least some cases though, the internal membranes are passed from mother cell to daughter as shown in Figure 23. This electron micrograph shows a cell in the process of budding. These organisms may divide by binary fission or by budding, the latter preceding the formation of a spore. A fracture through a spore is shown in Figure 24. The complex system of outer layers, membranes, etc. suggests that the membranes passed along during budding may be important in the formation of the spore.

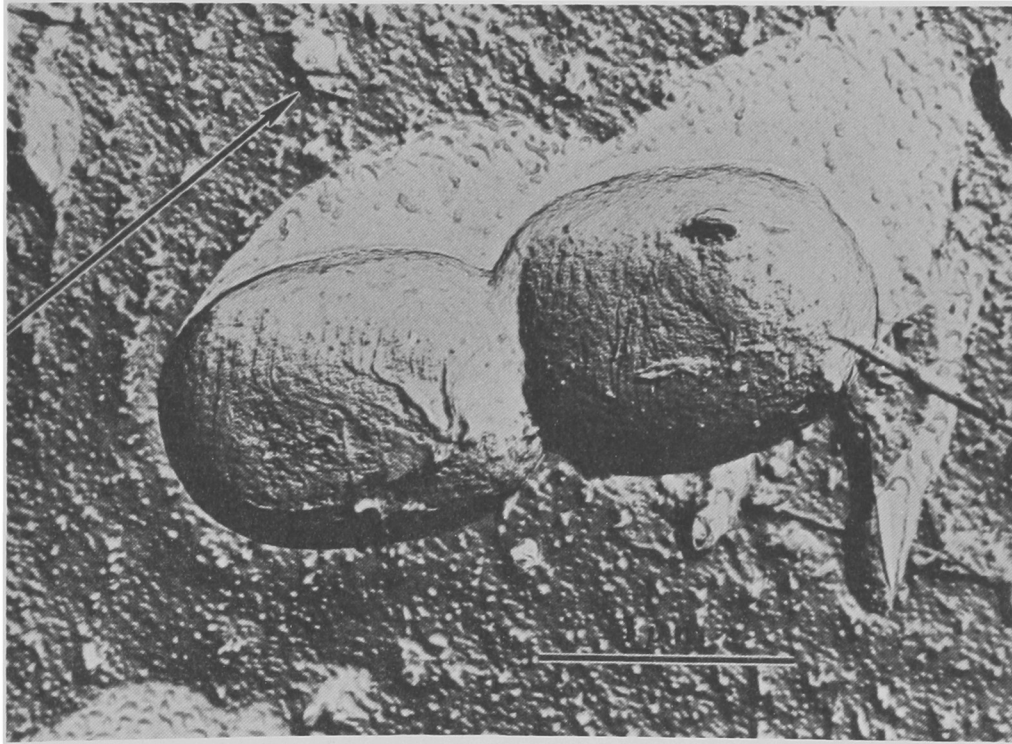


Figure 17. Electron micrograph of a carbon replica of *M. methanica*. The arrow denotes the direction of shadowing.

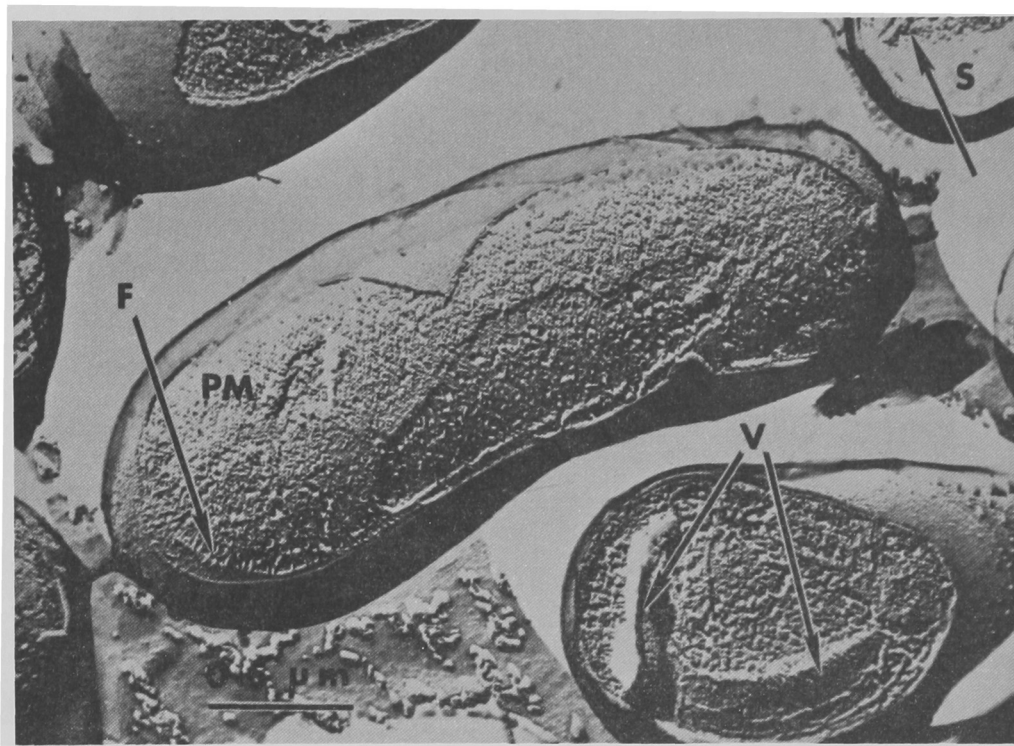


Figure 18. Electron micrograph of a freeze etch preparation of M. trichosporium showing:

- F = fibers
- PM = plasma membrane
- V = venticles
- S = direction of shadowing

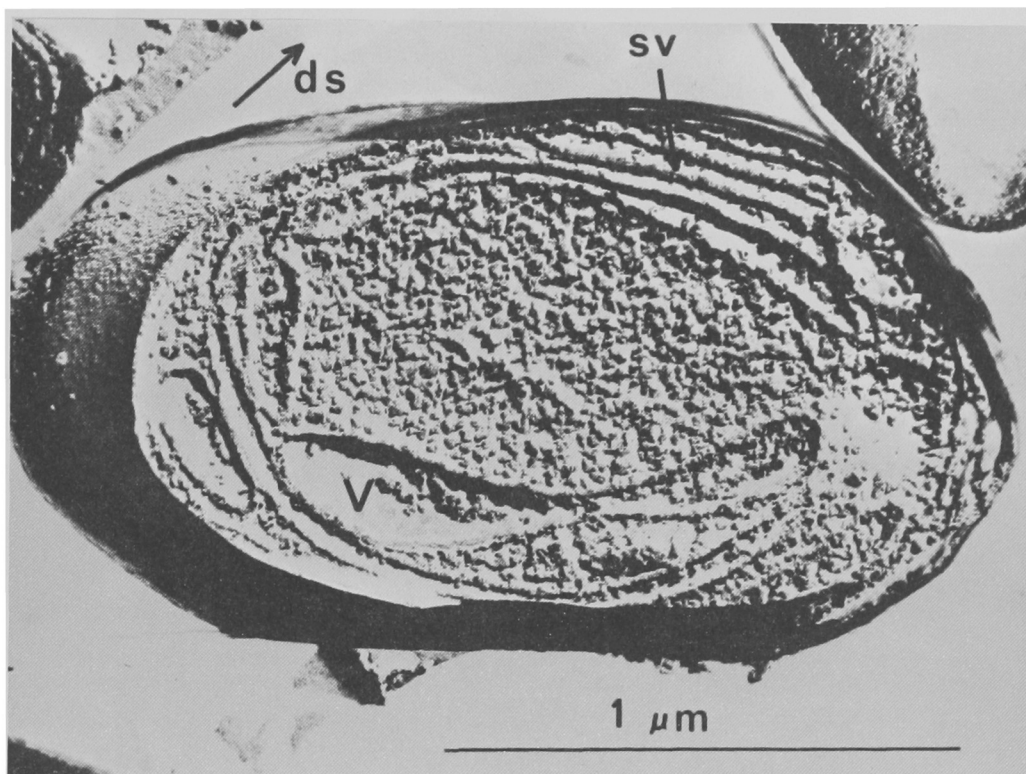


Figure 19. Electron micrograph of a freeze etch preparation of M. trichosporium showing:

SV = stacked vesticles
V = vesticle
DS = direction of shadowing

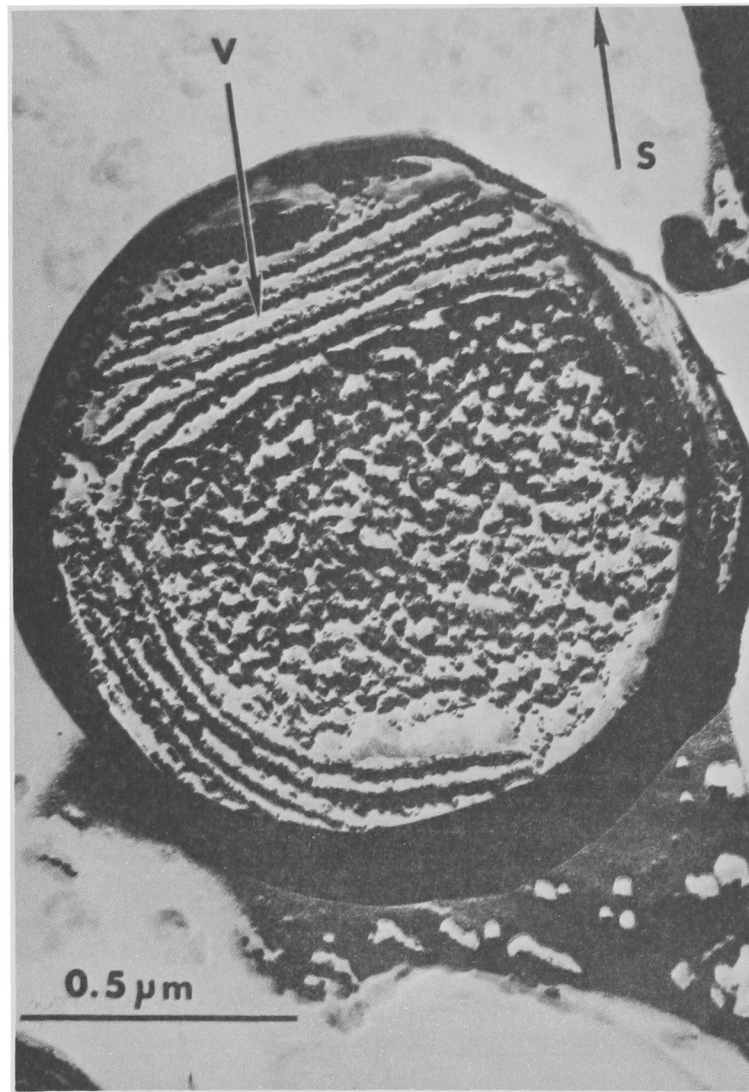


Figure 20. Electron micrograph of a freeze etch preparation of M. trichosporium showing:

V = vesicle

S = direction of shadowing

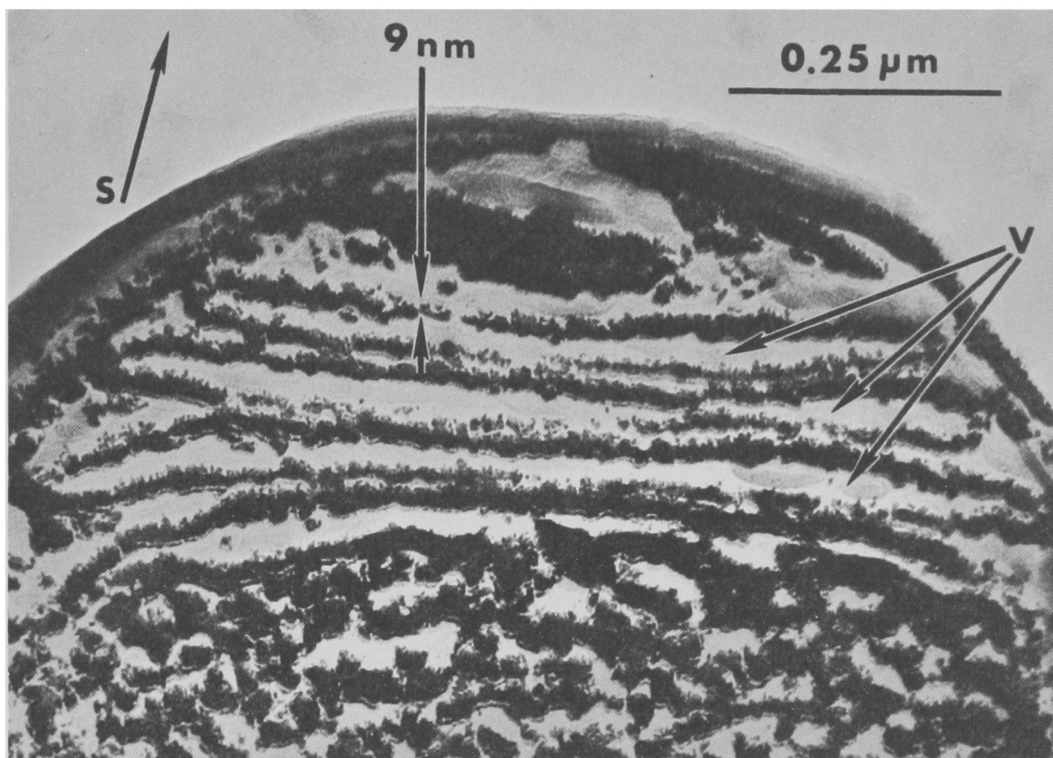


Figure 21. Electron micrograph of a freeze etch preparation of M. trichosporium showing:

V = vesticle

S = direction of shadowing

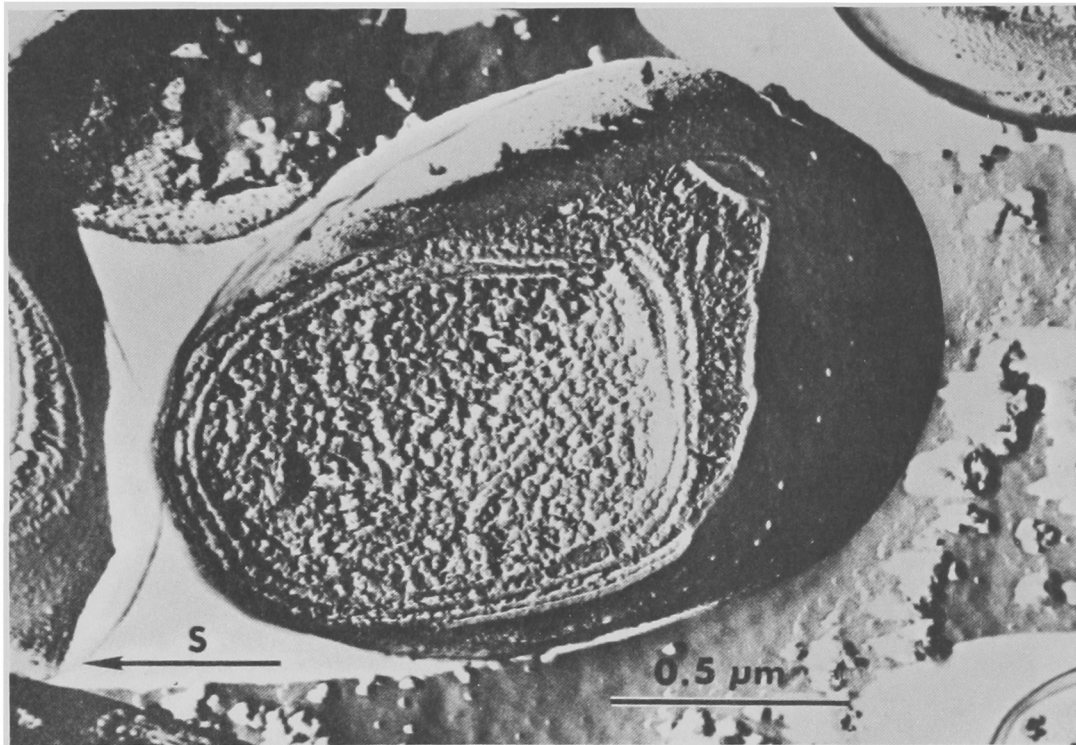


Figure 22. Electron micrograph of a freeze etch preparation of M. trichosporium showing extent of internal membranes.

S = direction of shadowing

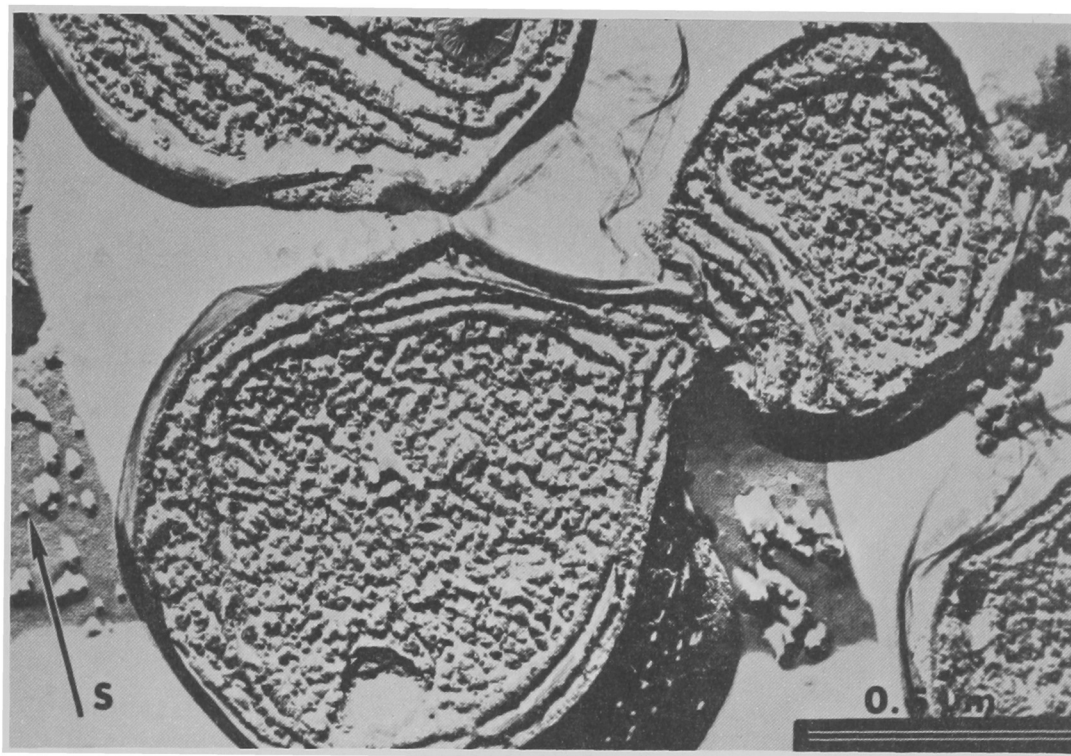


Figure 23. Electron micrograph of a freeze etch preparation of building M. trichosporium cell showing the division of membranes.

S = direction of shadowing

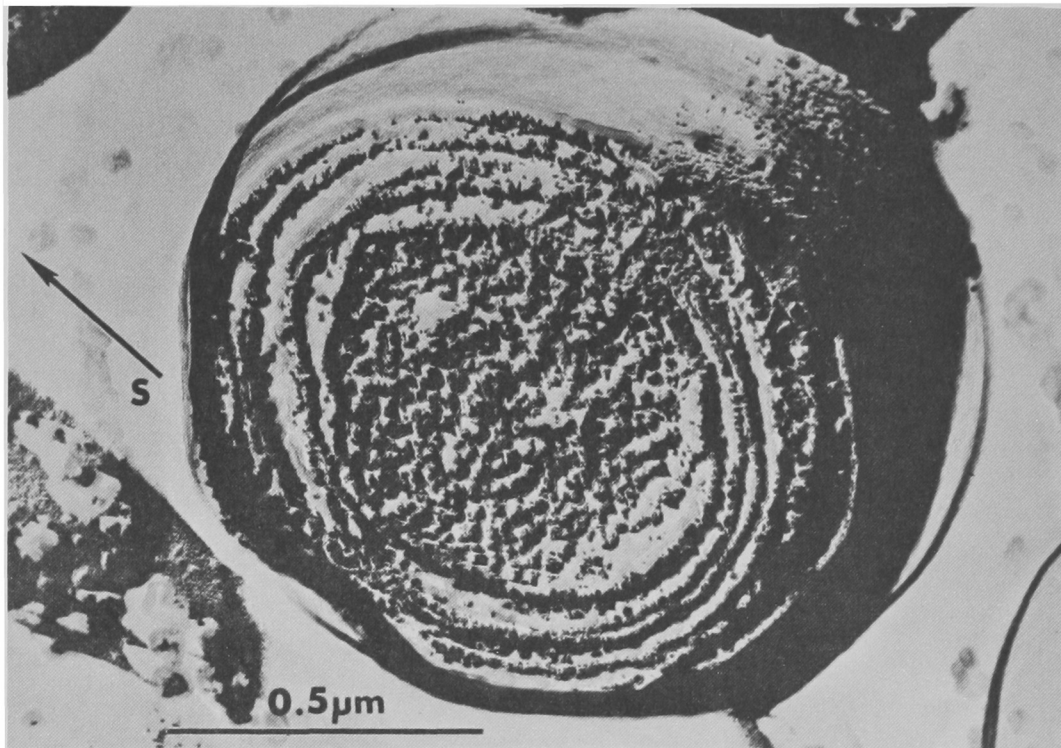


Figure 24. Electron micrograph of a freeze etch preparation of a M. trichosporium spore.

S = direction of shadowing

Figure 25 not only shows the peripheral membrane vesticles but also reveals a rodlike structure 4.5 nanometers in diameter with a repeating subunit every 4.5 nanometers. Although different in appearance from the membranes, the size of this structure suggests that it may be membrane material (i.e. 1/2 a membrane). The structure could also be a virus. Figure 26 shows another of these rodlike structures and also shows intercellular bridges (B) 30 x 75 nanometers in size that are of unknown origin and unknown function. In Figure 27, the bacteria from a liquid culture can be seen in short chains due to these intercellular connections.

Figure 28 reveals granules of PHB that range in size from 0.2-0.25 micrometers in diameter. The PHB granules were observed near the centers of cells, neither within the membrane vesticles nor attached to them. Identification of these granules as PHB was based upon a similar appearance in other bacteria in addition to chemical identification, as well as explained in a subsequent section.

This peripheral arrangement of balloon-like vesticles is a Type II membrane system. The proposed organization of the Type II membranes in M. trichosporium is illustrated diagrammatically in Figure 29.

For comparison, a freeze etching and a thin section of M. methanica are shown in figures 30 and 31 respectively. These intracytoplasmic membranes are representative of a Type I system, a lamellar arrangement of stacked membrane vesticles lying in the center of the cell. Figure 31 reveals that this bacterium also accumulates PHB. Vesticular arrangement and membrane ultrastructure are shown in Figure 32. The membranes were 9.15 nanometers thick enclosing vesticles 15-18 nanometers in diameter. Figure 33 indicates that these Type I membranes are also passed along during cell division.

Both the Type I and the Type II membrane systems are very similar in appearance to the intracytoplasmic membranes of the photosynthetic bacteria (83) and the nitrifying bacteria (127). Nevertheless, while these membranous microorganisms are similar in membrane structure, they are all distinguishably unique. Therefore, the potential exists for methane oxidizing bacteria to be detected and quantitated via their membrane morphology.

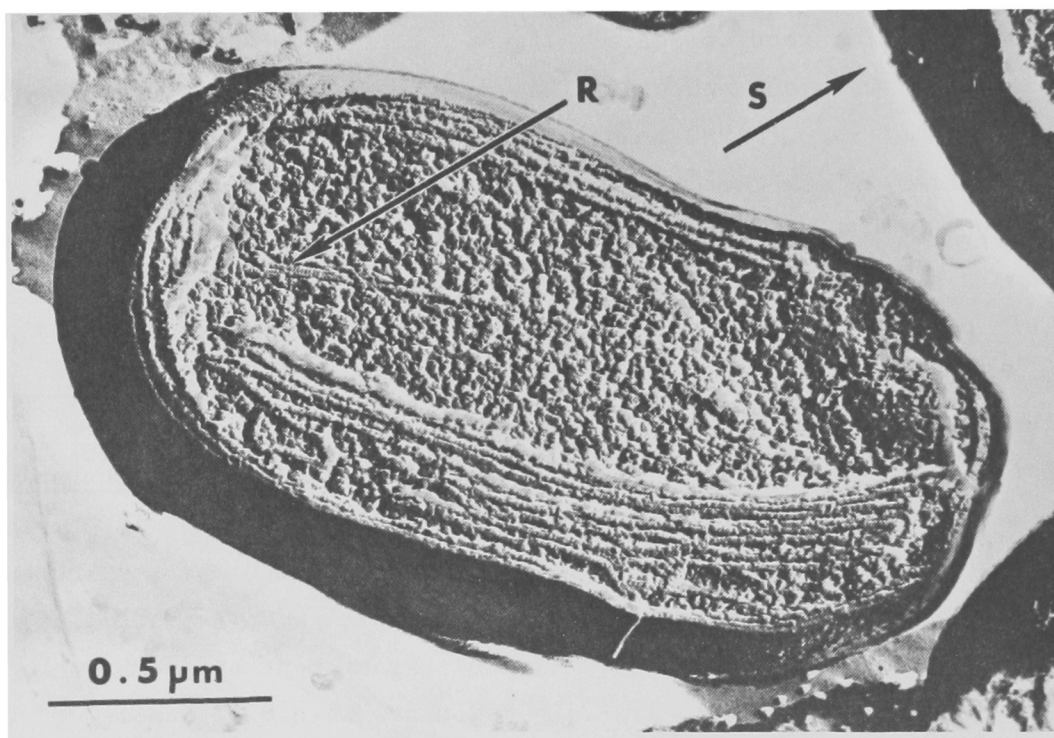


Figure 25. Electron micrograph of a freeze etch preparation of M. trichosporium showing:

R = rod structure

S = direction of shadowing

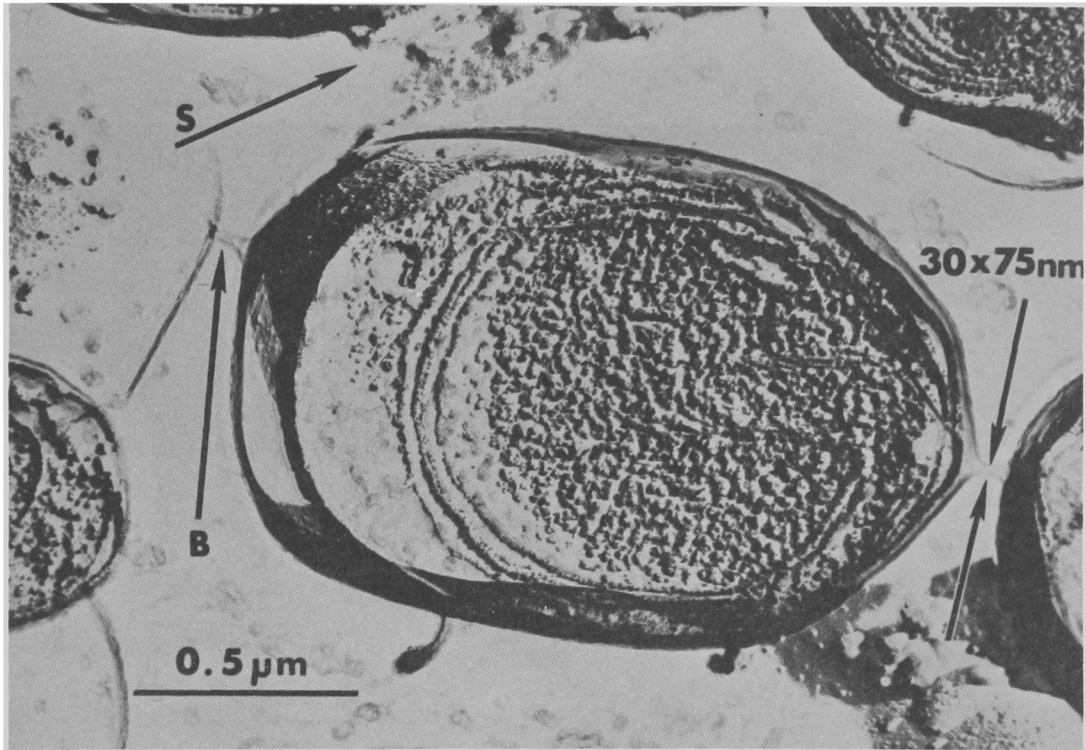


Figure 26. Electron micrograph of a freeze etch preparation of M. trichosporium showing:

B = intercellular bridge
S = direction of shadowing

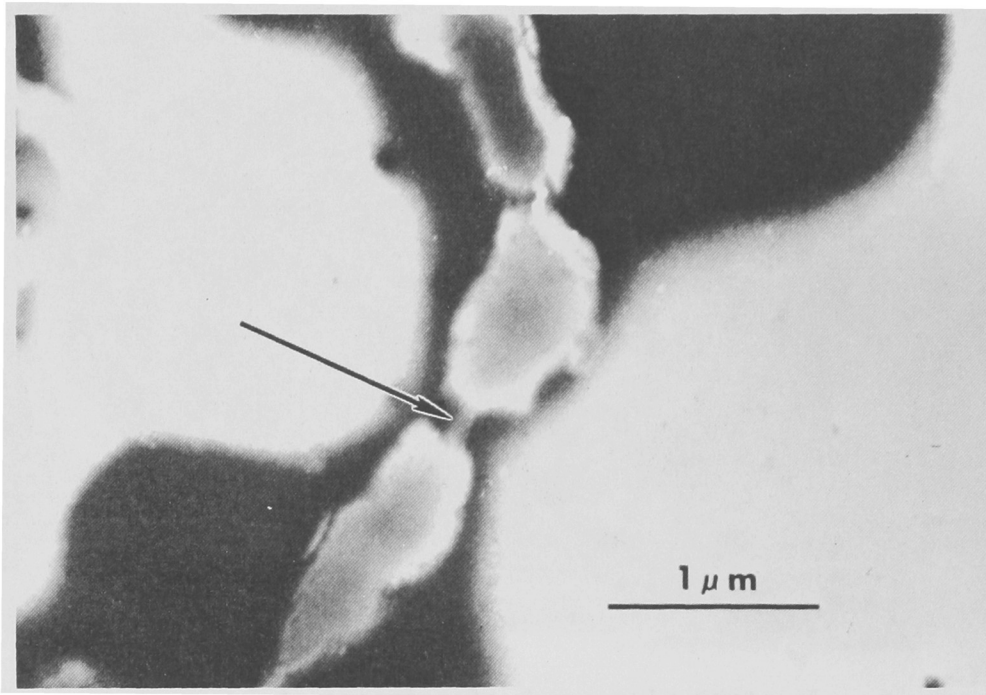


Figure 27. Electron micrograph of a negatively stained sample of liquid M. trichosporium culture showing an intercellular bridge (B).

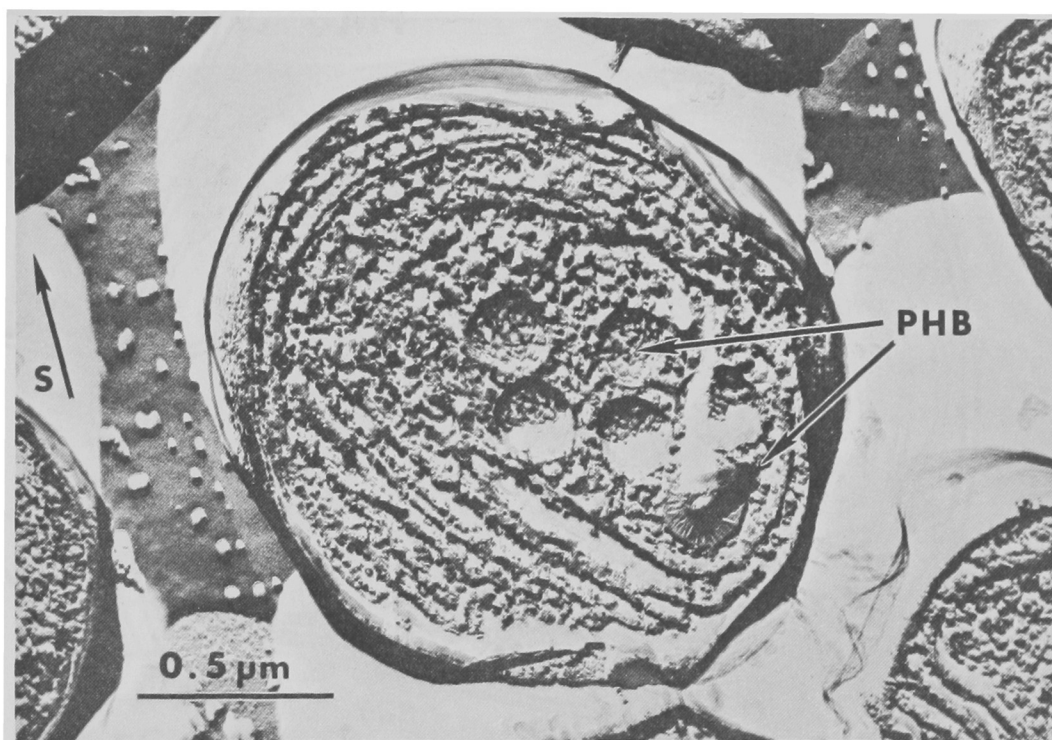


Figure 28. Electron micrograph of a freeze etch preparation of M. trichosporium showing:

PHB = poly-beta-hydroxybutyrate
S = direction of shadowing

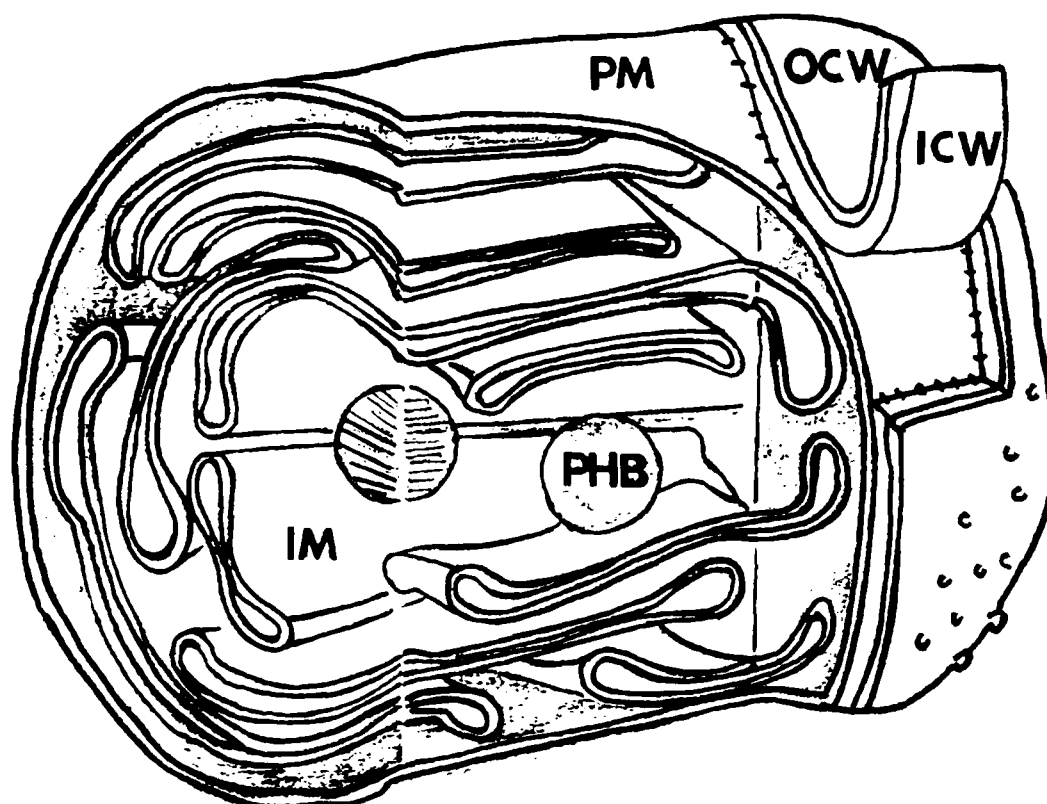


Figure 29. Illustration representing the proposed morphology of M. trichosporium.

OCW = outer cell wall
 ICW = inner cell wall
 PM = plasma membrane
 IM = intracytoplasmic membrane
 PHB = poly-beta-hydroxybutyrate

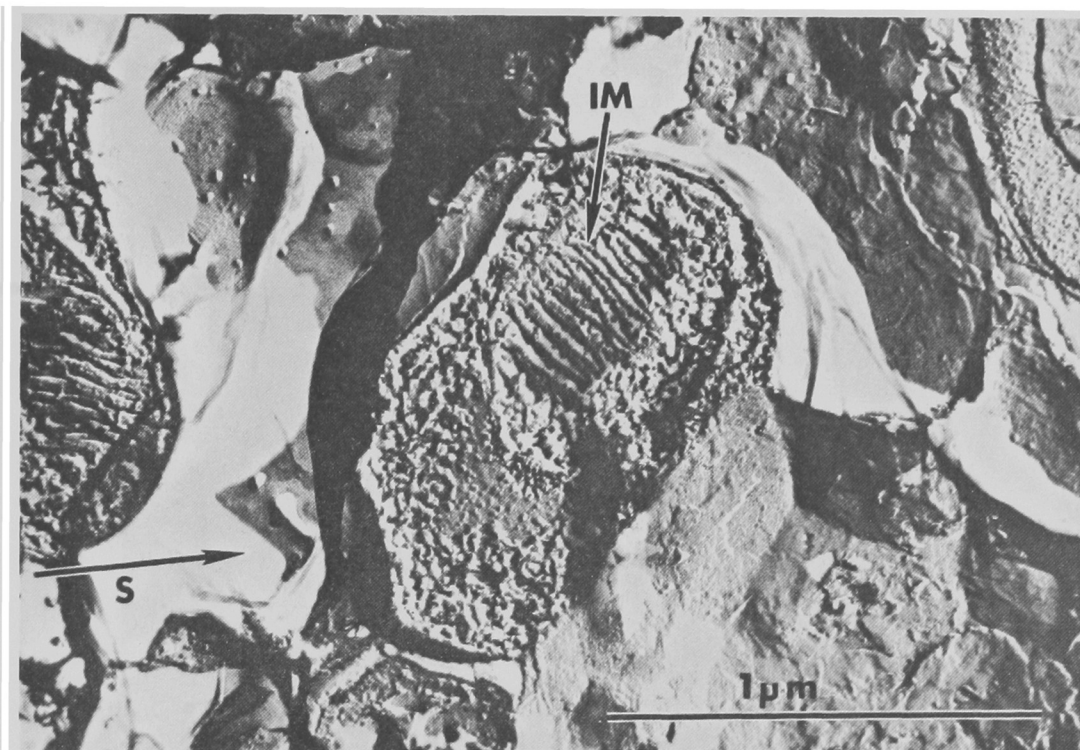


Figure 30. Electron micrograph of a freeze etch preparation of M. methanica showing Type I membranes.

IM = internal membranes
S = direction of shadowing

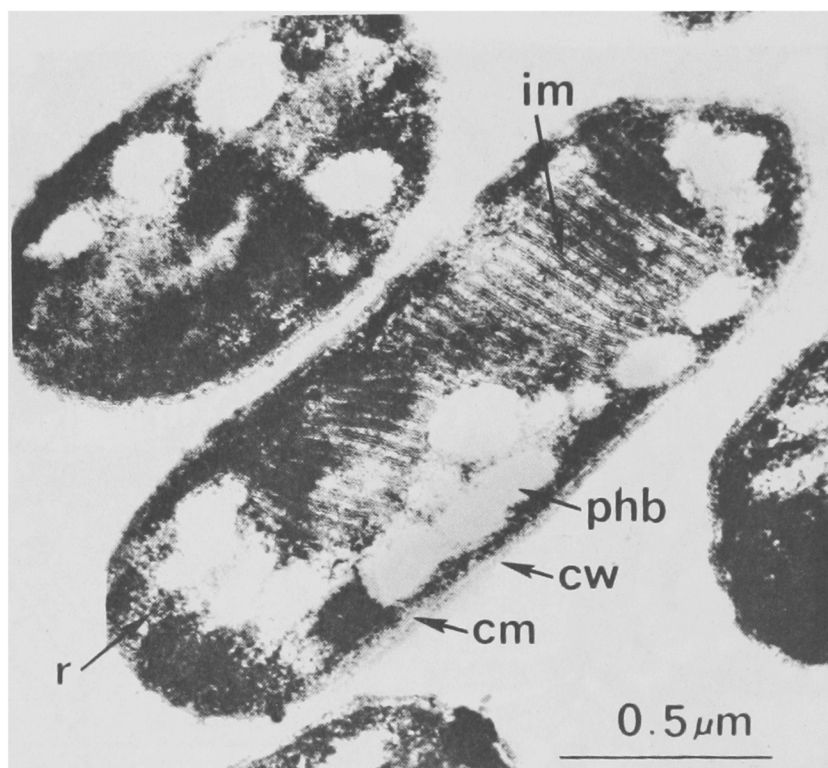


Figure 31. Electron micrograph of a thin section preparation of M. methanica showing:

im = internal membranes
cm = cell membrane
cw = cell wall
phb = poly-beta-hydroxybutyrate
r = ribosomes

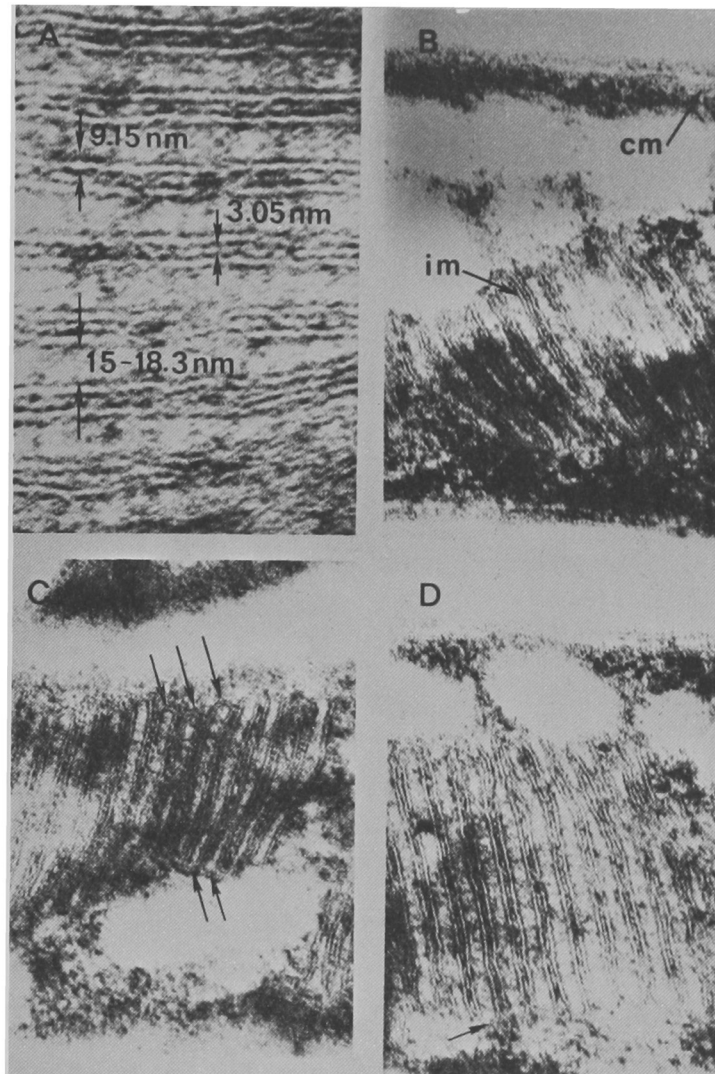


Figure 32. Electron micrographs of thin sections of membranes in *M. methanica* showing:

- A. Membrane dimensions
- B. Comparison of cell membrane with internal membranes
cm = cell membrane
im - internal membranes
- C. Membrane vesticles
Arrows denote membrane continuity
- D. Membrane vesticles

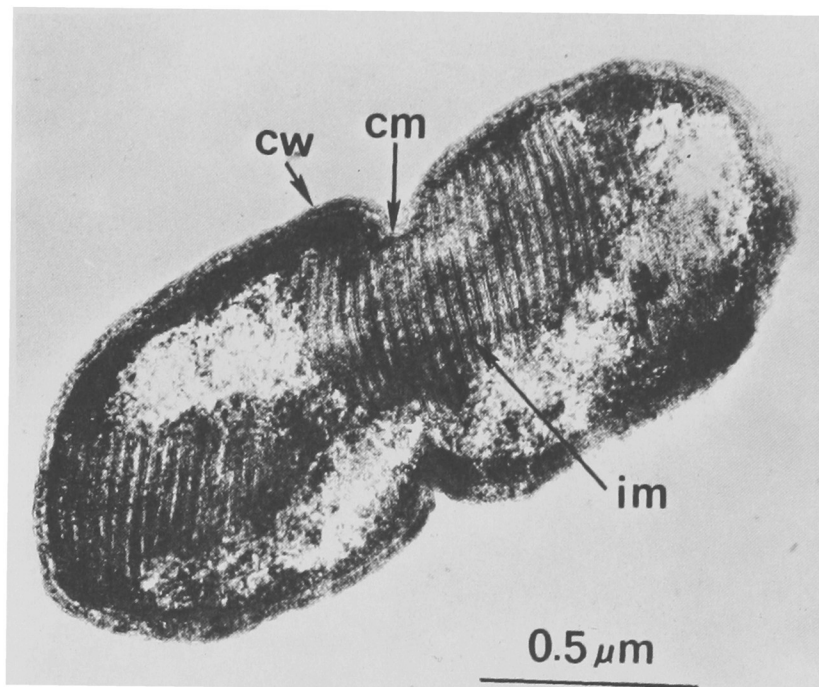


Figure 33. Electron micrograph of a thin section preparation of M. methanica showing:

cm = cell membrane

cw = cell wall

im = internal membranes

6. ISOLATION OF INTRACYTOPLASMIC MEMBRANES

Since intracytoplasmic membranes were the predominant morphological characteristic of the methane oxidizing bacteria, biochemical characteristics of these membranes could serve as specific identifying labels. Subsequent sections will describe biochemical studies directed at revealing unique characteristics of the membranes of methane oxidizing bacteria. A method for obtaining purified membranes was developed as a prerequisite to these studies.

MATERIALS AND METHODS

M. trichosporium grown as previously described was used for this study.

Bacterial cells (200 mg/ml wet weight) were disrupted by shaking with 0.45-0.5 millimeter acid washed glass beads in a Braun MSK cell homogenizer at 4000 RPM for 3 min. The homogenizer unit was continuously cooled with liquid carbon dioxide during the process.

Various cell fractions were separated by differential centrifugation using 5/8 x 4 inch polyallomer tubes in a SW27 rotor with a Beckman Model L2-65B Ultracentrifuge. The fractionation was performed as follows:

1. Centrifuge 30 minutes at 5,000 x g.
2. Save the pellet as the 5P fraction and recentrifuge the supernatant for 30 minutes at 10,000 x g.
3. Save the pellet as the 10P fraction and recentrifuge the supernatant for 30 minutes at 20,000 x g.
4. Save the pellet as the 20P fraction and recentrifuge the supernatant for 30 minutes at 40,000 x g.
5. Save the pellet as the 40P fraction and recentrifuge the supernatant for 30 minutes at 80,000 x g.
6. Save the pellet as the 80P fraction and the supernatant as the 80S fraction.

Each fraction was examined electromicroscopically after negative staining with 1% (w/v) phosphotungstic acid. This procedure is outlined in Section IV. Each fraction was also analyzed for total protein, total hexose, and poly-beta-hydroxybutyrate.

Total protein in each differential centrifugation fraction was determined by the procedure of Lowry et al. (75).

The Folin phenol reagent was that of Folin and Ciocalteu (31).

Sugars in concentrated H_2SO_4 react with the acid to form furfural derivatives which in turn react with anthrone to form a blue-green color. Total sugar in each fraction was determined using the anthrone test of Whistler and Wolfram (130).

Poly-beta-hydroxybutyrate (PHB) was quantitated by the method of Law and Slepecky (65).

RESULTS AND DISCUSSION

An electron micrograph of negatively stained material from the 5P fraction is shown in Figure 34 and is typical of the material found in this fraction. This is indicative of the relatively heavy cell wall material that was in the 5P fraction. Also of significance is the fact that the cells were not grossly disrupted by this breakage procedure. There were large chunks of cell wall debris and PHB in the low speed fractions, but the relatively mild cell disruption evidenced in Figure 34 was the norm rather than the exception. The 20P fraction shown in Figure 35 shows that even at this moderate speed, the large pieces of cell debris had been previously sedimented. Figure 36 shows the 80P fraction containing relatively pure membrane material. Clumps seen in this fraction are characteristic of membrane material which forms aggregates due to hydrophobic areas in the membranes. Figure 37 shows a thin section of a membrane preparation revealing the typical ultrastructure of osmium fixed membranes.

Perhaps more valuable are the quantitative data listed in Table 5. These data show that most of the PHB sediments in the 5P fraction, a moderate amount in the 80S fraction, and little or none in the other fractions. The PHB in the 80S fraction could be due to buoyancy of the lipid material, but this seems unlikely since no granules appearing similar to PHB were observed in 80S. negative strains. The possibility of fragments of PHB granules in the 80S fraction seems remote since such small quantities were observed in the 10P through 80P fractions. Another hypothesis that may explain this observation would be the presence of short chain partially polymerized and single molecules of beta-hydroxybutyrate in the 80S fraction (27).

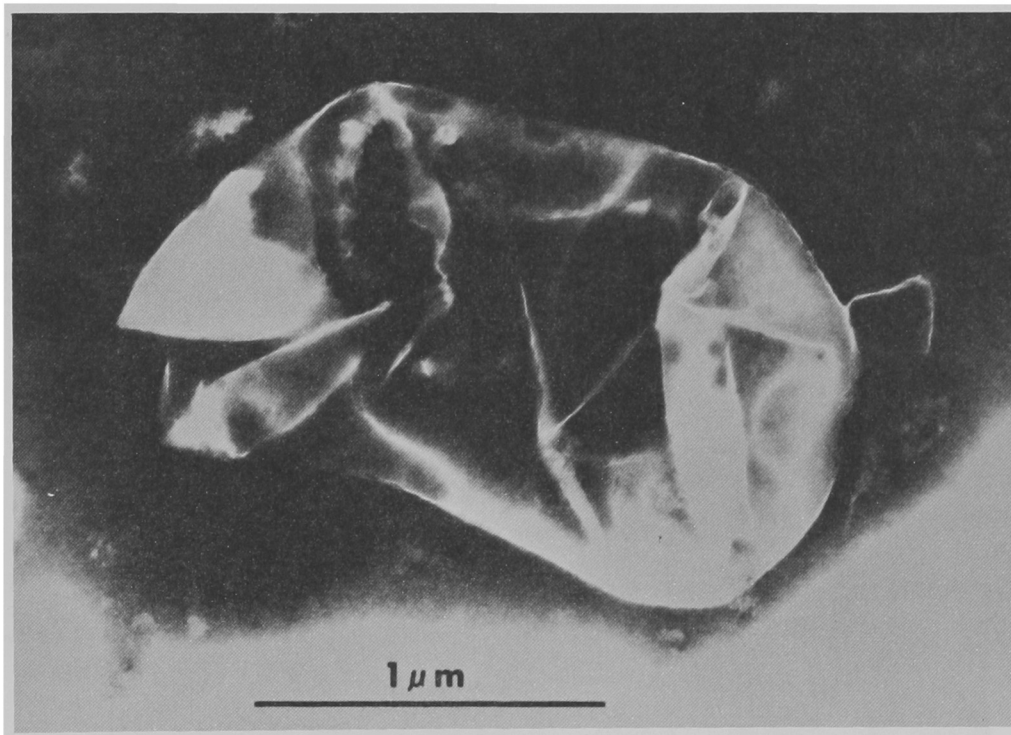


Figure 34. Negative stain of the 5P differential centrifugation fraction of disrupted M. trichosporium cells.

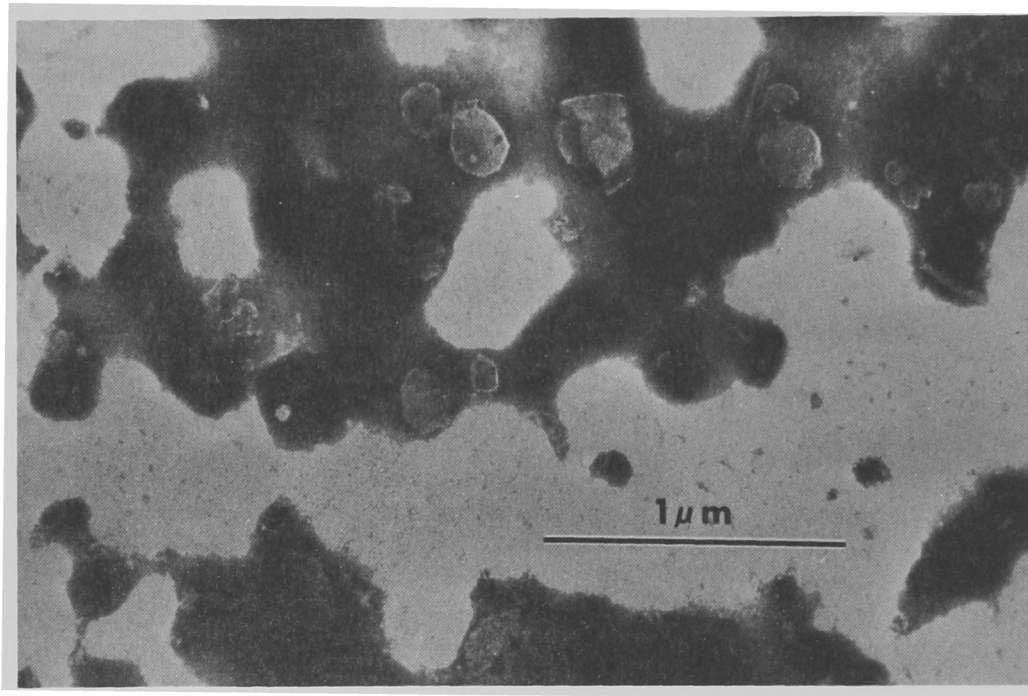


Figure 35. Negative stain of the 20P differential centrifugation fraction of disrupted M. trichosporium cells.

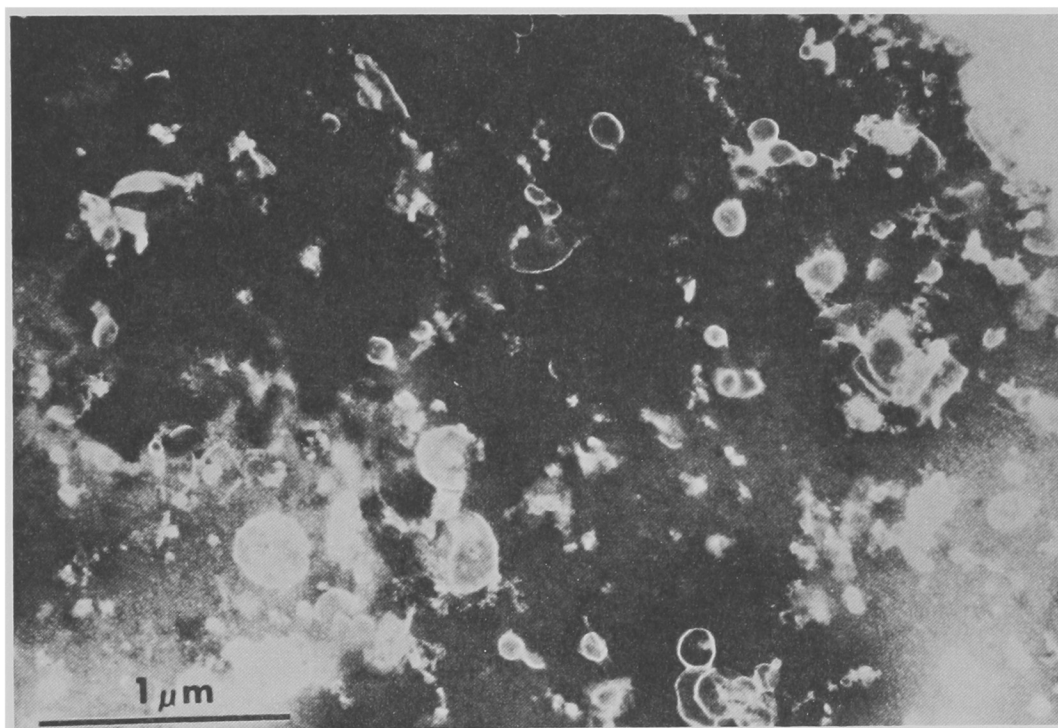


Figure 36. Negative stain of the 80P differential centrifugation fraction of disrupted M. trichosporium cells.

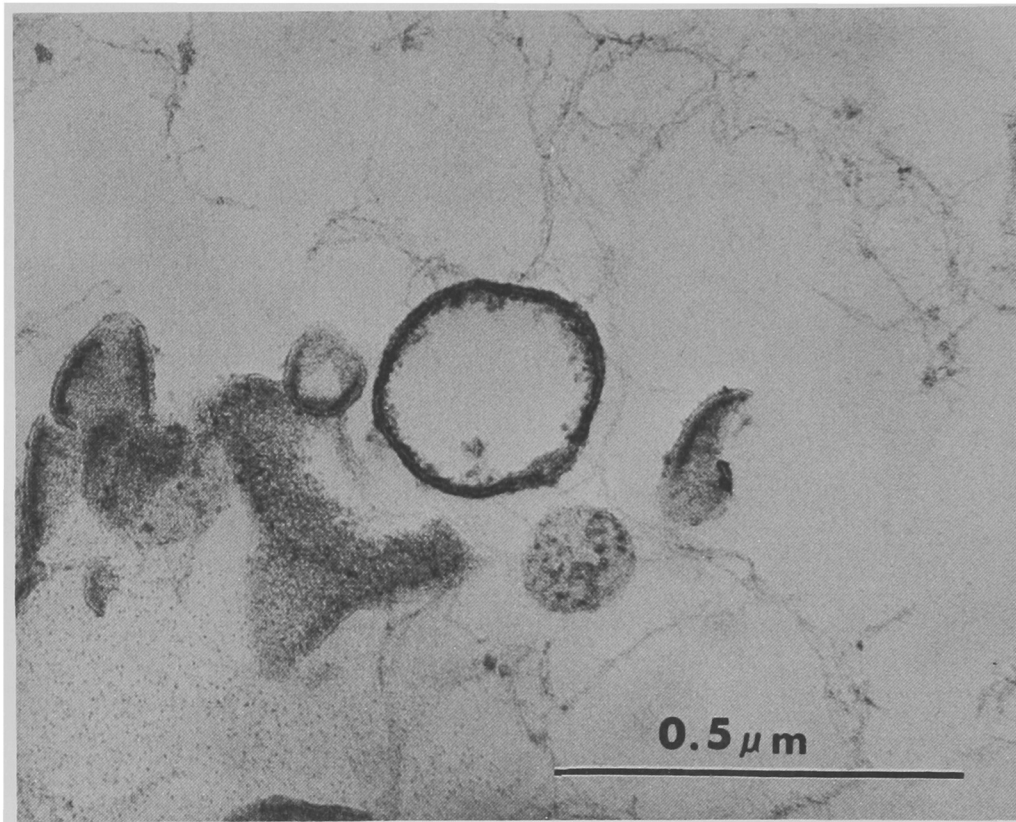


Figure 37. Thin section of an intracytoplasmic membrane preparation 20P, 40P, 80P, fractions from M. trichosporium.

TABLE 5

Relative weight of protein, hexose, and PHB in various differential centrifugation fractions of broken M. trichosporium cells.

<u>FRACTION</u>	<u>PROTEIN (mg)</u>	<u>HEXOSE (mg)</u>	<u>PHB (ug)</u>	<u>PROTEIN/HEXOSE</u>
Broken Cell	37.4	17.0	692	2.2
5P	17.2	7.57	567	2.3
10P	0.59	0.05	1.67	12
20P	0.50	0.05	0.93	10
40P	0.36	0.05	0.74	7.2
80P	0.24	0.05	0	4.8
80S	13.3	6.46	63.2	2.1

The quantity of both protein and hexose decreased through the 80P fraction; this was expected since the total amount of material decreased. More important is the fact that the protein/hexose ratio increased in the 10P, 20P, 40P, and 80P fractions as compared with broken cells and the 5P fraction. Because cell walls contain large amounts of hexose while membranes are lipid-protein structures, this indicates membrane enrichment in the higher speed pellets. Since the cell wall material sedimented in the low speed fractions and because it has already been shown that in these bacteria the plasma membrane is attached to the cell wall, the higher speed pellets represent relatively purified intracytoplasmic membranes. Thus, the plasma membrane-cell wall association of Gram negative bacteria that has so bothered membrane investigators in the past has in this study been an advantage making it possible to obtain preparations of intracytoplasmic membranes. While this investigation employed only one methane oxidizing bacterial isolate, since the methane oxidizers are mostly gram negative, this or a similar technique should be applicable to other isolates as well.

7. LIPIDS OF CELLS AND MEMBRANES

Biological membranes are comprised mostly of lipid and protein.

Pursuing the search for a biochemical label among methane oxidizing bacteria, lipids of cells and membranes of M. trichosporium were analyzed.

MATERIALS AND METHODS

Lipids were extracted by the procedures of either Folch et al. (39) or Bligh and Dyer (6).

Following both extractions, the lipid preparation was concentrated using an RAE Vacuum Evaporator (RAE Motor Corp.). When preparing lipids for fatty acids studies, all procedures were done under nitrogen.

PHB was precipitated from the lipid extract by adding 2 volumes of methanol and holding at -10 C. for several hours. The sample was then centrifuged and the PHB free lipid was recovered and concentrated as described previously. Removal of PHB was found to be necessary as a prerequisite for satisfactory separation of the various lipid components.

Silicic acid (Fisher Scientific Co.) was washed in chloroform: methanol (2:1) and heated at 110 C. for 12 hours. The following procedure was used to prepare the silicic acid column and separate the extracted lipids:

1. Mix the silicic acid with chloroform to form a slurry.
2. Pour the slurry into a 10 ml column.
3. Run about 25 ml of chloroform through the column to pack it.
4. Place some glass wool on top of the silicic acid to prevent mixing.
5. Layer the lipid sample (in chloroform) on top of the silicic acid.
6. Elute neutral lipids with 50 ml of chloroform.
7. Elute glycolipids with 50 ml of acetone:chloroform (1:1) and 50 ml of acetone.
8. Elute phospholipids with 50 ml methanol.
9. Collect all fractions in chloroform:methanol washed vessels.
10. Fractions concentrated as described previously.

Traces of water soluble components were removed from the phospholipid fraction by passage through a liquid/liquid partition column. The aqueous phase was immobilized by beads of Sephadex G-25. The procedure was as follows:

1. Soak the Sephadex G-25 (Pharmacia) overnight in 4 volumes of Folch's upper phase (FUP) prepared as previously described.
2. Wash the beads several times in FUP.
3. Pack the Sephadex slurry into a 10 ml column under slight pressure.
4. Cover the Sephadex with a piece of glass wool.
5. Run about 10 ml of FUP through the column.
6. Run about 20 ml of Folch's lower phase (FLP) through the column to displace FUP in void space.
7. Place the sample on top of the Sephadex.
8. Run about 50 ml of FLP through the column to elute the phospholipids.

Thin layer chromatographic plates (TLC) were prepared by shaking 40 gm of Camag silica gel type D-O (Arthur Thomas Co.) with 85 ml water for 5-10 minutes. This slurry was then spread over clean 8 x 8 x 1/8 inch glass plates using a Desaga-Brinkman plate spreader at 0.35 millimeters. These plates were heated at 110°C for 2-4 hours prior to use. Ascending development in a solvent saturated atmosphere was the procedure always used.

For separation of the simple lipids, hexane:diethyl ether:acetic acid (70:30:1) was found to be an excellent solvent. While several different solvents were used for separation of phospholipids, chloroform:methanol:water (65:25:4) was excellent and was used for routine separations. Buranol:acetic acid:water (60:20:20) was used for comparative purposes with standards. When running phospholipids, the TLC plate was always prewashed in acetone:petroleum ether (1:3).

Since the simple lipids were only separated into major classes (i.e. diglycerides, triglycerides, free fatty acids, and hydrocarbon) and because the TLC separation worked so well, these could be identified simply by running a representative standard for each class.

PHB was identified by infrared spectrophotometry. The methanol precipitate from total lipids, obtained as described previously, was used for this purpose. The sample was dissolved in chloroform, dried on a KBr pellet, and scanned through the infrared using a Perkin Elmer Model 237B recording infrared spectrophotometer. The resulting spectrum was compared to the PHB spectra of Blackwood and Agnes (5). Comparison was also made with a spectrum prepared using a purified PHB standard isolated in this laboratory from Zoogloea ramigera

Because the phospholipids were separated to individual chemical compounds and because the phospholipids were of principal interest in this study, a more rigorous means of identification was pursued.

1. Of prime importance in identification of a phospholipid was TLC along with phospholipid standards (Supelco, Inc.) in at least 2 different solvents.
2. The various spray reagents described previously were used to identify unknown compounds.
3. Paper chromatography of the water soluble mild alkaline hydrolysis products was used to identify phospholipids. Phospholipids, separated by TLC as described previously, were eluted from the TLC plate with chloroform: methanol (2:1), concentrated, and dissolved in 1 ml of chloroform:methanol (1:4). Mild alkaline hydrolysis (i.e. removal of the fatty acyl esters) was accomplished by the following procedure:
 - a. To the 1 ml sample add 0.1 ml 1.2 N NaOH:water (1:1).
 - b. Mix well and incubate at 37 C. for 10 minutes.
 - c. Neutralize the mixture with 1 N acetic acid.
 - d. Add 2 ml chloroform:methanol (9:1).
 - e. Add 1 ml isobutanol.
 - f. Add 2 ml of water.
 - g. Shake well and centrifuge for 10 minutes at 300Xg.
 - h. Draw off the upper aqueous phase with a Pasteur pipette.
 - i. Re-extract the lower phase 2 times with 1 ml of methanol:water (1:2)

The water soluble hydrolysis products were run on descending Whatman #1 paper chromatograms using phenol saturated water:acetic acid:ethanol (100:10:2) solvent. Phospholipids (Supelco, Inc.) treated in the same manner were used as standards.

4. TLC of acid hydrolyzed water soluble mild alkaline hydrolysis products was also done. The water soluble products from mild alkaline hydrolysis were further hydrolyzed in 1 ml of 2 N HCL at 100 C. for 3 hours to release the nitrogenous constituents. These products were run on ascending silica gel TLC plates in isopropanol:28% ammonium hydroxide (7:3) against appropriate standards.
5. Phosphatidyl glycerol was identified by detecting the free glycol group. The analysis was performed by the following procedure:

- a. Scrape the proposed phosphatidyl glycerol spot from the TLC plate into a clean test tube.
- b. Add 0.5 ml 95% ethanol to elute.
- c. Add 0.5 ml 0.5 N H_2SO_4 and 0.1 ml of freshly made 0.1 M NaIO_4 .
- d. Incubate 15 minutes in the dark.
- e. Add 0.1 ml M NaHSO_3 .
- f. Mix and incubate 10 minutes.
- g. Add an equal volume of chromotropic acid reagent.
- h. Heat in a boiling water bath for 30 minutes.
- i. Read optical density at 570 nanometers.

Formaldehyde production was quantitated by referring to a standard curve prepared by treating various concentrations of formaldehyde with chromotropic acid reagent as above and plotting optical density against concentration. Phosphatidyl ethanolamine and silica gel were carried through this procedure as controls.

Stock chromotropic acid reagent consisted of 5% aqueous chromotropic acid. Working reagent contained 1 ml stock and 10 ml concentrated H_2SO_4 .

Developing a thin layer chromatogram through silica gel impregnated with silver nitrate is called argentation chromatography. Plates were prepared by spraying 3/4 of a standard silica gel TLC plate with 15% (w/v) AgNO_3 . By leaving 1/4 of the plate free of AgNO_3 , the first direction of development could proceed up through this strip of AgNO_3 free silica gel. The plate was then dried, turned 90 degrees, and developed through the AgNO_3 impregnated silica gel. A mixed phospholipid sample was processed in this manner developing in chloroform:methanol:water (65:25:4) in both directions.

Lipids were quantitated by the following techniques:

1. Gravimetric Analysis: Quantitation of PHB, total simple lipids, and total phospholipids by weight could be done with mg quantities of material. Samples were dried in preweighted aluminum weighing cups and weighed using an Ainsworth Analytical Balance. Whole cell lipids were compared to 20P membrane lipids.
2. Dichromate Oxidation: Lipids reduce $\text{Cr}_2\text{O}_7^{2-}$ to Cr^{3+} . Increased absorbance at 575 nanometers due to lipid oxidation was measured using a Gilford Model 2400 Recording Spectrophotometer. Acid dichromate reagent contained 2.5 gm $\text{K}_2\text{Cr}_2\text{O}_7$ in 1 liter of concentrated

H₂SO₄. Whole cell and membrane simple lipids were analyzed by the following procedure:

- a. Scrape the TLC spot into a clean test tube.
- b. Add 2 ml dichromate reagent.
- c. Shake tubes to mix contents.
- d. Incubate 45 minutes at 100 C. with periodic shaking.
- e. Centrifuge to pellet silica gel.
- f. Remove 1 ml of sample.
- g. Dilute with 5 ml water.
- h. Read optical density at 575 nanometers.

Use silica gel treated as above for the spectrophotometric blank.

3. Radioactive Phosphorus: P³² was used to quantitate phospholipids. To label the phospholipids, 1 mCi P³² or orthophosphate (Amersham-Searle) was added to 2 liters of CM medium in a vacuum flask. The flask was inoculated, gassed with methane:air (1:1), and incubated in a fume hood. During incubation, the culture was stirred with a magnetic stirring apparatus. Cells were harvested and phospholipids were obtained by the usual methods. Labeled phospholipids on a silica gel thin layer plate were analyzed in several ways.
 - a. The spots were located using a Baird-Atomic Deluxe Radiochromatogram Scanner Model RSC-363. The instrument was operated at 1100 volts with a detector gas consisting of 0.95% isobutane in helium. The scanner tracing served not only to locate the spots but to quantitate them. Peak areas were measured using an A.O. Ott planimeter.
 - b. The phospholipid spots were scraped from the TLC plate into polyethylene scintillation vials containing 10 ml of cocktail, and radioactivity was counted using a Packard Tricarb Liquid Scintillation Spectrophotometer. The scintillation cocktail contained the following:

Cabosil (Packard)	40 gm
PPO (Packard)	5 gm
Dimethyl PPO (Packard)	0.25 gm
Toluene	1 liter
 - c. The TLC plate containing labelled phospholipids was also analyzed

autoradiography. A sheet of Kodak X-ray film was placed over the TLC plate, and both were stored in a light tight box for 24 hours. The X-ray film was developed in Dektol (Kodak) for 3 minutes and fixed for 10 minutes.

Fatty acids of phospholipids were analyzed as follows:

1. Preparation of Methyl Esters: Deacylation and methylation were accomplished by mild methanolysis (131) after elution of the phospholipids from silica gel with chloroform:methanol (3:1).
2. Gas Chromatography of the Methyl Esters: Separation of the fatty acid methyl esters was achieved using a Varian Aerograph Model 200 Gas Chromatograph equipped with a flame ionization detector and a 8 ft x 1/8 inch diethylene glycol succinate column. Injector and detector were 200 C. while the column was 170 C. Nitrogen carrier gas was adjusted to 25 ml/min. Various size samples were injected with a 100 microliter syringe (Hamilton).
3. Detection of Unsaturation: Since saturated and monounsaturated fatty acids come off the column very close to one another, a large peak in the vicinity could be either one. The sample was mixed with a few drops of bromine water, and the resulting chromatogram was compared with that of an untreated sample. Bromine will change the column retention time of an unsaturated fatty acid.

RESULTS AND DISCUSSION

Because of its simplicity and better yields, the Folch extraction was used throughout this study rather than the Bligh and Dyer technique.

The methanol precipitate of the total lipid extract was identified as poly-beta-hydroxybutyrate. Results of an infrared spectrophotometric comparison of this precipitate with purified PHB are shown in Figure 38. The dominant characteristic of this spectrum is the large ester peak at 1725 cm^{-1} . These spectra both compare well with the published Bacillus megaterium PHB spectra of Blackwood and Agnes (5).

The results of a gravimetric analysis of whole cell and 20P membrane lipids are listed in Table 6. Only about 9.2% of the cell dry weight was extracted as lipid while 27.9% of the membrane dry weight extracted was lipid. This lipid enrichment in the membrane fraction would be expected since membranes

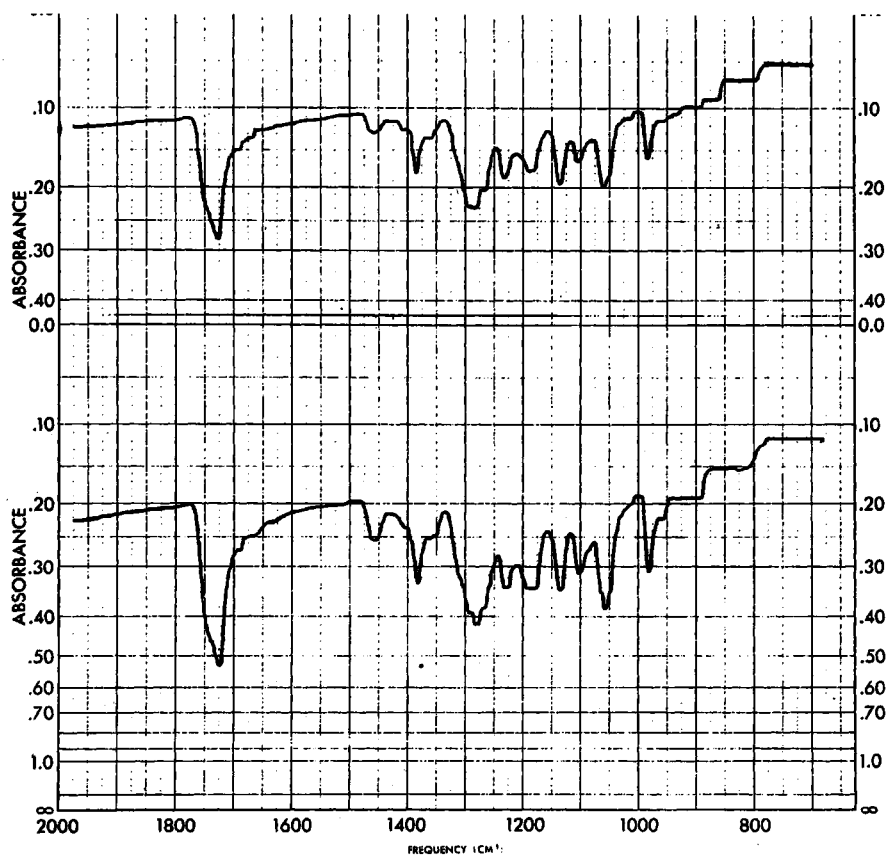


Figure 38. Infrared spectra of (upper spectrum) menthanol precipitate from total lipids of M. trichosporium and (lower spectrum) purified PHB.

TABLE 6

Graviometric analysis of lipid components of whole cells and membranes.

	<u>Weight Extracted From Cells (mg)</u>	<u>Weight Extracted From Membranes (mg)</u>
PHB	18.9	0.1
simple lipid	28.0	3.8
phospholipid	24.7	19.6
total	71.6	23.5

	<u>% Dry Weight of Cells</u>	<u>% Dry Weight of Membranes</u>
PHB	2.4	0.11
simple lipid	3.6	4.5
phospholipid	3.2	23.3
total	9.2	27.9

	<u>% Dry Weight of Total Cell Lipids</u>	<u>% Dry Weight of Total Membrane Lipids</u>
PHB	26.4	0.4
simple lipid	39.1	16.2
phospholipid	34.5	83.4

are basically lipid-protein structures. This compares very favorably with previous reports of 24% lipid in inner mitochondrial membrane and 25% lipid in Gram positive bacteria plasma membrane (39). However these in turn are very different from the 42% lipid in liver cell membranes, 43% lipid in erythrocyte membranes, and 75% lipid in myelin (39). Myelin may have increased lipid because of its requirement for insulation. The relatively low lipid in these intracytoplasmic membranes probably indicates the important enzymatic role (ergo, more protein) performed by these internal membranes. The relatively large amount of PHB found in whole cells (i.e. 26.4% of total lipid) indicates that this compound must play an important role in the physiology of this organism. Presumably, the trace of PHB in the membrane sample was due to contamination. The percent phospholipid was greatly increased from the 34.5% of whole cell lipids to 83.4% in the membrane sample. This would be expected since phospholipids almost exclusively comprise bacterial membrane lipids. This value is higher than the 67% phospholipid reported for erythrocyte membranes (39), but it is not unusual because eucaryotic membranes contain steroids while procaryotic membranes usually do not. Because of the relatively large amount of phospholipid and because of their importance in membrane structure, the phospholipids were investigated more intensely in this study.

The results of the simple lipid separation are listed in Table 7. Spot #1 (simple lipid #1 or SL-1) was identified as hydrocarbon, SL-2 was identified as triglyceride, SL-3 was identified as free fatty acid, SL-4 was identified as 1, 3-diglyceride, and SL-5 was tentatively identified as 1, 2-diglyceride based upon the fact that it is a common lipid component and is known to migrate slightly behind 1, 3-diglyceride in this solvent.

Quantitative data from the simple lipid analysis are shown in Table 8. The fact that whole cell simple lipids were different from membrane simple lipids could be expected, but the magnitude of the difference was surprising. Even though simple lipids are relatively minor components, their composition in membranes was found to be very different from that of whole cells. The predominance of triglycerides in whole cells is not unusual since these simple lipids are commonly reported in bacteria although usually in lower quantities (84). The prevalence of free fatty acids in membrane simple lipids is not unusual either because of the amphipathic nature of these molecules. With their part hydrophilic and part hydrophobic structure, fatty acids fit

TABLE 7

R_f values of cell and membrane simple lipids and standards on silica gel TLC in hexane-diethyl etheracetic acid.

<u>Spot #</u>	<u>R_f</u>
1	.95
2	.66
3	.44
4	.36
5	.27

<u>Standard</u>	<u>R_f</u>
free fatty acid	.44
triglyceride	.64
1,3-diglyceride	.36
hydrocarbon	.96

TABLE 7

Quantitative analysis of simple lipids from whole cells and membranes.

	Percent of Total Simple Lipid	
	<u>Whole Cells</u>	<u>Membranes</u>
hydrocarbon	6.8	43.5
triglycerides	73.7	6.7
diglycerides	2.5	0
free fatty acids	17	49.8

nicely into membrane structure as currently theorized. However, the large amount of hydrocarbon found in the membrane fraction is difficult to explain. Whatever role hydrocarbons play in membrane structure, they must be isolated in the hydrophobic regions of the membrane interior.

Five phospholipids were detected by TLC. The same five spots in the same ratios were detected whether analyzing whole cells or membranes. This was expected since nearly all cellular phospholipids are in membranes (83). A summary of the TLC data for membrane phospholipids is shown in Table 9. By comparing these data with the R_f values of phospholipid standards listed in Table 10, the phospholipids were identified. Phospholipid #1 (PL-1) was identified as diphosphatidyl glycerol; PL-2 was identified as phosphatidyl ethanolamine; PL-3 was identified as phosphatidyl glycerol; PL-4 was identified as phosphatidyl serine; PL-5 was identified as phosphatidyl choline. Since PL-5 was not Dragendorff positive, it could be a lysocompound. However, in view of the unreliability of the Dragendorff test and since this spot ran with phosphatidyl choline in 2 solvents, this was ample evidence to identify PL-5 as phosphatidyl choline.

Results of the argentation TLC are listed in Table 11. Development in the second direction through silver nitrate did not yield any further separation of the individual spots. This indicated homogeneity of the spots. If there were different species varying in fatty acid saturation, they would have separated in the second direction. Diphosphatidyl glycerol was not present in sufficient quantity to be detected on this plate. Further evidence of phospholipid homogeneity will be described later.

The results of the phospholipid hydrolysis experiments are listed in Table 12. Only the hydrolysis products of phosphatidyl ethanolamine were detected, presumably because of their quantity and ninhydrin reactivity. The water soluble products ran exactly with the appropriate standards and verify the identification of PL-2 as phosphatidyl ethanolamine.

Table 12 shows the results of the glycol analysis with PL-3; PL-2 and silica gel were used as controls. A thousand times more formaldehyde was produced with PL-3 than with either of the other samples. This supports the identification of PL-3 as phosphatidyl glycerol.

An autoradiogram of a thin layer plate after separation of phospholipids labeled with P^{32} is shown in Figure 39. This autoradiogram verifies the previous identification of 5 phospholipid spots. Relative abundance is also

TABLE 9

Summary of silica gel TLC data concerning membrane phospholipids.

	<u>1</u>	<u>2</u>	<u>3</u>	<u>4</u>	<u>5</u>
R _f in CMW ¹	.53	.39	.32	.21	.18
R _f in BAW ²	.57	.38	.48	.48	.23
ninhydrin	-	+	-	+	-
iodine	+	+	+	+	+
plasmalogen	-	-	-	-	-
orcinol	-	-	-	-	-
Goswami	+	+	+	+	+
Dragendorff	-	-	-	-	-

1 Chloroform:methanol:water (65:25:4)

2 Butanol:acetic acid:water (60:60:20)

TABLE 10

R_v values of phospholipid standards.

	R_f	
	<u>CMW¹</u>	<u>BAW²</u>
diphosphatidyl glycerol	.53	.57
phosphatidyl ethanolamine	.39	.38
phosphatidyl serine	.22	.45
phosphatidyl choline	.19	.23
phosphatidyl glycerol	.33	.49

1 Chloroform:methanol:water (65:25:4)

2 Butanol:acetic acid:water (60:20:20)

TABLE 11

R_f values for membrane phospholipids on argenation TLC plates.

	<u>1st</u>	R_f <u>2nd</u>
phosphatidyl ethanolamine	.39	.43
phosphatidyl glycerol	.32	.43
phosphatidyl serine	.21	.44
phosphatidyl choline	.18	.58

TABLE 12

R_f values for the hydrolysis products of phosphatidyl ethanolamine compared to standards.

A. Water soluble mild alkaline hydrolysis proudct.

	R_f
glycerophosphorylethanolamine	.74
hydrolysis product A	.72
glycerophosphorylserine	.39

B. Acid hydrolyzed product A.

	R_f
ethanolamine	.25
hydrolysis product B	.25
serine	.22

TABLE 13

Formaldehyde quantitation after periodate oxidation of phospholipids.

	<u>Color</u>	<u>Formaldehyde (micromoles)</u>
Blank	brown	less than 0.01
PL-2	brown/purple	0.01
PL-3	purple/black	10

in the autoradiogram with phosphatidyl ethanolamine and phosphatidyl glycerol comprising the bulk of the phospholipids. The radiochromatogram scanner tracing of this TLC plate is shown in Figure 40, and the relative peak areas from this tracing are listed in Table 14. Scintillation counts of spots scraped from these plates are listed in Table 15. From these data, it was observed that 93-94% of the total phospholipid consisted of phosphatidyl ethanolamine and phosphatidyl glycerol. The rest of the phospholipids made up about 6% of the total. It is not unusual for these 2 phospholipids to comprise 70-85% of total phospholipids in bacteria, but the magnitude of predominance found in this study is higher than normally observed. Several structurally and physiologically similar bacteria also have this higher percentage of phosphatidyl ethanolamine and phosphatidyl glycerol. For example, among the photosynthetic bacteria, these two phospholipids constitute 100% of the total in *Chromatium*, 98% of the total in *Rhodopseudomonas gelatinosa*, 90% of the total in *Rhodopseudomonas spheroides*, and 86% of the total in *Rhodospirillum rubrum* (83). Within the nitrifying bacteria, these two phospholipids account for 95% of the total phospholipids in both *Nitrocystis oceanus* and *Nitrosomonas europea* (40). The significance of this phospholipid composition is unknown, but the similarities with the other bacteria with intracytoplasmic membranes are obvious.

The results of the fatty acid analysis of these phospholipids is shown in Table 16. In view of the reduction of the major peak after bromine addition, it was identified as monounsaturated 10:1 fatty acid as opposed to 18:0 which also comes off in the vicinity of this very large peak. These results are similar to the report of Smith and Ribbons (115) concerning phospholipids from *Methanomonas methanoxidans* where over 90% of the esterified fatty acid was 18:1. Lack of diversity of fatty acids and a preponderance of 1 particular fatty acid is more characteristic of eucaryotic phospholipids than bacterial phospholipids which usually contain a variety of fatty acids. For example, White (131) described 36 relatively evenly distributed fatty acids ranging from 12-22 carbons in the phospholipids of *Haemophilus parainfluenzae*. Once again of interest are similarities between *M. trichosporium* and the photosynthetic and nitrifying bacteria. The ammonia oxidizing bacteria show a preponderance of 16:1 esterified fatty acid in the phospholipids while the nitrite oxidizing bacteria have mostly 18:1 fatty acid (7). Among the photosynthetic bacteria, *Rhodomicrobium vannielii* has 90% 18:1 fatty

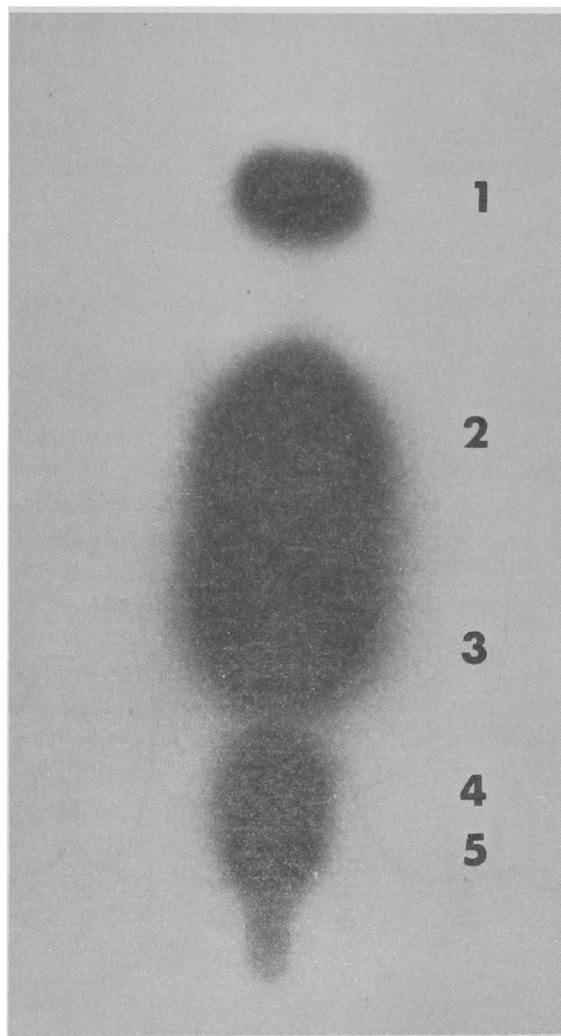


Figure 39. Autoradiogram of P^{32} labeled phospholipids separated by TLC.

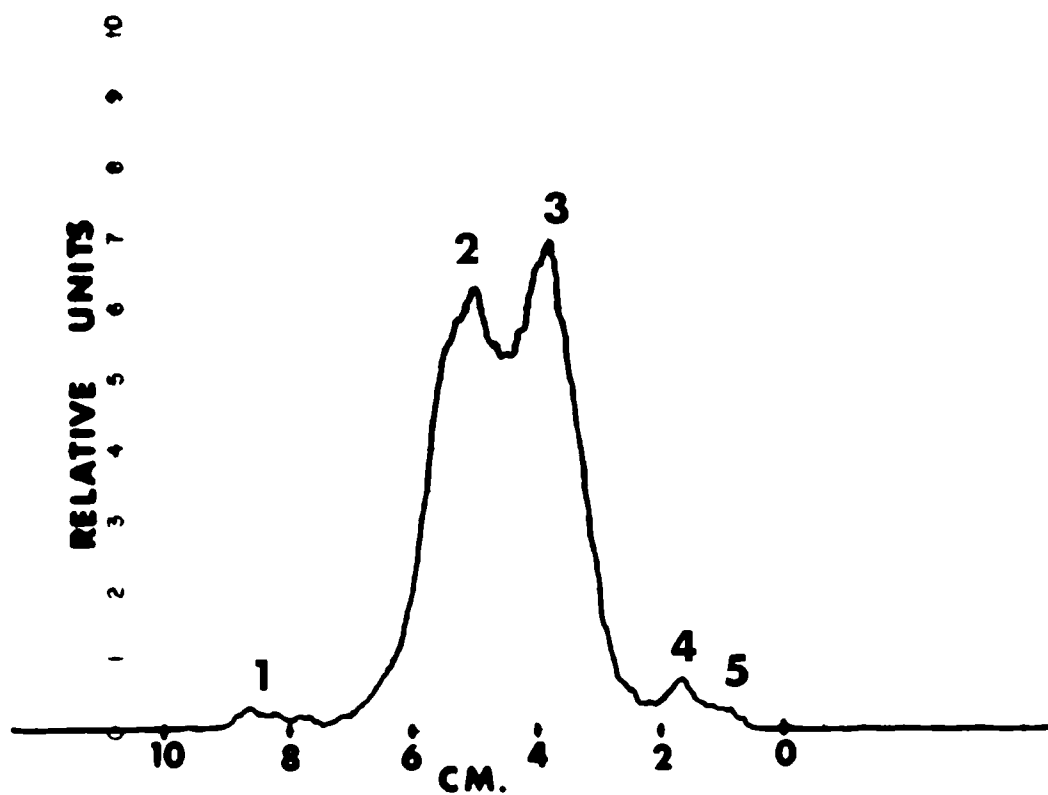


Figure 40. Radiochromatogram scanner tracing of P^{32} labeled phospholipids separated by TLC.

TABLE 14

Relative peak areas from radiochromatogram scanner tracing
of P^{32} labeled phospholipids separated by TLC.

	<u>Relative Area</u>	<u>% Total Activity</u>
diphosphatidyl glycerol	5	2
phosphatidyl ethanolamine	106	44
phosphatidyl glycerol	118	49
phosphatidyl serine	8	3
phosphatidyl chlorine	4	2

TABLE 15

Scintillation spectrophotometric quantitation of
p³² labeled phospholipids scraped from TLC plate.

	<u>C.P.M.</u>	<u>% Activity</u>
diphosphatidyl glycerol	2,956	1
phosphatidyl ethanolamine	150,198	37
phosphatidyl glycerol	229,583	57
phosphatidyl serine	16,862	4
phosphatidyl choline	2,419	1

TABLE 16

Fatty acid compositions of the phospholipids of *M. trichosporium*.

	Percent Total		
	<u>16:0</u>	<u>16:1</u>	<u>18:1</u>
diphosphatidyl glycerol	0	13	87
phosphatidyl ethanolamine	0.2	10.9	88.9
phosphatidyl glycerol	1	16	83
phosphatidyl serine	0	13	87
	<u>Ratio 18:1 to 16:1 to 16:0</u>		
fatty acids before bromine	190:50:1		
after bromine	4:1:1		

acid in its phospholipids, Rhodopseudomonas capsulata has 94.6% 18:1 fatty acid, and Rhodopseudomonas spheroides has 76.8% 18:1 fatty acid in its phospholipids (83). Similarity of fatty acid composition of phospholipids could be advantageous to an organism by facilitating transfer of components among the various phosphatides. This could be especially important to an organism whose metabolism is very dependent upon complex membrane systems and may explain the lack of diversity among the phospholipid fatty acids in M. trichosporium. The reason for the preponderance of 18:1 fatty acid is more difficult to explain. This is the longest fatty acid (with respect to the fatty acids normally found in bacteria) that would remain liquid at normal physiological temperatures. However, why only certain organisms have large amounts of 18:1 fatty acid is unknown. While the morphological and biochemical similarities among the methane oxidizing bacteria, photosynthetic bacteria, and nitrifying bacteria are obvious and interesting, their explanation and possible relationship remains to be elucidated.

Thus, the phospholipid compositions and phospholipid fatty acid compositions of membraneous bacteria are unique and rigidly uniform. Therefore, these could serve as biochemical labels for detecting and quantitating methane oxidizing bacteria in aquatic ecosystems.

8. PROTEINS OF CELLS AND MEMBRANES

Proteins, along with lipids which were discussed in the preceding section, are also major membrane constituents. In this study, membrane proteins of M. trichosporium were examined as chemicals and as enzymes.

MATERIALS AND METHODS

Protein amino acid composition was determined by a thin layer chromatographic system that resulted in separation of polar amino acids (i.e. glutamic acid, aspartic acid, lysine and arginine) from the apolar amino acids (i.e. all other amino acids). Membrane preparations were analyzed as follows:

1. Hydrolyze the sample in 6 N HCl for 36 hours at 110 C.
2. Evaporate the HCl, add water, and evaporate again.
3. Dissolve the amino acids in 0.1 ml water.
4. Spot the amino acid mixture on a silica gel TLC plate.
5. Develop in 95% ethanol:28% ammonium hydroxide (7:3).
6. Scrape the polar and apolar amino acid fractions, determined by running appropriate standards, into test tubes.
7. Elute the amino acids with 2 ml water.
8. Pellet the silica gel by centrifugation.
9. Remove 1 ml of sample, and quantitate the amino acids by the procedure described in the following section.

Amino acids were quantitated by the procedure of Rosen (1957).

Polyacrylamide gel electrophoresis was used to examine the size of membrane proteins. Proteins were solubilized from membranes by heating for 5 minutes in 5% sodium dodecyl sulfate (SDS) at 100 C. The sample was mixed with 1/2 volume of glycerol to facilitate layering on the gel.

The electrophoretic buffer was 0.05 M phosphate containing 0.1% SDS (w/v). The gel contained 7.5% acrylamide (Eastman Organic Chemicals) and 0.1% (w/v) methylene-bis-acrylamide (Eastman Organic Chemicals) in the SDS buffer. The mixture was polymerized with 0.2 ml of freshly made ammonium persulfate (Bio Rad) and 0.02 N,N',N',-tetramethylethylenediamine (Bio Rad).

Using a multitube electrophoresis apparatus, the gels were washed at 5 amps/gel for 30 minutes. Samples were they layered on the gels with a pipette,

and 2 amps/gel was applied for 30 minutes to move the samples into the gels. The gels were then run at 5 amps/gel for 1 hour. The gels were stained with 0.1% Amido Black (w/v) in ethanol:glacial acetic acid:water (20:7:73). The gels were decolorized and stored in 7% (v/v) glacial acetic acid. Bovine serum albumin (Sigma) was used as a standard. It contains a monomer with a molecular weight of 60,000 and a dimer with a molecular weight of 120,000. Molecular weights of membrane proteins were read from a standard curve prepared by plotting the log of the molecular weight of BSA standard versus migration distance.

Membrane cytochromes were examined using a Shimadzu Model MPS-50L Recording Spectrophotometer. Samples were scanned from 350 to 650 nanometers against a buffer blank or alternatively, oxidized versus reduced samples were used. Samples were reduced by adding a few grains of sodium dithionite and oxidized by adding a drop of hydrogen peroxide.

Various substrates were tested for their ability to reduce cytochromes in a 10S fraction. Methane was added as a drop of methane saturated buffer or by bubbling gas through the curvette. Methanol was added by the drop. Formaldehyde and formic acid were added dropwise as aqueous solutions.

Enzymes were prepared by growing, disrupting, and centrifuging cells as explained previously except the 20S fraction was centrifuged for 30 minutes at 100,000 X g. The 100,000 g pellet (100P) suspended in 0.05 M phosphate buffer pH 7 was used as a membrane enzyme preparation and the 100S fraction was used as a extra-membrane enzyme preparation. The sources of the chemicals used in the enzyme assays will be listed at the end of this section.

A. L-serine:tetrahydrofolate 5,10-hydroxymethyl transferase

This enzyme was assayed spectrophotometrically by measuring the reduction of NADP as described by Hatefi et al. (1957). The reaction mixture contained the following:

serine	10 micromoles
tetrahydrofolic acid	0.6 micromoles
NADP	0.6 micromoles
sodium phosphate (ph 7.5)	100 micromoles
enzyme preparation	0.1 ml
water	to make 3 ml

Change in optical density at 340 nanometers was measured using a Gilford

Model 2400 Recording Spectrophotometer. The extinction coefficient of NADH and NAD H is $6.22 \times 10^6 \text{ cm}^2/\text{mole}$. Controls containing NADPH, everything but substrate, and everything but enzyme were also run.

B. Formate:NAD Oxicoreductase

This enzyme was assayed as explained in the preceding section except NAD reduction was measured. The reaction mixture contained the following:

sodium phosphate (pH 7.5)	100 micromoles
NAD	10 micromoles
sodium formate	20 micromoles
enzyme preparation	0.1 ml
water	to make 3 ml

C. Formaldehyde:NAD Oxidoreductase

This enzyme was assayed as in part B. The reaction mixture contained the following:

sodium phosphate (pH 7.5)	100 micromoles
NAD	10 micromoles
Formaldehyde	20 micromoles
enzyme preparation	0.1 ml
water	to make 3 ml

D. D-glycerate:NAD Oxidoreductase

This enzyme was assayed spectrophotometrically as explained previously except NADH oxidation was measured. The reaction mixture contained the following:

sodium phosphate (pH 7.5)	100 micromoles
NADH	0.5 micromoles
3-hydroxypyruvate	10 micromoles
enzyme preparation	0.1 ml
water	to make 3 ml

E. 3-hydroxybutyrate:NAD Oxidoreductase

This enzyme was assayed spectrophotometrically as in section B. The reaction mixture contained the following:

sodium phosphate (pH 7.5)	100 micromoles
NAD	10 micromoles
3-hydroxybutyrate	20 micromoles

enzyme preparation	0.1 ml
water	to make 3 ml

F. Methanol:NAD Oxidoreductase

This enzyme was assayed spectrophotometrically as explained in part B. The reaction mixture contained the following:

Tris (pH 9)	0.3 millimoles
Methanol	20 micromoles
NH ₄ Cl	45 micromoles
NAD	10 micromoles
enzyme preparation	0.1 ml
water	to make 3 ml

G. NAD Independent Methanol Dehydrogenase

This enzyme was assayed similar to the preceding assay except NAD was deleted from the above reaction mixture and 3.3 micromoles phenazine methosulfate and 0.14 micromoles dichlorophenolindophenol were added. Optical density was measured at 600 nanometers.

H. NADH:Cytochrome C Oxidoreductase

This enzyme was assayed spectrophotometrically by measuring cytochrome reduction at 550 nanometers. The reaction mixture contained the following:

sodium phosphate (pH 7.5)	100 micromoles
cytochrome C (oxidized)	0.5 micromoles
NADH	0.5 micromoles
enzyme preparation	0.1 ml
water	to make 3 ml

I. ATP Phosphohydrolase

This enzyme was assayed by measuring the release of inorganic phosphate from ATP after 5 minutes reaction time. Controls minus substrate or enzyme were also analyzed. The reaction mixture contained the following:

ATP	100 micromoles
Histidine Buffer (pH 7.5)	100 micromoles
HgCl ₂	5 micromoles
enzyme preparation	0.1 ml
water	to make 3 ml

The histidine buffer was prepared as 0.2 M histidine in 0.15 KCl, pH 7.5.

The inorganic phosphate assay was that of Ames.

Histidine, cytochrome C, NADH, 3-hydroxybutyrate, 3-hydroxypyruvate, serine, tetrahydrofolic acid, NADP, and phenazine methosulfate were obtained from Nutritional Biochemicals Corp. ATP and NAD were obtained from General Biochemicals Corp. Tris was obtained as Trizma Base from Sigma Chem. Corp. Methanol, ammonium chloride, formaldehyde, and ammonium molybdate were obtained from J.T. Baker Co. DCIP and sodium formate were purchased from Fisher Chem. Co. Ascorbic acid was obtained from Merck and Co.

RESULTS AND DISCUSSION

The suggestion that membranes tend to have less polar amino acids than other proteins was made by Vanderkooi and Capaldi (124). Vanderkooi and Capaldi used a relatively complex procedure for their analyses which required knowledge of absolute amino acid composition for computations. Therefore, one of the goals in this study was to investigate the proposal of Vanderkooi and Capaldi by simpler and faster techniques. The percent polarity for 100 ~~non~~membrane proteins whose composition is listed in the Handbook of Biochemistry (106) was compiled in Figure 41. The average polarity of these nonmembrane proteins was 33%. These computations were done to serve as the norm for subsequent amino acid analyses.

The observed R_f values for 19 amino acids in the previously described silica gel TLC system are listed in Table 17. The apolar amino acids have R_f values greater than 0.5 while the polar amino acids were less than 0.5. This convenient separation made it possible to perform this amino acid polarity study. The results of the polarity analyses are shown in Table 18. The whole cell and 80S samples both fall near the mean polarity of the nonmembrane protein analysis. All the membrane fractions had increased levels of apolar amino acids and exhibited a very low polarity as compared to the nonmembrane proteins in Figure 41. This can be explained by the hypothesis that if membranes contained excesses of polar amino acids, they would become solubilized in water and could not function as a carrier in an aqueous environment.

The detection of low polarity proteins is good evidence for the presence of membrane proteins. This could serve as a biochemical handle for detecting and quantitating membranous microorganisms, i.e. algae, blue-green algae,

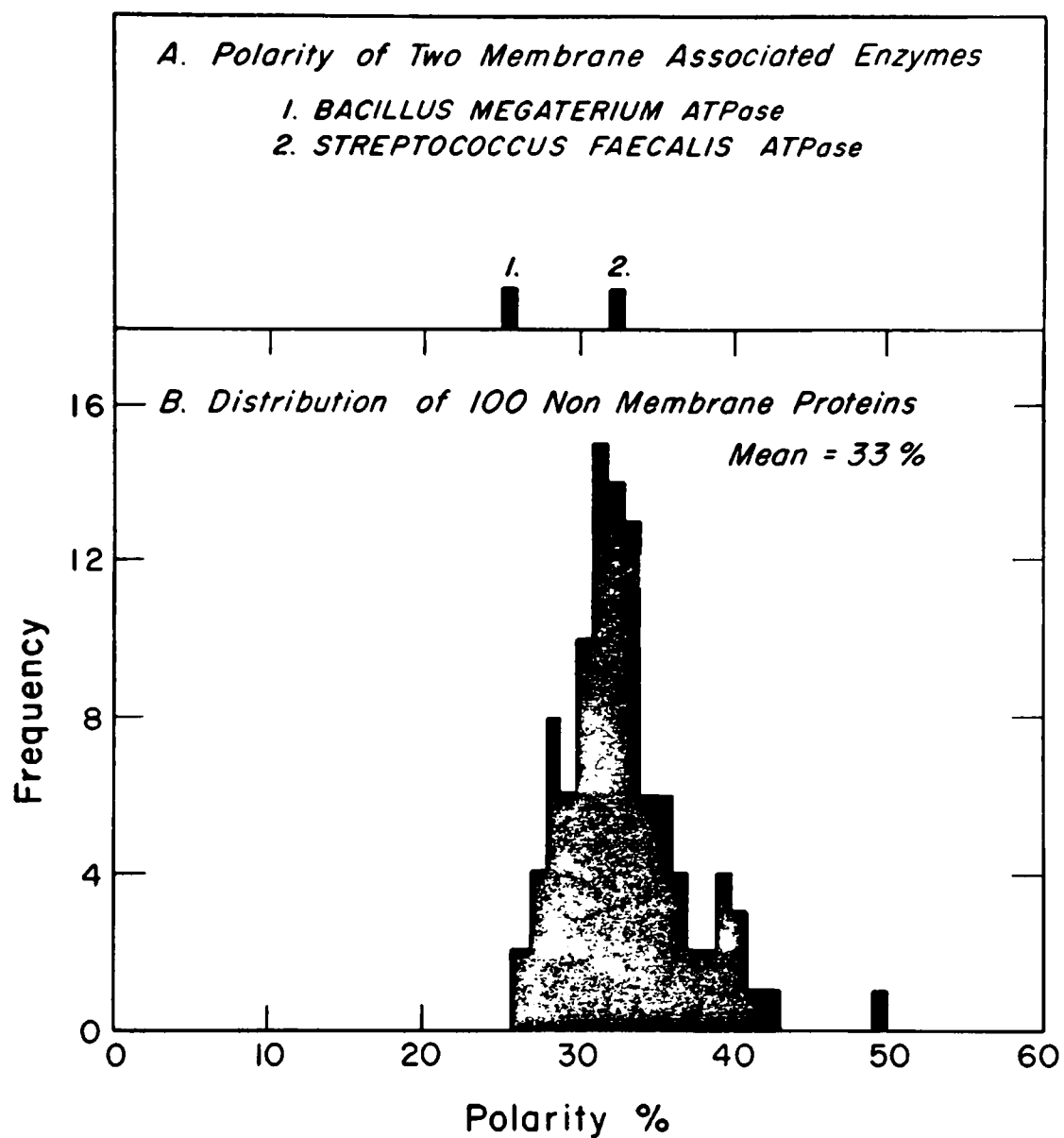


Figure 41. Histogram showing (A) polarity of 2 membrane associated enzymes and (B) distribution of polarity among 100 nonmembrane proteins.

TABLE 17

R_f values for amino acids on silica gel TLC plates developed with ethanol and ammonium hydroxide.

<u>Amino Acid</u>	<u>R_f</u>
phenylalanine	.75
leucine	.75
isoleucine	.75
tryptophane	.74
methionine	.70
valine	.69
alanine	.67
threonine	.66
histidine	.64
serine	.62
glycine	.62
proline	.59
hydroxy proline	.59
cystine	.58
cysteine	.58
glutamic acid	.49
aspartic acid	.33
lysine	.25
arginine	.22

TABLE 18

Polarity of amino acids in various protein samples from M. trichosporium.

<u>Sample</u>	<u>Apolar</u>	<u>Polar</u>
whole cells	68.4	31.6
10P	71.6	28.4
20P	73.9	26.1
80P	71.4	28.6
80S	67.2	32.8

photosynthetic bacteria, nitrifying bacteria, and methane oxidizing bacteria, in aquatic ecosystems. These membranous microbes are all intimately related to the eutrophication process.

A photograph of the stained membrane protein polyacrylamide gels is shown in Figure 32, and the appropriate molecular weights of the proteins are listed in Table 19. Guidotti (38) observed 9 proteins in human erythrocyte membranes ranging in molecular weight from 25,000 to 250,000. Two of these proteins (47,000 and 80,000) had identical molecular weights to M. trichosporium intracytoplasmic membrane proteins. The intracytoplasmic membranes analyzed in this study contained 5 major proteins ranging in molecular weight from 47,000 to 180,000 which is similar to the distribution reported by Guidotti (38) with erythrocyte membranes. Due to the problem of obtaining solubilized membrane protein in sufficient quantities to detect on a gel, the proteins observed in this study probably represent only the major membrane proteins. Membrane enzymes, for example, that may be required in catalytic amounts probably wouldn't have been detected by this technique.

Results of a spectrophotometric examination of an 80P membrane preparation indicated that the oxidized spectrum absorbed maximally at 410 nanometers, and the reduced spectrum has absorbance peaks at 416, 522, and 550 nanometers, which is the spectrum of a C type cytochrome. The shift of the gamma or Soret peak to a longer wavelength, i.e. 410 to 416 nanometers, and the appearance of the alpha and beta peaks, i.e. 550 and 522 nanometers, when reduced are typical of C cytochromes. More specifically, these data correspond to cytochrome C₂. Previously reported cytochromes categorized as C₂ include the cytochrome C from denitrifying bacteria with reduced absorption peaks at 550, 522, and 416 nanometers and oxidized Soret peak at 410 nanometers, and a C cytochrome from Rhodospirillum rubrum which absorbs maximally when reduced at 550, 521, and 416 nanometers and at 409 nanometers when oxidized (76). Once again, similarities among this methane oxidizing bacterium, the photosynthetic, and the nitrifying bacteria are evident. Upon close examination of the reduced spectrum, a shoulder could be seen at 445 nanometers. All peaks were enhanced by using oxidized membranes in the reference cuvette against reduced membranes in the sample cuvette. The small shoulder was much better resolved in the difference spectrum and absorbed maximally 445, 600, and 630 nanometers which is characteristic of cytochrome A. C cytochromes have a reduction potential around 220 millivolts

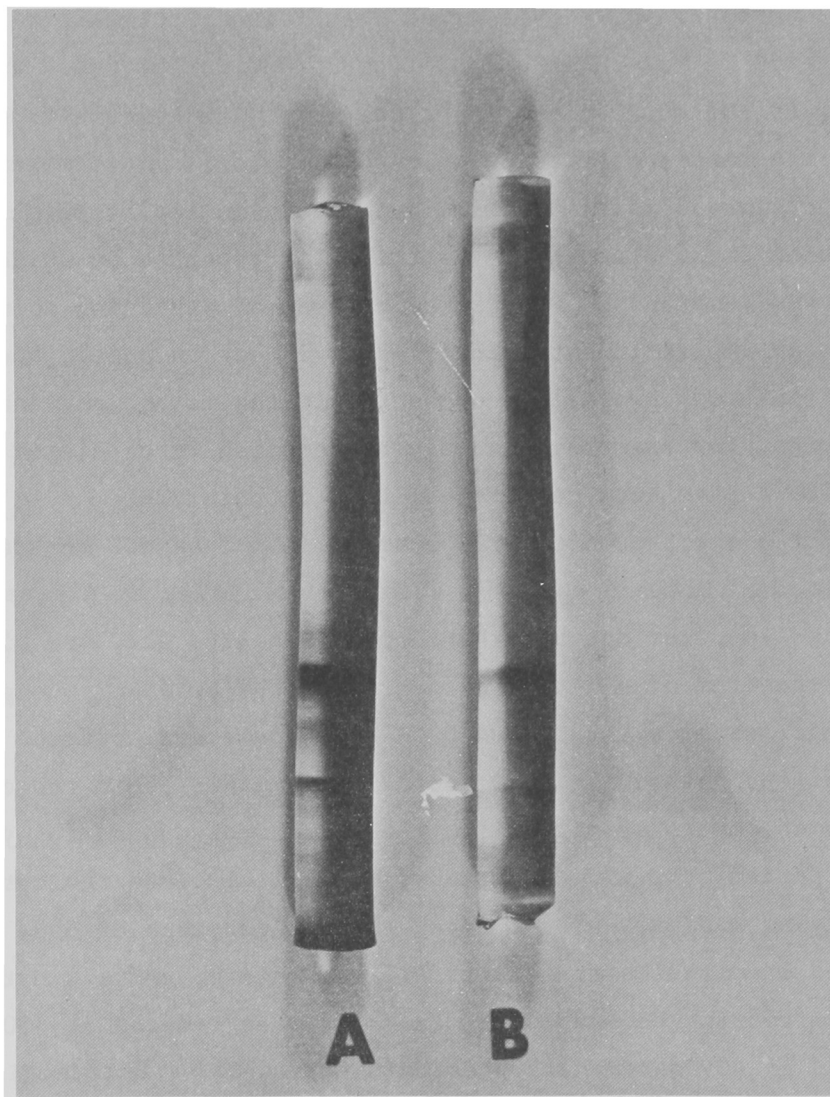


Figure 42. Photograph of electrophoretic polyacrylamide gels containing (A) bovine serum albumin and membrane proteins, and (B) bovine serum albumin.

TABLE 19

Migration distances and molecular weights of membrane proteins and bovine serum albumin standard as related to polyacrylamide gel electrophoresis.

	<u>Migration Distance (mm)</u>	<u>Molecular Weight</u>
BSA (monomer)	22	60,000
BSA (dimer)	13	120,000
membrane protein 1	25	47,000
membrane protein 2	18	80,000
membrane protein 3	12	125,000
membrane protein 4	9	160,000
membrane protein 5	7	180,000

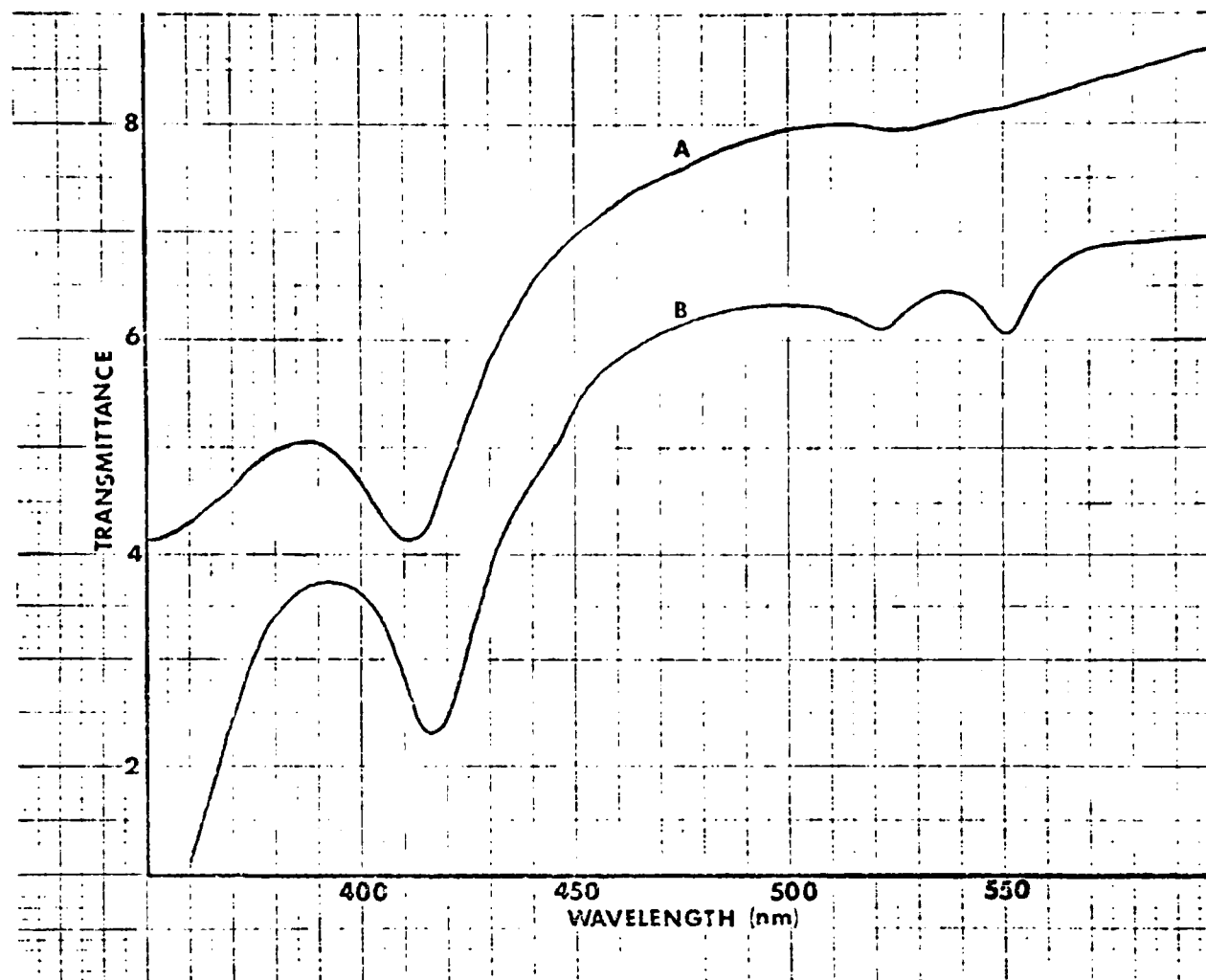


Figure 43. Absorption spectra of a 80P membrane preparation from *M. trichosporium* when (A) oxidized and (B) reduced.

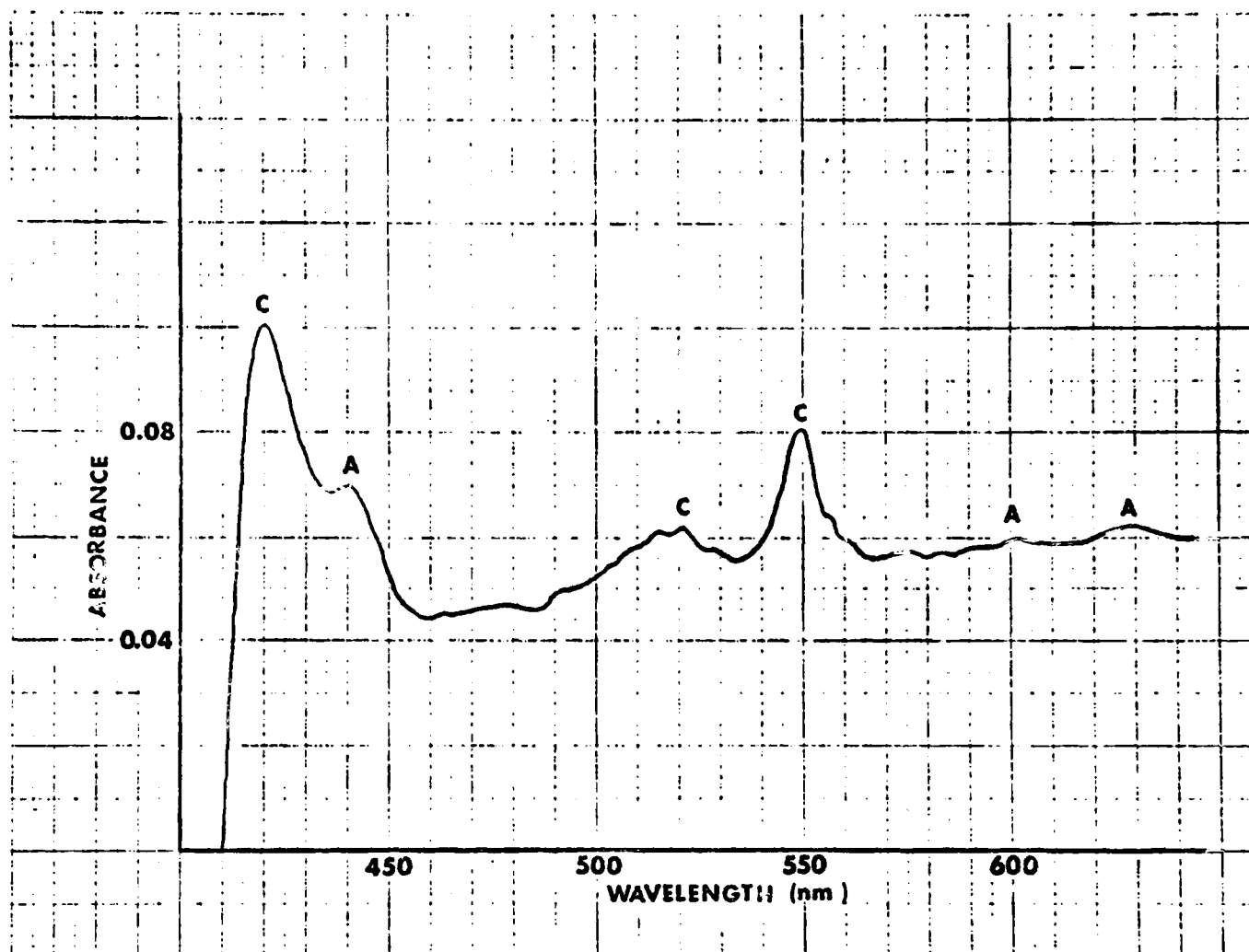


Figure 44. Difference spectrum of oxidized 80P membranes versus reduced 80P membranes.

and A cytochromes are around 300 millivolts. Assuming these two components function in an electron transport system, the flow of electrons would be from cytochrome C_2 to cytochrome A to oxygen. There are probably other carriers in this electron transport chain between cytochrome C_2 and NAD, however, these remain to be found. Oxidation of NADH and the intermediates in the methane oxidization pathway could be coupled to cytochrome reduction. The addition of methanol, formaldehyde, formate, and NADH to the 20S fraction resulted in cytochrome C_2 reduction as evidenced by the shift in the Soret peak and the appearance of the alpha and beta peaks. The results with methane were inconclusive but it certainly didn't reduce the cytochrome C_2 like the other compounds. This is consistent with the earlier observation that only 1 oxygen atom is consumed per oxidative step in the oxidation of methane by M. trichosporium. If the initial step in methane oxidation, which is probably a monooxygenase, resulted in cytochrome reduction, then 2 oxygen atoms would be required for this step.

The detection of C_2 cytochrome could serve as biochemical label for membranous bacteria which are deeply implicated in eutrophication. C_2 cytochrome is easily released from membranes, is usually present in high concentration, is easily detected, and is specific for these bacteria.

In order to avoid confusion, the Commission on Enzymes of the International Union of Biochemistry (CEIUB) numbers, systematic names, trivial names, and reactions of the enzymes assayed are listed in Table 20. Results of the various enzyme assays are shown in Figures 36-42. The initial velocities and activities of the enzymes are listed in Table 20.

The activities of the enzymes range from 0.87 to 2700 nanomoles/minute/mg protein. In this study, formaldehyde dehydrogenase had the lowest activity. This enzyme could function as a control point for the channeling of carbon into cell materials. The separation of activity between cytoplasm and membrane is very evident in these data. It is proposed that the extra-membrane enzymes are cytoplasmic rather than contained inside membrane vesticles. This is based upon the observation that many vesticles in the membrane fractions appear intact and yet most of the enzymes are restricted either to cytoplasm or membrane with no overlap of activity. If the enzymes were intravesticular, overlap of activity would be expected. The overlap of activity with ATPase has been observed before with other bacteria (107) and may be due to release of membrane bound enzyme, or to the fact that the ATPase is

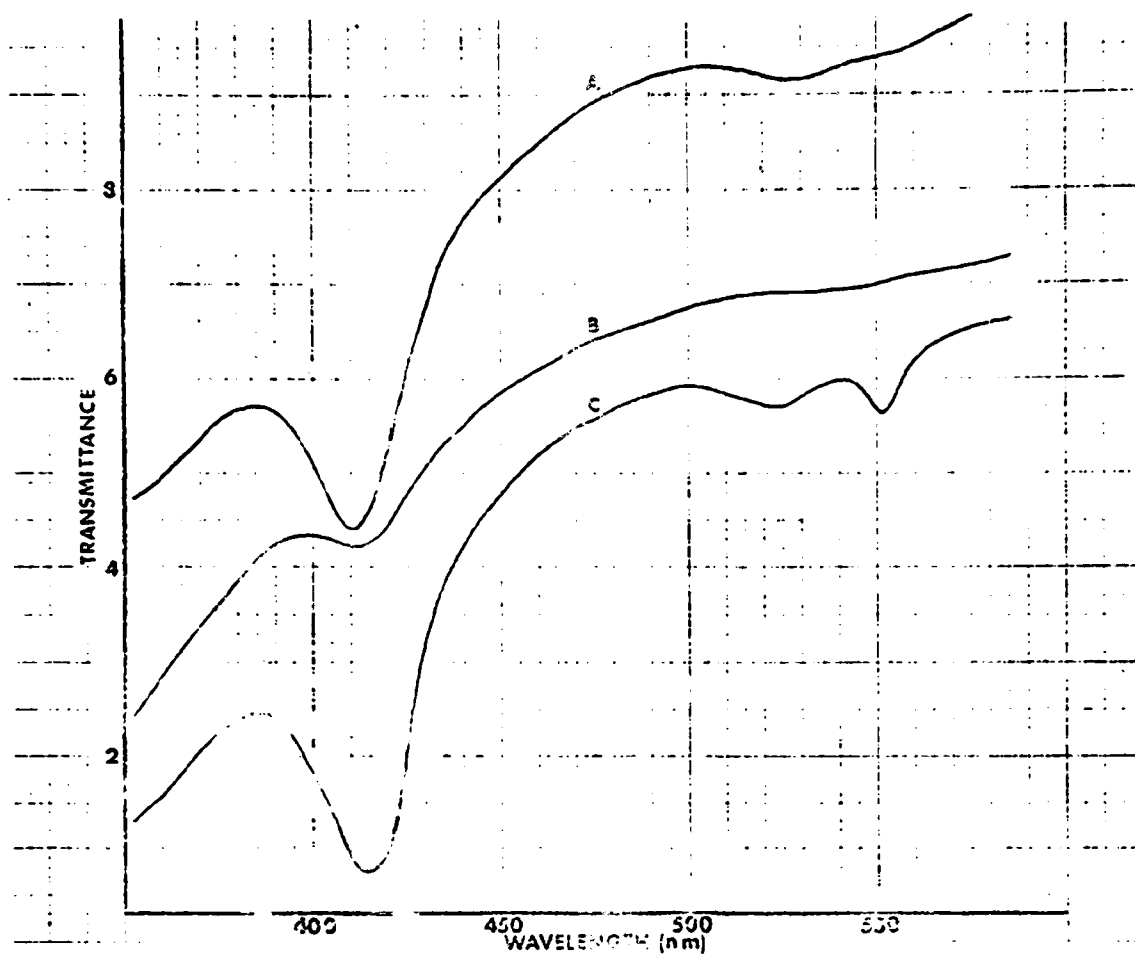


Figure 45. Absorption spectra of 20S centrifugation fractions. Spectra represent (A) oxidized spectrum, (B) sample plus methane, and (C) sample plus methanol, formaldehyde, formate, or NADH.

TABLE 20

Enzyme nomenclature listing (1) CEIUB number
(2) systematic name (3) trivial name (4) reaction.

- A.
1. 2.1.2.1
 2. L-serine:tetrahydrofolate 5,10-hydroxymethyl transferase
 3. serine trans hydroxymethylase
 4. L-serine + tetrahydrofolate = glycine + 5,10-methylene THF
- B.
1. 1.1.1.1
 2. alcohol:NAD oxidoreductase
 3. alcohol dehydrogenase
 4. alcohol + NAD = aldehyde or ketone + NADH
- C.
1. 1.2.1.3
 2. formaldehyde:NAD oxidoreductase
 3. formaldehyde dehydrogenase
 4. formaldehyde + NAD = formate + NADH
- D.
1. 1.2.1.2
 2. formate:NAD oxidoreductase
 3. formate dehydrogenase
 4. formate + NAD = CO₂ + NADH
- E.
1. 1.6.2.1
 2. NADH:cytochrome C oxidoreductase
 3. cytochrome C reductase
 4. NADH + oxidized cytochrome C = NAD + reduced cytochrome C
- F.
1. 3.6.1.3
 2. ATP phosphohydrolase
 3. ATPase
 4. ATP + H₂O = ADP + orthophosphate
- G.
1. 1.2.1.29
 2. D-glycerate:NAD oxidoreductase
 3. glycerate dehydrogenase or hydroxypyruvate reductase
 4. glyceric acid + NAD = NADH + hydroxypyruvate
- H.
1. 1.1.1.31
 2. 3-hydroxybutyrate:NAD oxidoreductase
 3. beta-hydroxybutyrate dehydrogenase
 4. 3-hydroxybutyrate + NAD = acetoacetate + NADH

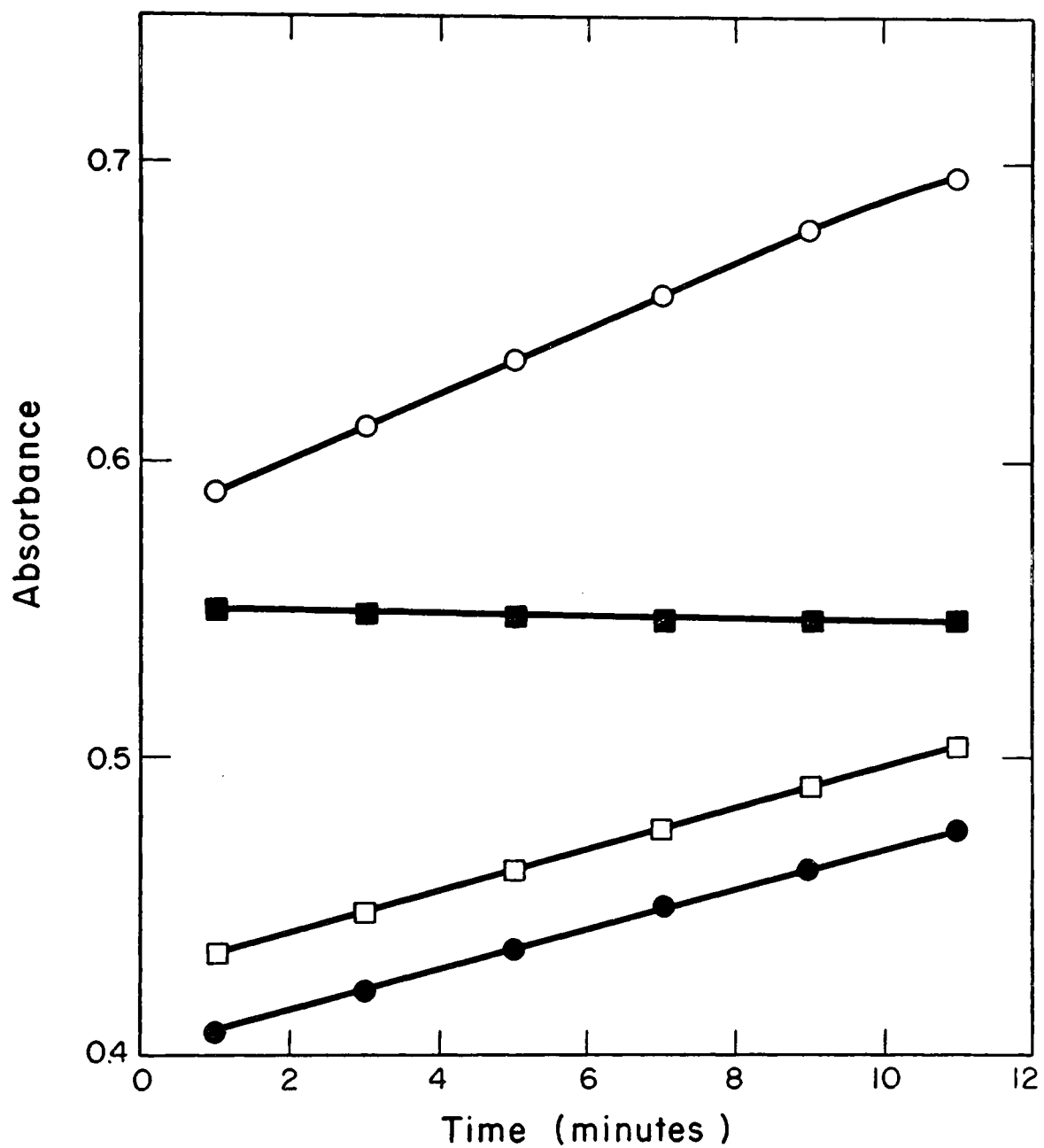


Figure 46. Graphs showing activity of serine transhydroxymethylase.

- supernatant activity
- membrane activity
- NADPH control, membranes
- no substrate

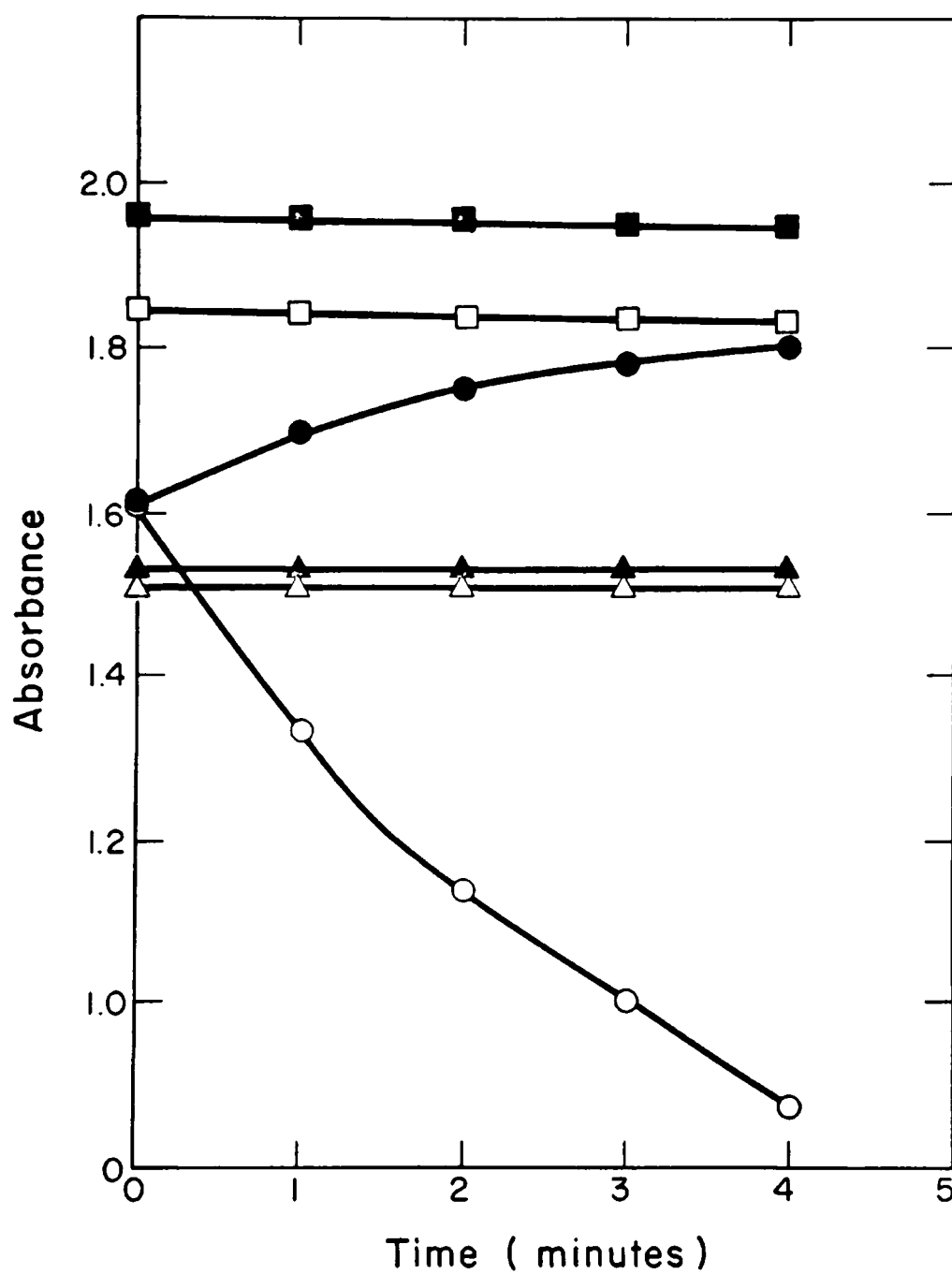


Figure 47. Graphs showing methanol dehydrogenase activity.

- membrane activity
- membrane control-no methanol
- supernatant activity
- supernatant control-no methanol
- △ supernatant activity with NAD
- ▲ NAD linked supernatant control

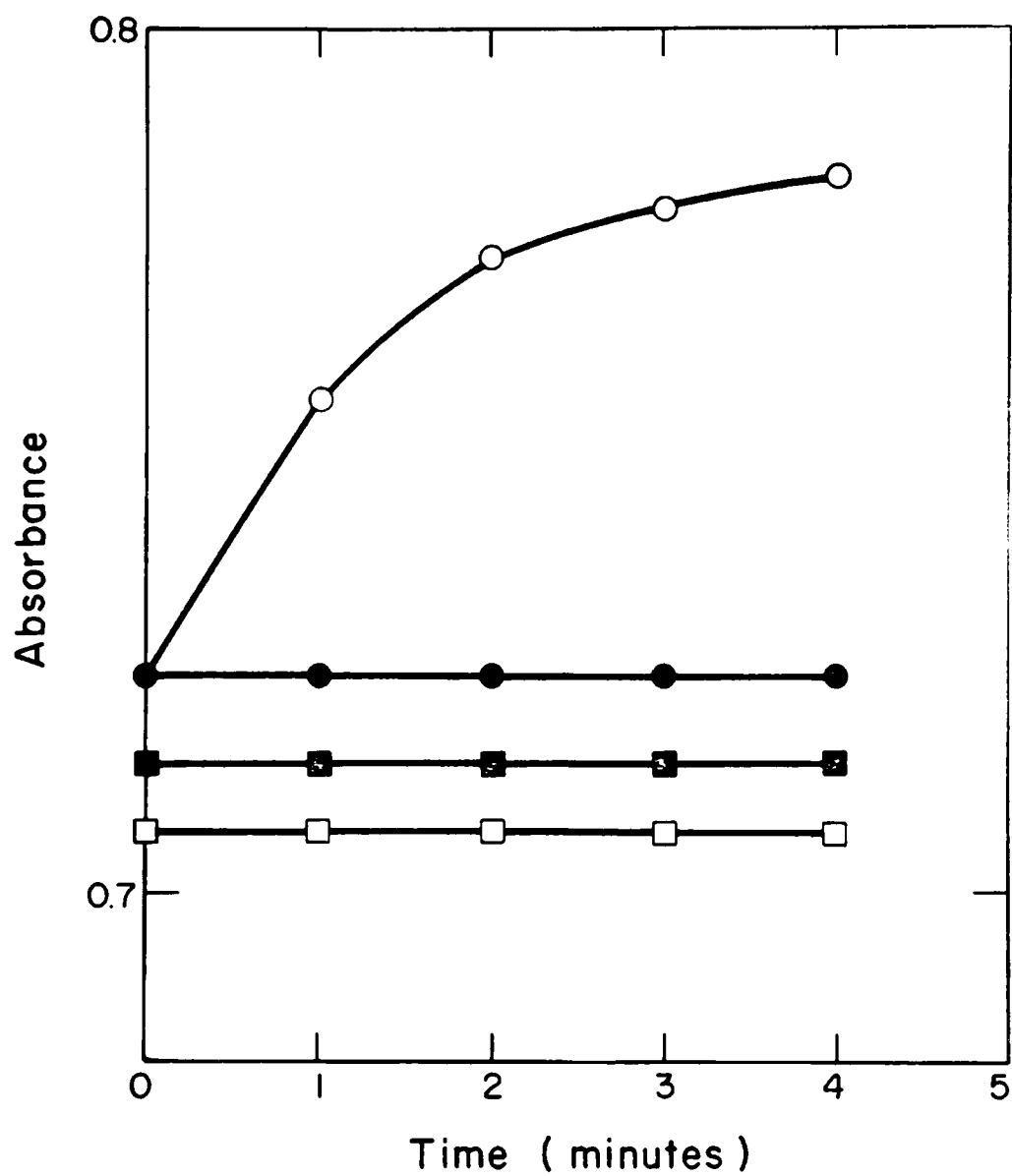


Figure 48. Graphs showing formaldehyde dehydrogenase activity.

- membrane activity
- membrane control-no formaldehyde
- supernatant activity
- supernatant control-no formaldehyde

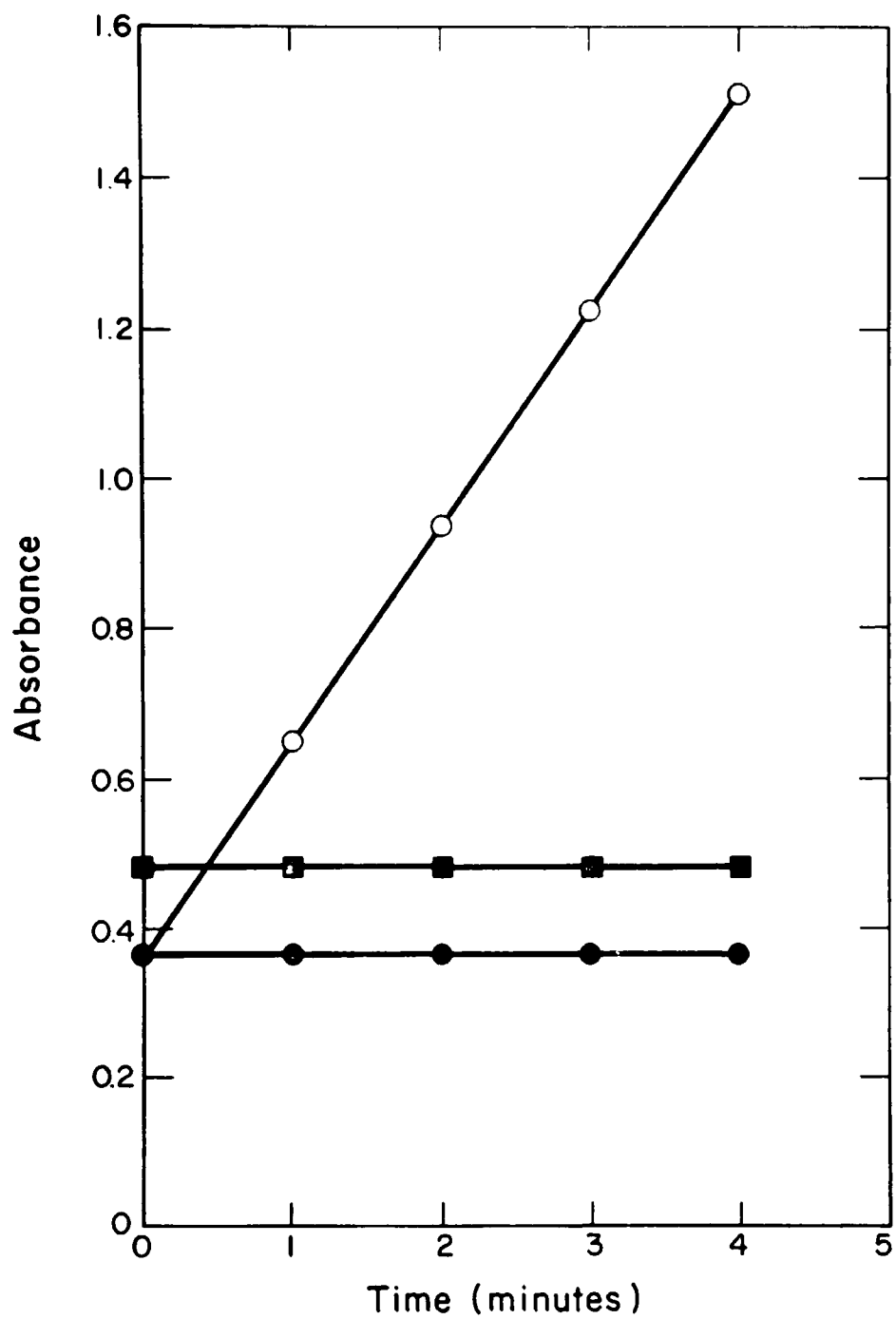


Figure 49. Graphs showing formate dehydrogenase activity.

- membrane activity and control
- supernatant activity
- supernatant control-no formate

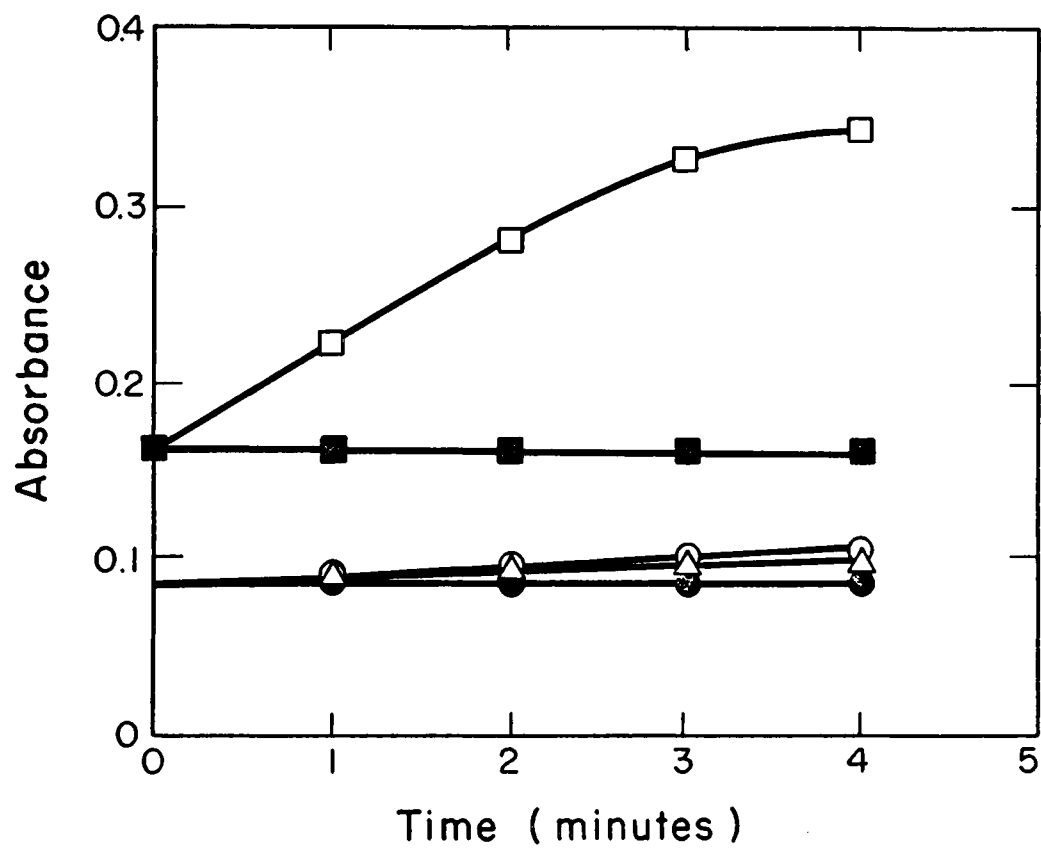


Figure 50. Graphs showing cytochrome C reductase activity.

- Membrane activity
- Membrane control-no NADH
- Supernatant activity
- Supernatant control-no NADH
- △ Control-no enzyme

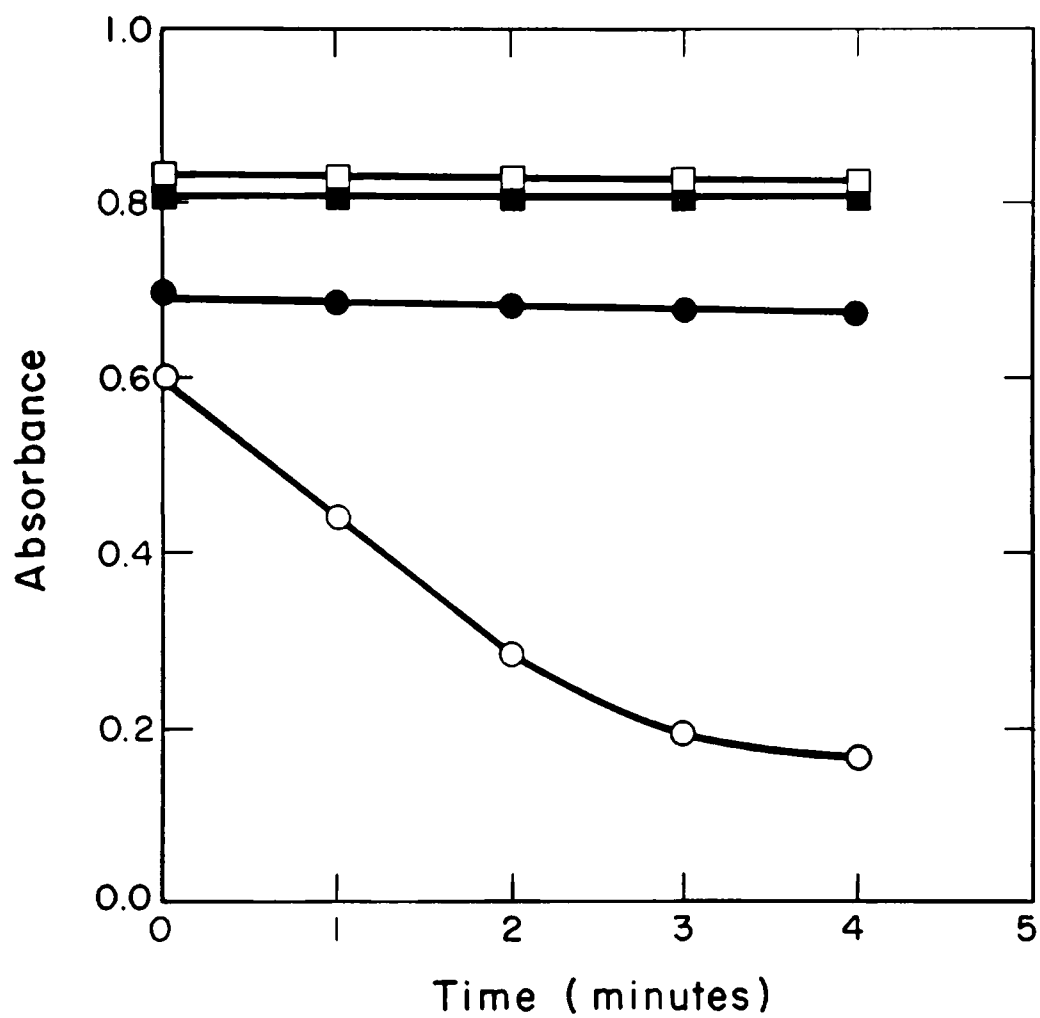


Figure 51. Graphs showing hydroxypyruvate reductase activity.

- Membranes activity
- Membrane control-no hydroxyp
- Supernatant activity
- Supernatant control-no hydroxyp

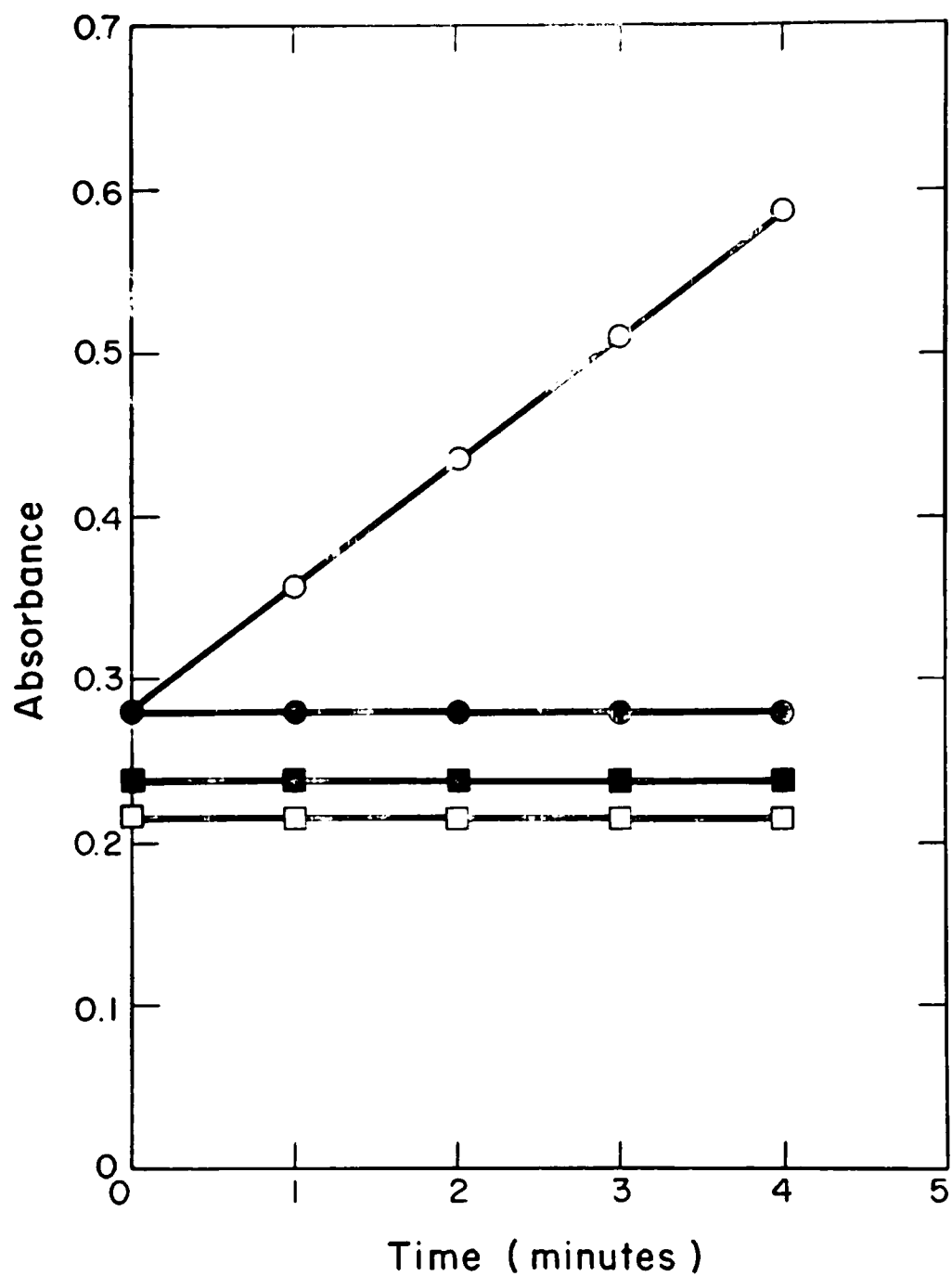


Figure 52. Graphs showing beta-hydroxybutyrate dehydrogenase activity.

- membrane activity
- membrane control-no beta-hydroxybutyrate
- supernatant activity
- supernatant control-no beta-hydroxybutyrate

TABLE 21

Initial velocities and activities of enzymes
in membrane and cytoplasmic preparations.

	Initial Velocity Activity			
	(nmoles/min)		(nM/min./mg)	
	Cyt.	Mem.	Cyt.	Mem.
serine hydroxymethyltransferase	0.56	0	1.4	0
methanol dehydrogenase	303	0	78	0
formaldehyde dehydrogenase	3.4	0	0.87	0
formate dehydrogenase	51	0	13.1	0
NADH:cyt. C reductase	0	3.1	0	1.2
ATPase	3100	10600	910	2700
hydroxypyruvate reductase	21	0	5.38	0
beta-hydroxybutyrate dehydrogenase	17	0	5	0

intravesticular. Since the intracytoplasmic membranes contain cytochromes, NADH-Cytochrome C reductase, and ATPase, they must serve as organelles of electron transport and energy entrapment. The oxidation and fixation of methane are cytoplasmic processes.

Hydroxypuruvate reductase and serine transhydroxymethylase may be useful as the biochemical labels for methane oxidizing bacteria sought in these studies. Both are soluble, easily extracted and easily assayed, and may be specific for methane oxidizing bacteria. The latter suggestion requires further evidence for conclusive statement.

9. SUMMARY

Suspended clay particles enhance bacterial methane oxidation by decreasing the lag phase of growth, increasing total methane oxidized, and by increasing the rate of methane oxidation. Bacterial methane oxidation enhancement increases with increasing clay concentrations up to 4.0%. The clay types kaolinite, illite, vermiculite, and bentonite equally stimulated bacterial methane oxidation. Clay particles less than $2\mu\text{m}$ in size elicit a greater stimulation of methane oxidation than particles greater than $2\mu\text{m}$ in size. The silicious remains of diatoms slightly enhance bacterial methane oxidation.

Calcium phosphate and calcium carbonate in suspension almost completely inhibit bacterial methane oxidation. However, calcium chloride did not inhibit methane oxidation when used in concentrations below 1%, suggesting the inhibitory effect was not due to solubilized calcium ions. Ferrous phosphate in suspension has no affect on bacterial methane oxidation. *Anacystis nidulans* produces an extracellular substance that inhibits bacterial methane oxidation. *Chlorella vulgaris* and *Anabaena variabilis* inhibit bacterial methane oxidation when exposed to light.

Increased methane utilization rates increase rates of dissolved oxygen composition. *Methylosinus trichosporium* is one of the bacteria responsible for methane oxidation. It is an obligate methylophilic Gram negative rod shaped bacterium which has a generation time of about 5.3 hours and a growth constant in log phase growth of about 0.1312 hours^{-1} . A variety of amino acids, organic acids, pentoses, and hexoses (e.g. organic pollutants) enhance methane oxidation by this bacterium. The bacterium fixes about 50% of the methane it oxidizes into cell material and one oxygen atom is consumed at each oxidative step during methane oxidation which is consistent with a monooxygenase. High speed differential centrifugation fractions contain relatively purified intracytoplasmic membranes which occur as flattened balloon-like vesicles near the cell periphery.

Intracytoplasmic membranes are organelles of electron transport and energy entrapment in this bacterium and are morphologically and biochemically similar to the internal membranes of the photosynthetic and nitrifying bacteria. Methane is fixed into cell material by the cytoplasmic enzyme serine hydroxymethyl transferase. An NAD independent methanol dehydrogenase is present in the cytoplasm. The bacterium has a specific formaldehyde dehydrogenase in the

cytoplasm. Formate dehydrogenase, beta-hydroxybutyrate dehydrogenase, and hydroxypruvate reductase are cytoplasmic enzymes. NADH: cytochrome C reductase is a membrane enzyme. The cytochromes are membrane-associated. ATPase was observed in both cytoplasm and membranes.

10. CONCLUSIONS

The methane oxidizing bacteria were found to be difficult to isolate. Most standard techniques had to be modified to accommodate growth of these bacteria. While growth of the methane oxidizers was relatively slow in pure cultures, mixed cultures enriched from aquatic ecosystems grew rapidly. Rapid growth is directly related to methane utilization and oxygen consumption. The influence of this phenomenon on dissolved oxygen in the aquatic environment must be significant and has been shown to be affected by a variety of environmental factors. Notably, clay minerals and various soluble organic compounds have been shown in this study to stimulate methane oxidation. Therefore, minimizing input of these materials into aquatic ecosystems would minimize methane carbon retention in those waters. This would reduce the rate of carbon accumulation in an aquatic ecosystem which plays a key role in the eutrophication process. Conversely, other factors such as certain algae and minerals were found to inhibit methane oxidation. The use of insoluble minerals to regulate methane carbon retention, in aquatic ecosystems, is a possibility. For example, selection of a reservoir site with large amounts of apatite over another site with high clay content may minimize methane carbon retention in the water.

Standard techniques such as plate counts were found to be of little use for quantitating methane oxidizing bacteria. However, in order to understand the process of microbial methane fixation in aquatic ecosystems, in situ rates of methane oxidation must be coupled with quantitation of methane oxidizing bacteria. For this reason, considerable effort was directed at developing methods for quantitative detection of the methane oxidizing bacteria. Biochemical and morphological studies directed at finding labels useful in quantitation resulted in some potentially valuable information. Methane oxidizing bacteria membranes, enzymes, cytochromes, protein composition, and lipid composition all had unique characteristics that could be valuable in obtaining quantitative data. This would represent a biochemical approach to obtaining quantitative data related to eutrophication and aquatic ecology. These techniques could be useful in studying groups of microorganisms such as methane oxidizing bacteria, photosynthetic bacteria, and nitrifying bacteria that were heretofore not amenable to standard quantitative techniques. Future research endeavors using this approach in addition to newer techniques such as identification in situ via fluorescent labeled antibody should be rewarding.

11. LITERATURE CITED

1. Ames, B.N. 1966. Assay of Inorganic Phosphate, Total Phosphate and Phosphates. *Methods in Enzymology*. 8:115-118.
2. Barker, H.A. 1936. On the Biochemistry of the Methane Fermentations. *Arch. Mikrobiol.* 7:404-419.
3. Barker, H.A. 1936. Studies Upon the Methane Producing Bacteria. *Arch. Microbiol.* 7:420-438.
4. Bigger, J.W. and J.H. Nelson. 1941. The Growth of Coliform Bacilli in Distilled Water. *J. Path. Bacteriol.* 53:189-206.
5. Blackwood, A.C. and E.P.P. Agnes. 1957. Identification of Beta-hydroxybutyric Acid in Bacterial Cells of Infrared Spectrophotometry. *J. Bacteriol.* 74:266-267.
6. Bligh, E.G. and W.J. Dyer. 1959. A Rapid Method of Total Lipid Extraction and Purification. *Can. J. Biochem. Physiol.* 37:911-917.
7. Blumer, M., T. Chase, and S. W. Watson. 1969. Fatty Acids in the Lipids of Marine and Terrestrial Nitrifying Bacteria. *J. Bacteriol.* 99:366-370.
8. Bremner, J.M. 1949. Studies on Soil Organic Matter. *J. Ag. Sci.* 39:280-282.
9. Brown, R.L. and R.J. Strawinski. 1957. The Bacterial Metabolism of Methane, *Bacteriol. Proc.* 1957:18.
10. Brown, L.R. and R.J. Strawinski. 1958. Intermediates in the Oxidation of Methane. *Bacteriol. Proc.* p. 122.
11. Brown, L.R. and R.J. Strawinski, and C.S. McCleskey. 1964. The Isolation and Characterization of Methanamonas methanoxidans.
12. Cashen, J. 1966. Extraction of Organic Material From Soils. *J. Soil Sci.* 17:303-316.
13. Casper, V.L. 1965. A Phytoplankton Bloom in Western Lake Erie. Pub. #13, Great Lakes Res. Div., Univ. of Michigan. pp. 29-34.
14. Coleman, R. 1973. Membrane Bound Enzymes and Membrane Ultrastructure. *Biochim. Biophys. Acta.* 300:1-30.
15. Conn, H.J. and J.E. Conn. 1940. The Stimulating Effect of Colloids Upon the Growth of Certain Bacteria. *J. Bacteriol.* 39:99-100.
16. Cralley, K.E. 1968. The Effect of Particulates on the Growth of Selected Actinomycetes. M.S. Thesis, The Ohio State University.
17. Danielli, J.F. and H.A. Davson. 1936. A Contribution to the Theory of Permeability of Thin Films. *J. Cell. Comp. Physiol.* 9:89-92.

18. Davis, J.B., V.F. Coty, and J.P. Stanley. 1964. Atmospheric Nitrogen Fixation by Methane Oxidizing Bacteria. *J. Bacteriol.* 88:468-472.
19. Davis, S.L. and R. Wittenbury. 1970. Fine Structure of Methane and Other Hydrocarbon Utilizing Bacteria. *J. Gen. Microbiol.* 61:227-233.
20. Davies, T.R. 1973. Isolation of Bacteria Capable of Utilizing Methane as a Hydrogen Donor in the Process of Denitrification. *Water Res.* 7:575-579.
21. Davis, B.D., R. Dulbecco, H.N. Eisen, and H.S. Ginsberg. W.B. Wood-Microbiology. 1968. Harper and Row.
22. Davis, J.B., V.F. Coty, and J.P. Stanley. 1964. Atmospheric Nitrogen Fixation by Methane Oxidizing Bacteria. *J. Bacteriol.* 88:468-472.
23. D'Mello, J. 1972. A Study of the Amino Acid Composition of Methane Utilizing Bacteria. *J. Appl. Bacteriol.* 1:145-148.
24. Dugan, P.R., R.M. Pfister, and J.I. Frea. 1970. Implications of Microbial Polymer Synthesis in Waste Treatment and Lake Eutrophication. *Proc. 5th Int. Conf. Water Pollution Res.* 1970.
25. Dworkin, M. and J.W. Foster. 1956. Studies on Pseudomonas methanica (Söhngen). *J. Bacteriol.* 72:646-659.
26. Dworkin, M. and J.W. Foster. 1956. Studies on Pseudomonas methanica *J. Bacteriol.* 72:646-655.
27. Eller, D. and D.G. Lundgren. 1968. Morphology and Poly-beta-hydroxybutyrate Granules. *J. Mol. Biol.* 35:489-502.
28. Emerson, R.W. 1870. *Society and Solitude.* Fields, Osgood, and Co., Boston, Mass. p. 142.
29. Erickson, D. 1941. Studies on Some Lake Mud Strains of Micromonospora. *J. Bacteriol.* 41:277-303.
30. Folch, J., M. Lees, and G.H. Sloane Stanley. 1957. A Simple Method for the Isolation and Purification of Total Lipids from Animal Tissues. *J. Biol. Chem.* 226:497.
31. Folin, O. and V. Ciocalteu. 1927. On Tyrosine and Tryptophane Determinations in Protein. *J. Biol. Chem.* 73:627-650.
32. Foster, J.W. and R.H. Davis. 1966. A Methane Dependent Coccus with Notes on Classification and Nomenclature of Obligate Methane Utilizing Bacteria. *J. Bacteriol.* 91:1924-1931.
33. Friedman, B.A. and P.R. Dugan. 1968. Concentration and Accumulation of Metallic Ions by the Bacterium Zoogloea. *Develop. Ind. Microbiol.* 9:381-388.
34. Giglioni, I. and G. Masoni. 1914. Nuove osservazioni sull'assorbimento Biologico del Metano; e sulla Distribuzione nei Terreni, nelle Melme e negli ingrassi, degli Organismi Metanici di Kaserer e di Söhngen. Pisa Università, Istituto di Chimica Agraria, Studi e Ricerche. 22:76-94.

35. Gorter, E. and R. Grendel. 1925. On Bimolecular Layers of Lipoid on the Chromocytes of Blood. J. Exp. Med. 41:439-443.
36. Goswami, S.K. and C.F. Frey. 1971. Spray Detection of Phospholipids on Thin Layer Chromatograms. J. Lipid Res. 12:509-510.
37. Grim, R.E. 1968. Clay Mineralogy. McGraw-Hill Book Co., New York, N.Y. pp.596.
38. Guidotti, G. 1972a. Membrane Proteins. Ann. N.Y. Acad. Sci. 195:139-141.
39. Guidotti, G. 1972b. The Composition of Biological Membranes. Arch. Int. Med. 129:194-201.
40. Hagen, P.O. 1966. Phospholipids of Bacteria with Extensive Intracytoplasmic Membranes. Science. 151:1546.
41. Håggström, L. 1969. Studies on Methanol Utilizing Bacteria. Biothec. Bioeng. 11:1043-1054.
42. Hamer, G. and C.G. Heden. 1967. Methane as a Carbon Substrate for the Production of Microbial Cells. Biothec. Bioeng. 2:499-514.
43. Hanes, C.S. and F.A. Isherwood. 1949. Separation of Phosphoric Esters on the Filter Paper Chromatogram. Nature. 164:1107-1112.
44. Harder, W., and J.R. Quayle. 1971b. Aspects of Glycine and Serine Biosynthesis During Growth of *Pseudomonas* A1 on C₁ Compounds. Biochem. J. 121:763-769.
45. Harrington, A.A., and R.E. Kallio. 1960. Oxidation of Methanol and Formaldehyde by *Pseudomonas methanica*. Can. J. Microbiol. 6:1-7.
46. Harrison, W.H. and P.A.S. Aiyer. 1914. The Gases of Swamp Rice Soils: Their Composition and Relationship to the Crop. Mem. Dept. Agr. India, Chem. Ser. 3:65-107.
47. Harrow, B. and A. Mazur. 1967. Biochemistry. W.B. Saunders Co., Philadelphia, Pa. pp.648.
48. Hatefi, Y., M.J. Osborn, L.D. Kay, and F.M. Huennekens. 1957. Hydroxymethyl Tetrahydrofolic Dehydrogenase. J. Biol. Chem. 227:637-647.
49. Hazeu, W. and P.J. Stennis. 1970. Isolation and Characterization of Two Vibrio-Shaped Methane Oxidizing Bacteria. Ant. van Leeuwenhoek. 36:67-72.
50. Heptinstall, J. and J.R. Quayle. 1970. Pathways leading to and from Serine During Growth of *Pseudomonas* A1 on C₁ Compounds or Succinate. Biochem. J. 117:563-572.
51. Heukelekian, H. and A. Heller. 1940. Relation Between Food Concentration and Surface for Bacterial Growth. J. Bacteriol. 40:547-558.

52. Higgins, I.J. and J.R. Quayle. 1970. Oxygenation of Methane by Methane Growth Pseudomonas methanica and Methanomonas methanoxidans. Biochem. J. 118:201-208.
53. Howard, D.L., J.I. Frea, and R.M. Pfister, 1971. The Potential for Methane-Carbon Cycling in Lake Erie. Proc. 14th Conf. Great Lakes Res. 1971.
54. Hutton, W.E. and C.E. Zobell. 1949. The Occurrence and Characteristics of Methane Oxidizing Bacteria in Marine Sediments. J. Bacteriol. 58:463-473.
55. Hutton, W.E. and C.E. Zobell. 1952. Pruduction of Nitrite from Ammonia by Methane Oxidizing Bacteria. J. Bacteriol. 65:216-219.
56. Johnson, P.A. and J.R. Quayle. 1965. Microbial Metabolism of C₁ Compounds. Biochem. J. 95:859.
57. Johnson, J.L. and K.L. Temple. 1962. Some Aspects of Methane Oxidation. J. Bacteriol. 84:456-458.
58. Jorgensen, E.G. 1962. Antibiotic Sybstances From Cells and Culture Solutions of Unicellular Algae with Special References to Some Chlorophyll Derivatives. Phys. Plant. 15:530-545.
59. Kaneda, T. and J.M. Roxburgh. 1959. Service as an Intermediate in the Assimilation of Methanol by a Pseudomonas. Biochem. Biophys. Acta. 33:106-110.
60. Kaserer, H. 1905. Ueber die Oxydation des wasserstofes und des Methane durch Midroorganismen. Z. Landy. Versuchsw. Deut. Oesterr. 8:789.
61. Kemp, M.B. and J.R. Quayle. 1967. Microbial Growth or C₁ Compounds: Uptake of C¹⁴ Formaldehyde and C¹⁴ Formate by Methane Grown Pseudomonas methanica and Determination of the Hexose Labelling Pattern After Brief Incubation with C¹⁴ Methanol. Biochem. J. 102:94-102.
62. Large, P.J., D. Peel, and J.R. Quayle. 1961. Microbial Growth on C₁ Compounds: Synthesis of Cell Constituents by Methanol and Formate Grown Pseudomonas Aml. Biochem. J. 81:470-480.
63. Large, P.J., D. Peel. and J.R. Quayle. 1962. Microbial Growth on C₁ Compounds: Distribution of Radioactivity in Metabolites of Methanol Grown Pseudomonas Aml After Incubation with C¹⁴ Methanol and C¹⁴ Bicarbonate. Biochem. J. 82:483-488.
64. Large, P.J. and J.R. Quayle. 1963. Microbial Growth on C₁ Compounds: Enzyme Activities in Extracts of Pseudomonas Aml. Biochem. J. 87:386-396.
65. Law, J.H. and R.S. Slepecky. 1961. Assay of Poly-beta-hydroxybutric Acid. J. Bacteriol. 82:33-36.
66. Lawrence, A.J. and J.R. Quayle. 1970. Alternative Carbon Assimilation Pathways in Methane Utilizing Bacteria. J. Gen. Microbial. 63:371-374.

67. Lawrence, A.J., M.B. Kemp, and J.R. Quayle. 1970. Synthesis of Cell Constituents by Methane Grown Methylococcus capsulatus and Methanomonas methanoxidans. Biochem. J. 116:631-639.
68. Leadbetter, E.R. and J.W. Foster. 1957. Some New Methane Utilizing Bacteria. Bacteriol. Proc. 1957:17.
69. Leadbetter, E.R. and J.W. Foster. 1958. Studies on Some Methane Utilizing Bacteria. Arch. for Microbiol. 30:91-118.
70. Leadbetter, E.R. and J.W. Foster. 1959. Incorporation of Molecular Oxygen in Bacterial Cells Utilizing Hydrocarbons for Growth. Nature. 184:1428-1429.
71. Leadbetter, E.R. and J.W. Foster. 1960. Bacterial Oxidation of Gaseous Alkanes. Arch. for Microbiol. 35:92-104.
72. Leonard, J. and S.J. Singer. 1966. Protein Conformation in Cell Membrane Preparations as Studied by Optical Rotatory Dispersion and Circular Dichorism. Prac. Nat. Acad. Aci. U.S.A. 56:1828-1835.
73. Leshniowsky, W.O., P.R. Dugan, R.M. Pfister, J.I. Frea and C.I. Randles. 1970. Aldrin: Removal From Lake Water by Flocculent Bacteria. Science. 169:993-995.
74. Lewin, R.A. 1962. Physiology and Biochemistry of Algae. Academic Press, New York, N.Y. pp. 929.
75. Lowry, O.H., N.J. Rosebrough, A.L. Farr, and R.J. Randall. 1951. Protein Measurement with the Folin Phenol Reagent. J. Biol. Chem. 193:265-275.
76. Mahler, H. and E. Cordes. 1966. Biological Chemistry. Harper and Row, New York, N.Y.
77. Maze', P. 1903. Volatile Gas Production by Bacteria. Compt. Rend. 137:887-891.
78. Meadows, P.S. and J.G. Anderson. 1966. Microorganisms Attached to Marine and Freshwater Sand Grains. Nature. 212:1059-1060.
79. Morrison, R.T. and R.N. Boyd. 1966. Organic Chemistry. Allyn and Bacon, Inc. Boston, Mass. pp. 36-37.
80. Nageli, C. and C. Cramer. 1972. Pflanzephysiologische Untersuchungen, 1855. The Development of Ideas on Membrane Structure. Sub. Cell. Biochem. 1:363-373.
81. Naguib, M. and J. Overbeck. 1970. On Methane Oxidizing Bacteria in Fresh Waters. Zeit. für Allg. Mikrobiol. 10:17-36.
82. Nechaeva, N.G. 1949. Two Species of Methane Oxidizing Mycobacteria. Mikrobiologiya. 18:310-317.

83. Oelze, J. and G. Drews. 1972. Membranes of Photosynthetic Bacteria. *Biochem. Biophys. Acta.* 265:209-239.
84. O'Leary, W.M. 1967. The Chemistry and Metabolism of Microbial Lipids. The World Pub. Co., Cleveland, Ohio.
85. Op Den Kamp, J.A.F. and L.L.M. Van Deenen. 1969. Bacterial Phospholipids and Membranes as in Structural Aspects of Lipoproteins in Living Streams. Academic Press. New York, N.Y. pp. 227-325.
86. Overton, E. 1895. Uber die osmotischen Eigenshafter der Lebenden Pflanzen und tierzelle. *Vjschr. Naturf. Ges Zurich.* 40:159-201.
87. Patel, R.N. and D.S. Hoare. 1971. Physiological Studies of Methane and Methanol Oxidizing Bacteria: Oxidation of C-1 Compounds by Methylococcus capsulatus. *J. Bacteriol.* 107:187-192.
88. Patel, R.N., H.R. Bose, W.J. Mandy, and D.S. Hoare. 1972. Physiological Studies of Methane and Methanol Oxidizing Bacteria: Comparison of a Primary Alcohol Dehydrogenase from Methylococcus capulatus (Texas Strain) and Pseudomonas Species M27. *J. Bacteriol.* 110:570-577.
89. Parsons, A.B. 1970. Investigation of Zoogloea ramigera Isolate 115 with Emphasis on Composition and Synthesis of the Extracellular Matrix Polymer. M.S. Thesis, The Ohio State University.
90. Parsons, A.B. and P.R. Dugan. 1971. Production of Extracellular Polysaccharide Matrix by Zoogloea ramigera. *Applied Microbiol.* 21:657-661.
91. Pauling, L. 1930. The Structure of Micas and Related Minerals. *Proc. Natl. Acad. Sci. U.S.* 16:123-129.
92. Peel, D. and J.R. Quayle. 1961. Microbial Growth on C-1 Compounds: Isolation and Characterization of Pseudomonas AML. *Biochem. J.* 81:465-469.
93. Perry, J.J. 1968. Substrate Specificity in Hydrocarbon Utilizing Microorganisms. *Ant. van Leeuwenhoek.* 34:27-36.
94. Pfister, R.M. P.R. Dugan, and J.I. Frea. 1968. Particulate Fractions in Water and the Relationship to Aquatic Microflora. *Proc. 11th Conf. Great Lakes Res.* 1968:111-116.
95. Pfister, R.M., J.I. Frea, P.R. Dugan, C.I. Randles, K. Zaebst, J. Duchene, T. McNair, and R. Kennedy. 1970. Chlorinated Hydrocarbon, Microparticulate Effects of Microorganisms Isolated From Lake Erie. *Proc. 13th Conf. Great Lakes Res.* 1970:82-92.
96. Proctor, H.M., J.R. Norris, and D.W. Ribbons. 1969. Fine Structure of Methane-Utilizing Bacteria. *J. Appl. Bacteriol.* 32:118-121,
97. Protz, R. 1970. Sedimentation Times for Particle Size Analysis. Laboratory Particle Analysis, Agronomy Dept., The Ohio State University.

98. Reynolds, E.S. 1963. The Use of Land Citrate at High pH as an Electron Opaque Stain in Electron Microscopy. J. Cell. Biol. 17:208.
99. Ribbons, D.W., J.E. Harrison, and A.M. Wadzinski. 1970. Metabolism of Single Carbon Compounds. Ann. Rev. Microbiol. 24:135-158.
100. Ribbons, D.W. and I.J. Higgins. 1971. Enzymic Oxidation of Methane by Particles from Methylococcus capulatus. Bacteriol. Proc. p. 107.
101. Ribbons, D.W. and J.L. Michalover. 1970. Methane Oxidation by Cell-Free Extracts of Methylococcus capulatus. FEBS Letters 11:41-44.
102. Robertson, J.D. 1972. The Structure of Biological Membranes. Arch. Int. Med. 129:202-228.
103. Rosen, H. 1957. A Modified Ninhydrin Colorimetric Analysis for Amino Acids. Arch. Biochem. Biophys. 67:10-15.
104. Rosen, H. 1957. Ninhydrin Procedure for Amino Acids. Arch. Biochem. Biophys. 67:10.
105. Round, F.E. 1966. The Biology of Algae. E. Aronod Pub. LTD. London, England. p. 218.
106. Saber, H.A., R.A. Harte, and E.K. Saber. 1970. Handbook of Biochemistry. Chem. Rubber Co. Cleveland, Ohio. pp. C:282-287.
107. Salton, M.R. 1971. Bacterial Membranes. Crit. Rev. Microbiol. May:161-197.
108. Schwimmer, M. and D. Schwimmer. 1955. The Role of Algae and Plankton in Medicine. Grune and Stratton, New York, N.Y. p. 56.
109. Sheehan, B.T. and M.J. Johnson. 1970. Production of Bacterial Cells From Methane. Applied Microbiol. 21:511-515.
110. Sheehan, B.T. and M.J. Johnson. 1971. Production of Bacterial Cells from Methane. Appl. Microbiol. 21:511-515.
111. Singer, S.J. 1973. Are Cell Membranes Fluid? Science. 180:983.
112. Singer, S.J. and G.L. Nicolson. 1972. The Fluid Mosaic Model of Membrane Structure. Nature. 175:720
113. Sjöstrand, F.S. 1969. Morphological Aspects of Liporprotein Structures, in Structural and Functional Aspects of Liporprotein in Living Systems. Academic Press. New York, N.Y. pp. 73-139.
114. Skipshi, V.P. and M. Barclay. 1969. Thin Layer Chromatography of Lipids. Methods in Enzymology. 14:530-598.
115. Smith, U. and D.W. Ribbons. 1970. Fine Structure of Methanomonas methanoxidans. Arch. Mikrobiol. 74:116-122.

116. Smith, U., D.W. Ribbons, and D.S. Smith. 1970. The Fine Structure of Methylococcus capsulatus. Tissue and Cell. 2:513-520.
117. Söhngen, N.L. 1906. Ueber Bakterien, welch Methan als Kohlenstoffnahrung und Energiequelle gebrauchen. Zentr. Bakt. Parasitenk. 15:513-517.
118. Stocks, P.K. and C.S. McCelskey. 1964. Morphology and Physiology of Methanomonas methanoxidans. J. Bacteriol. 88:1071-1077.
119. Stotzky, G. and L.T. Rem. 1966. Influence of Clay Minerals on Microorganisms. Can. J. Microbiol. 12:547-563.
120. Stotzky, G. and L.T. Rem. 1967. Influence of Clay Minerals on Microorganisms. Can. J. Microbiol. 13:1535-1550.
121. Strawinski, R.J. and J.A. Tortorich. 1955. Preliminary Studies of Methane Oxidizing Bacteria and Their Possible Role in Oil Prospecting. Bacteriol. Proc. 1955:27.
122. Strawinski, R.J. and L.R. Brown. 1957. Isolation Criteria and Characterization of a New Methane Oxidizing Bacterium. Bacteriol. Proc. p. 18.
123. Swinnerton, J.W., V.J. Linnenbom, and C.H. Cheek. 1969. Distribution of Methane and Carbon Monoxide Between the Atmosphere and Natural Waters. Environ. Sci. Technol. 3:836-838.
124. Vanderkooi, G. and R.A. Capaldi. 1972. A Comparative Study of the Amino Acid Compositions of Membrane Proteins and Other Proteins. Ann. N.Y. Acad. Sci. 195:135-138.
125. Vary, P.S. and M.J. Johnson. 1967. Cell Yields of Bacteria Grown on Methane. Applied Microbiol. 15:1473-1478.
126. Waksman, S.A. 1950. The Actinomycetes: Their Naturek Occurrence, Activity, and Importance. Chronica Botanica Co., Waltham, Mass.
127. Watson, S.W. 1965. Characteristics of a Marine Nitrifying Bacterium, Nitrocystis oceanus sp. n. Limmol and Ocean. 10:274-189.
128. Weaver, T.L. and P.R. Dugan. 1972. The Eutrophication Implications of Interactions between Naturally Occurring Particulates and Methane Oxidizing Bacteria. Water Res. 6:817-828.
129. Wertlieb, D. and W. Vishniac. 1967. Methane Utilization by a Strain of Rhodopseudomonas gelatinosa. J. Bacteriol. 93:1722-1724.
130. Whistler, R.L. and M.L. Wolfrom. 1962. Methods in Carbohydrate Chemistry. MacMillan Co., New York, N.Y. p. 389.
131. White, D.C. 1968. Lipid Composition of the Electron Transport Membrane of Haemophilis parainfluenzoe. J. Bacteriol. 96:1159-1170.
132. Whittenbury, R. 1969. Microbiol Utilization of Methane. Proc. Biochem. 1:51-56.

133. Whittenbury, R., K.C. Phillips, and J.F. Wilkinson. 1970. Enrichment, Isolation, and Some Properties of Methane Utilizing Bacteria. J. Gen. Microbiol. 61:205-218.
134. Whittenbury, R., S.L. Davies, and J.F. Davey. 1970. Exospores and Cysts formed by Methane Utilizing Bacteria. J. Gen. Microbiol. 61:219-231.
135. Wiegner, G. and H. Jenny. 1927. Ueber Basenaustausch an Permutiten. Kolloid Z. 43:268-272.
136. Wolnak, B., B.H. Andreen, J.A. Chisholm, and M. Saadek. 1967. Fermentation of Methane. Biothec. Bioeng. 9:57-76.
137. Zobell, C.E. and Q. Anderson. 1936. Observations on the Multiplication of Bacteria in Different Volumes of Stored Sea Water and the Influence of Oxygen Tension and Solid Surfaces. Biol. Bull. 71:324-342.